Investigating the Influence of Metabolic Syndrome on Cancer Immunotherapy

Matthew J. Woodall

A thesis submitted for the degree of

Bachelor of Medical Science with Honours

University of Otago

Dunedin

New Zealand

December 2019

Abstract

Cancer is a significant cause of morbidity in New Zealand, with breast and colorectal cancers being amongst the most commonly diagnosed. Therapeutic research has moved into immunotherapies, harnessing the immune system to target tumours. One approach uses virus-like particles (VLP) to activate the immune system against specific antigens found on tumour cells. This has been successful in normal weight murine models of breast and colorectal cancer.

Obesity is a highly prevalent disease and contributes to the development of many cancers and may impact the efficacy of treatment. Uric acid is known to be highly immunogenic and chronic hyperuricemia (elevated serum urate) is likely to influence the immune system.

The project aimed to test a known efficacious VLP therapy combined with anti-programmed death ligand (PD-L)1, against models of breast and colorectal cancer in obese and hyperuricemic mice. Mice were grafted with either breast or colorectal cancer and treated with an empty vehicle, VLP alone, or VLP + anti-PD-L1. Tumours were either immunohistochemically stained or T-cells were stained for markers of exhaustion. Populations of immune cells were also determined in the blood.

Slight increases in survival were observed in obese and hyperuricemic mice with breast cancer treated with VLP, although these mouse strains had reduced survival compared to lean mice when treated with VLP + anti-PD-L1. Obese and hyperuricemic mice had reduced levels of tumour-infiltrating lymphocyte (TIL) infiltrate compared to lean mice. TILs tended to have a greater phenotype associated with exhaustion in obese mice.

In colorectal cancer, survival rates increased in obese mice in both treatment groups. Obese mice had similar levels of TIL infiltration to lean mice, which was reduced in

hyperuricemic mice. Treatment with VLP increased TIL frequency in obese and hyperuricemic mice but not in lean mice. There were no differences in TIL exhaustion in lean and obese mice. Obese mice had higher counts of circulating neutrophils and inflammatory monocytes in the blood, but had reduced lymphoid-derived dendritic cell and B-cell counts compared to lean mice.

This data suggests that obese and hyperuricemic mice may have reduced responses to immunotherapy, however this varies based on cancer type. Reduced TIL infiltration and increased T-cell exhaustion seen in the breast cancer model may play a role in this.

To examine the effect of obesity on cancer treatment in patients, data from stage I and II colorectal cancer patients were analysed for obesity metrics, muscle mass, and blood parameters to compare survival in designated subpopulations.

Analysing data about visceral fat showed that obese females had the lowest rate of survival, with non-obese females and all males having similar survival levels. Conversely, measuring waist circumference showed that non-obese females had lower rates of survival than obese females, while obese males had lower rates than non-obese males. Patients with low muscle mass tended to have higher survival compared to those with normal muscle mass. Obesity resulted in higher levels of lymphocytes and albumin, but lower levels of neutrophils and platelets. Sarcopenic patients had decreased levels of lymphocytes.

Using visceral fat as a measurement of obesity gives different survival rates compared with standard measures. This may be useful clinically when considering body composition during prognosis. Future research will investigate the effect of body composition on the survival of stage III and IV colorectal cancer patients and may facilitate the development of more personalised and effective treatment regimens.

Acknowledgements

Firstly, I would like to express my immense gratitude to my primary supervisor, Professor Sarah Young. She willingly allowed me to become part of her team, and her respect for all of us was a great motivator to make the most out of my project. Her guidance and advice, not always related to my experiments, was refreshing. I have been interested in the field of immunotherapy for several years now and it was exciting to be part of her laboratory.

To my wonderful co-supervisors, Drs. Katrin Kramer and Silke Neumann – the most profound thank you is needed here. Your friendly nature and willingness to help with experiments and proof-reading alleviated a lot of stress I had coming into this year. I would especially like to mention Katrin, who was heavily involved in my project. I do not think that I could have done it without you.

Dr. Sharon Pattison became an advisor for the patient side of my project. Her willingness to expand my project and involve me in as much as possible was unexpected but much appreciated. I look forward to continuing working with you next year. I would also like to thank Dr. Gabriel Lau, for helping me with my CT analysis.

I felt very welcome in the Young laboratory from the moment I started, and for this, I thank the above people but also everyone else – Donata Maciaczyk, Estelle Peyroux, Hein Nguyễn, Nick Shields, Niki Zach, Peng Luo, Serena Bielli, and Yasmin Wilkinson. I would also like to thank Meghan Evans, who started this project for her Bachelor of Biomedical Science (honours). Your work has proved immensely helpful.

Finally, to my friends, family, and the team of Anatomy demonstrators, thank you for your love and support. Being able to get away from the laboratory and talk with people doing other things meant that I could relax and then work my hardest when I was here.

Table of Contents

List of Figures

List of Tables

List of Abbreviations

AMPK	5'-AMP-activated protein kinase
ANOVA	Analysis of variance
APC	Antigen-presenting cell
Bcl	B-cell lymphoma
BMI	Body mass index
C57BL/6	Lean mice
CD	Cluster of differentiation
CEA	Carcinoembryonic antigen
CLS	Crown-like structures
CpG	Cytosine-phosphate guanosine
CRP	C-reactive protein
CT	Computed Tomography
CTL	Cytotoxic T cell ($CD8^+$ T-cells)
CTLA-4	Cytotoxic T-lymphocyte-associated Protein-4
CXCR3	CXC chemokine receptor-3
DAB	3,3′-Diaminobenzidine
DAMP	Danger-associated molecular protein
DC	Dendritic cell
DHEA	Dehydroepiandrosterone
DIO	Diet-induced obesity
DMEM	Dulbecco's Modified Eagle Medium
DNA	Deoxyribonucleic acid
EDTA	Ethylenediaminetetraacetic acid
ESR	Erythrocyte sedimentation rate
FACS	Fluorescence-Activated Cell Sorting
FCS	Foetal Calf Serum
GHR	Growth hormone receptor
GM-CSF	Granulocyte-macrophage colony-stimulating factor
H&E	Haematoxylin and eosin
HIF	Hypoxia-inducible factor
HRC CRC	Health Research Council Colorectal Cancer
HTRU	Hercus Taieri Research Unit
i.p	Intraperitoneal

IFN	Interferon
Ig	Immunoglobulin
IGF	Insulin-like growth factor
IGF-1R	Insulin-like growth factor-1 receptor
IL	Interleukin
IR	Insulin receptor
IRS1	Insulin receptor substrate-1
L3/4/5	Lumbar vertebra 3/4/5
L3SMI	Skeletal muscle index at the level of the third lumbar vertebra
LAG-3	Lymphocyte activation gene-3
MHC	Major Histocompatibility Complex
MSU	Monosodium urate
mTOR	Mammalian target of rapamycin
MUC1	Mucin-1
NF-κB	Nuclear factor kappa-light-chain-enhancer of activated B cells
NHI	National Health Index
NK	Natural killer cell
NLR	Neutrophil lymphocyte ratio
NLRP	NOD-like receptor protein
NOD	Nucleotide-binding oligomerisation domain-like receptors
OS	Overall survival
PD-1	Programmed death-1
PD-L1	Programmed death ligand-1
PI-3K	Phosphatidylinositol-3 kinase
POUND	Obese mice
PSA	Prostate-specific antigen
RBC	Red blood cell
RHDV	Rabbit haemorrhagic disease virus
RNA	Ribonucleic acid
RPMI	Roswell Park Memorial Institute media
s.c	Subcutaneous
SEM	Standard error of the mean
STAT-3	Signal transducer and activator of transcription-3

surv.VLP	Survivin-VLP
surv.VLP-SS-MUC1	Survivin-VLP + mucin-1
TAA	Tumour-associated antigen
TCR	T-cell receptor
TGF	Tumour growth factor
T_H	T helper cell ($CD4^+$ T-cells)
TIL	Tumour-infiltrating lymphocyte
Tim-3	T-cell immunoglobulin and mucin-domain containing-3
TLR	Toll-like receptor
TME	Tumour microenvironment
TNF	Tumour necrosis factor
Urah$^{Plt2/Plt2}$	Hyperuricemic mice
VEGF	Vascular endothelial growth factor
VFA	Visceral fat area
VLP	Virus-like particle
VP60	Viral protein-60
WBC	White blood cell
WC	Waist circumference

Chapter 1

Introduction

1.1 An overview of cancer

Cancer is a non-communicable disease brought about by changes within cells, resulting in their uncontrolled growth and division. Accumulated mutations of deoxyribonucleic acid (DNA) in these cells means that they have abnormalities in multiple regulatory systems, such as losing their ability to suppress cell division, becoming unresponsive to signals which would otherwise evoke apoptosis (programmed cell death), or over responding to growth factors (1).

Cancer is one of the leading causes of mortality worldwide, and the leading cause of death in New Zealand (2). While frequencies in cancer type differ between geography, income and sex, most deaths attributed to cancer worldwide are from lung, breast, colorectal, stomach and liver cancers (3). Furthermore, the number of new cancer registrations is increasing globally (3). Low-income countries tend to be the most affected, with an expected increase in incidence of more than 80% by 2030. In high-income countries, this rate is expected to increase by 40%. Low-income countries have the greatest burden of cancer for reasons such as reduced resource ability, fewer trained medical personnel, and less implemented cancer prevention strategies. Patients also tend to present at a later stage to a medical professional due to costs, so the disease tends to be more advanced and thus harder to treat (4).

According to the latest published New Zealand Cancer Registry data (2016), breast cancer and colorectal cancer have significant numbers of new registrations in New Zealand (50.7 cases per 100,000, 41 cases per 100,000 respectively). Rates for breast (which almost only affects women) and colorectal cancers are higher in Māori than non-Māori (5).

1.1.1 Breast cancer

Along with lung cancer, breast cancer is the most common cancer globally (3). Invasive ductal carcinoma, which makes up 70-80% of breast cancer cases, is a result of the epithelial cells lining the lactiferous ducts of the breast proliferating. The cells eventually breach the basement membrane and expand into the surrounding tissue, becoming malignant (6). Successful public awareness campaigns in high-income countries have contributed to early detection and subsequent treatment of breast cancer, which has resulted in an estimated 5-year survival of 80%. In contrast, constraints in resources in low-income countries resulting in later detection when the cancer is at a more advanced stage means that the 5-year survival is less than 40% (7).

1.1.2 Colorectal cancer

Adenocarcinoma of the colon accounts for 95% of all colorectal cancers and is the result of an accumulation of acquired genetic and epigenetic changes (8). Together, they result in the formation of polyps from the normal tubular epithelium of the colon, and the polyps into invasive carcinoma (9). Lifestyle choices, such as cigarette smoking, obesity, increased red meat intake and reduced fruit and vegetable intake, have all been shown to be risk factors for colorectal carcinoma (10). The 5-year survival rate of localised colorectal cancer is at 90%, however, as the cancer becomes more widespread this drops significantly.

1.2 The anti-tumour immune response

The immune system, while best known for protecting the body from foreign invaders, is also capable of mounting a response against endogenous tissue. Changes in cancerous cells alert the immune system to recognise and respond to tumours as well. Figure 1 shows this process in a diagrammatic form.

1.2.1 Tumour-associated antigens

Tumour-associated antigens (TAAs) are abnormal proteins expressed in tumour cells which are the result of genetic mutations and dysregulations in genetic transcription. TAAs can be immunogenic and therefore be detected by the immune system, particularly by T-cells. TAAs vary based on the tumour and can form in different ways. Most commonly they can be self-antigens which are normally expressed by the specific type of cell, however, they are expressed in a different location or are abnormally expressed to the point where they become immunogenic. Other forms of TAAs are neoantigens which have had mutations in their structure and differ from the normal version by a few amino acids, antigens produced by oncogenic viruses, oncofoetal proteins such as carcinoembryonic antigen (CEA), or tumour-specific antigens which are expressed only by the tumour and are often crucial to the malignancy of the tumour itself (11).

TAAs can be taken up and presented by antigen-presenting cells (APCs) in several ways. Cytoplasmic proteins can be ubiquitinated, which marks the protein for degradation in the proteasome, and subsequently presented on the surface of the tumour cells on Major Histocompatibility Complex (MHC)-I molecules (11). Another common way TAAs can stimulate the immune system is by being released into the extracellular environment. Tumour cells lose the regulation of a controlled death, so they die via a necrotic process (12). In this process, antigens from the tumour are released and consequently phagocytosed by APCs, most commonly immature dendritic cells (DCs), and presented on both MHC class I and II (13).

1.2.2 Processing of TAAs by dendritic cells (DCs)

DCs are APCs that exist in an immature state in most tissues. When tumour cells necrotise, danger associated molecular patterns (DAMPs), such as heat shock proteins and calreticulin (among others), and immunostimulatory signals are released. DAMPs

bind to pattern recognition receptors such as toll-like receptors (TLRs) on or within DCs and stimulate the DC to become activated (14). Phagocytosis of TAAs results in the presentation of peptide fragments on MHC-II, where extracellular peptides are presented. Extracellular peptides can also be displayed on MHC-I molecules through a process called cross-presentation. This occurs in DCs, where exogenous antigens are internalised first and then processed and presented on MHC-I molecules (15). Once presentation on MHC molecules has occurred and DCs are activated, they are able to migrate to the tumour-draining lymph node. There DCs interact with, and present TAAs to, T-cells via MHC class I and II (16).

1.2.3 Activation of the adaptive immune system

The activation of naïve T-cells is crucial for the induction of an anti-tumour response. This occurs when the antigen-MHC complex binds to the T-cell receptor (TCR), which recognises the particular peptide. Depending on whether this cell is a cluster of differentiation (CD)4^+ or $CD8^+$ origin, the CD4 or CD8 co-receptor will also bind to the MHC complex. Co-stimulation via CD80/86 receptors on DCs, which bind to CD28 on naïve T-cells, provides the second signal required for activation, differentiation and proliferation of T-cells into millions of clones (17). Cytokines make up a third signal, and determine the differentiation pathway of T-cells into different types of effector cells (18).

1.2.4 T cells and the effector response

There are two basic types of effector T-cells, $CD8^+$ cytotoxic T lymphocytes (CTLs) and $CD4^+$ T helper cells (T_H cells). They differ in how they recognise and respond to antigens and therefore have different roles in the anti-tumour response.

$CD4^+$ T-cells recognise antigens presented on MHC-II molecules. Most solid tumour cells lack MHC-II on their surface, resulting in activated $CD4^+$ T cells being unable to directly recognise the tumour cells (19). $CD4^+$ T-cells are the first effector cells activated by DCs in lymph nodes and most of their action is through helping prime CTLs. Numerous mouse studies have shown that this occurs through $CD4^+$ T-cells 'licensing' lymph node-resident DCs through CD40/CD40 ligand interaction. This causes the upregulation of signals such as CD80/86 and the release of interferon (IFN)γ and tumour necrosis factor (TNF)-α, which increase the activation and differentiation of $CD8^+$ T-cells (20). $CD4^+$ T-cells, particularly T_H1 cells are able to help the effector CTL response by releasing cytokines at the tumour site. The release of IFNγ causes an upregulation of MHC-I molecules on tumour cells, facilitating enhanced T-cell recognition (15, 21). IFNγ also helps to increase the production of ligands for CXC chemokine receptor (CXCR)3, which is upregulated on T_H1 and $CD8^+$ T-cells and is important in the migration of T-cells to the tumour site (22).

The other type of effector cell, $CD8^+$ T-cells, recognise antigens presented on MHC-I molecules which is present on all nucleated cells, including malignant cells (23). Once activated, CTLs leave the lymph node and scan peripheral tissue in order to find target cells (24). When CTLs recognise a target cell through binding of the peptide-MHC-I complex, there are two main methods through which they can kill the target cells. Firstly, binding of the Fas ligand on the surface of CTLs to the Fas receptor on the target cell triggers apoptosis via the classical caspase cascade. Secondly, CTLs release granules containing perforins and granzymes directly into the intercellular space, which induce apoptosis of the target cell (15). Pro-inflammatory cytokines also play a smaller role, mainly TNF-α and IFNγ (23). TNF-α causes amplification of the pro-inflammatory response, increasing the release of chemokines and cytokines, while IFNγ acts as a

chemoattractant, upregulates MHC-I, increases T_H1 polarisation, and may promote target cell death directly (25, 26).

1.2.5 Memory T-cells

Another important component in the anti-tumour response is the creation of memory $CD8^+$ T-cells (27). During the rapid expansion of effector T-cells, a small subset of these cells forms a memory $CD8^+$ T-cell population and are capable of persistent long-term survival through the actions of IL-7 (upregulates the anti-apoptotic protein B-cell lymphoma (Bcl)-2, promoting survival) and IL-15 (a potent inducer of proliferation independently of antigen) (28). $CD4^+$ T-cell help is required for the differentiation of $CD8^+$ T-cells into memory T-cells, provided through the secretion of IL-2. $CD4^+$ T-cells are also involved in the maintenance of the memory T-cell population, although the mechanism is not yet known (29). Memory T-cells are important as they reside throughout the body and can be rapidly reactivated when re-encountering a small amount of antigen, including re-expressing effector molecules (27).

1.2.6 Immune checkpoint molecules

In order to regulate this system, there are certain molecules which are activated and have either a stimulatory or inhibitory effect. Stimulatory molecules include receptors already discussed, such as CD28 and CD40. There are several inhibitory molecules however which play an important role in self-tolerance by preventing the immune system from becoming overactive (30).

The stimulation of CD28 on naïve T-cells during activation by DCs also triggers the production of the checkpoint molecule Cytotoxic T-lymphocyte-associated Protein (CTLA)-4. This molecule has a greater binding affinity with CD80/86 than CD28, thus acts as a competitive inhibitor by blocking a key part of T-cell stimulation. Some

evidence suggests that this binding may even produce inhibiting signals as well, further counteracting CD28-CD80/86 and TCR-MHC binding (30). The relative levels of CD28 to CTLA-4 production therefore determines whether T-cell stimulation and proliferation occur.

Another inhibitory checkpoint molecule is Programmed Death (PD)-1. This is expressed on the surface of T-cells, B-cells and Natural Killer (NK) cells, and binds to Programmed Death Ligand (PD-L)-1 and 2, which is upregulated on the surface of a wide variety of both immune and non-immune cells, including tumour cells (30). The binding of PD-1 to its ligand causes similar effects as CTLA-4, inhibiting T-cell proliferation, reducing T-cell survival, and reducing the production of key cytokines such as IFNγ and TNFα. The key difference between these two molecules occurs around where in the T-cell response cycle they have their effect. CTLA-4 functions during the priming of the adaptive immune system, while PD-1 has its effect during the effector response (30).

Other inhibitory immune checkpoint molecules include lymphocyte activation gene (LAG)-3 (effects progression of the cell cycle) and T-cell immunoglobulin and mucin-domain containing (Tim)-3, which inhibits the expression of cytokines such as TNF and IFNγ (31, 32). These are both present on the surface of T-cells.

1.2.7 Tumour-infiltrating lymphocytes

Tumour-infiltrating lymphocytes (TILs) are lymphocytes which have migrated into the tumour mass and surround or oppose the tumour cells (33). They play an important role within the tumour microenvironment, either targeting tumours cells through the process above or inducing immunosuppression as talked about in section 1.3.2 (34).

1.2.7.1 T-cell exhaustion

Cancer is a chronic condition, so T-cells located within tumours have been shown to convert to an exhausted state due to prolonged antigen stimulation (35). This involves a decreased ability to cause an effector response, resulting in poorer control over cancers. Eventually, there is a depletion of antigen-specific T-cells (32). A hallmark of T-cell exhaustion is an increased expression of cell surface inhibitory receptors, including the upregulation of several immune checkpoint molecules such as PD-1, Tim-3 and LAG-3 (32).

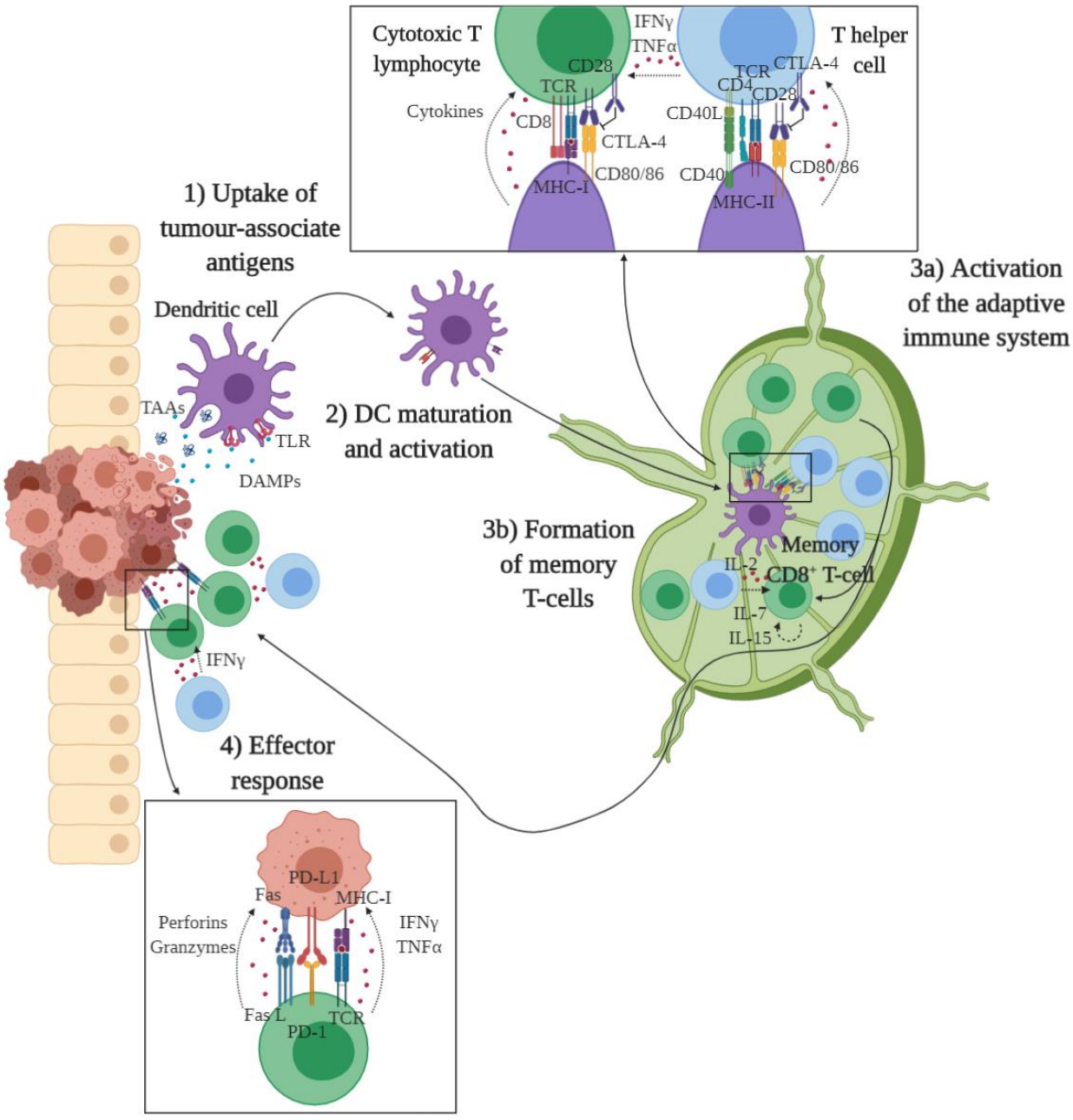

Figure 1: Overview of the anti-tumour immune response

TAAs and DAMPs are released from dying tumour cells and phagocytosed by nearby DCs. This causes activation and maturation of DCs, which present antigens on both MHC-I and MHC-II. DCs then migrate to local lymph nodes where they activate naïve T-cells via interaction with MHC and TCR. MHC-I binds to the TCR-CD8 complex while MHC-II binds to the TCR-CD4 complex. CD28-CD80/86 interaction and the release of cytokines provide further signals for activation. Activated T_H cells bind CD40 ligand to CD40 on DCs, causing the release of IFNγ and TNFα which helps activate cytotoxic T lymphocytes. Once activated, the T-cells multiply and migrate to the site of the tumour where CTLs locate tumour cells by binding to MHC-I and initiates tumour killing via several mechanisms. T_H cells increase the immune response by releasing IFNγ, stimulating CTLs.

Diagram made with *biorender.com*.

1.3 Tumour-induced immunosuppression

Ideally, the process outlined above would lead to the destruction of almost all tumours. However, tumour cells which can evade the immune system are selected through the process of tumorigenesis.

1.3.1 Downregulated MHC expression

One of the key ways that malignant cells are able to escape the immune system is by having reduced expression of the MHC-I molecule on the plasma membrane via epigenetic silencing (36). This results in CTLs being unable to recognise the tumour cells as foreign and prevents them from carrying out their effector role (37). In doing so, however, this makes tumour cells susceptible to killing by NK cells, which target cells with low levels of MHC-I. One of the main driving pressures for the selection process against MHC-I positive tumour cells is the interaction with $CD8^+$ T-cells themselves, as they are able to successfully recognise and kill off most tumour cells in the early stages of tumour development (38). The remaining tumour cells, which are able to proliferate, tend to be from MHC-I negative predecessors, resulting in a population which has significant numbers of tumour cells that are deficient in this receptor (38). It is thought that the downregulation of MHC-I molecules reduces the efficacy of immunotherapy interventions (38). However, many cancers with MHC-I deficiency can be stimulated to express MHC-I molecules by mimicking T_H1 cytokine release, such as IFNγ (38). However, around 30-40% of cancers with MHC-I downregulation are unable to be stimulated and so the use of gene therapy or T-cells that specifically recognise low MHC-I expression may be a potential therapeutic approach (38).

1.3.2 Tumour microenvironment

Various elements of the tumour microenvironment (TME) inhibits the immune system indirectly. The environment can be hypoxic, which inhibits TCR and CD28-mediated activation of lymphocytes (39). Furthermore, the poor vasculature created during angiogenesis, low extracellular pH and low glucose concentration found in some tumours are thought to affect T-cell movement, infiltration of the tumour, and function (36).

The TME can also actively hinder immune surveillance and the immune response. Myeloid-derived suppressor cells, tumour associated macrophages and regulatory T-cells (a type of $CD4^+$ T-cell) can be resident at the tumour site. These cells release cytokines such as tumour growth factor (TGF)-β and IL-10, which are immunosuppressive. They act by regulating lymphocyte proliferation and inhibiting the ability of DCs and macrophages to stimulate $CD4^+$ T-cells respectively (40-42). Furthermore, tumour-associated macrophages inhibit T-cell activation and also cause apoptosis of activated T-cells. This significantly reduces the amount of lymphocytes that infiltrate the tumour tissue, reducing the effectiveness of the anti-tumour response.

1.4 Current cancer treatments

The standard treatments for cancer are surgical resection, chemotherapy and radiation therapy. Depending on the type of cancer, combination therapy can be effective at slowing the progression of disease and may be curative. However, while these therapies are designed to target cancer cells by targeting rapidly dividing cells, they are not specific for them and significant adverse side effects are common (43).

In light of the significant side effects and in an attempt to increase the curative success of treatment, research has moved into new types of more targeted therapies, including immunotherapy.

1.5 Cancer immunotherapy

Immunotherapy is an up-and-coming approach to cancer treatment. This technique aims to provide either passive or active immunity against cancers by stimulating the immune system to specifically target tumour cells. The formation of a memory response against these cells is then able to prevent a reoccurrence of the tumour (44). Due to its specificity, it may also be a way of avoiding some of the side effects of chemotherapy and radiation therapy (45). In the past twenty years, there have been a significant number of proof-of-concept trials as well as clinical studies, which have shown that this is a promising approach. There are several types of immunotherapy being developed, including cancer vaccinations, adoptive cell transfer therapy, and immune checkpoint blockade (45).

1.5.1 Cancer vaccines

One form of immunotherapy that has shown to be promising is a cancer vaccine. It is an active immunotherapy that induces a specific immune response to TAAs already present in the patient's body by presenting one or more antigens to APCs and triggering an immune response (46). Viral vectors are used in the Young laboratory, however, a brief description of the other forms of cancer vaccines currently under development will also be given.

1.5.1.1 Viral vector vaccines

This involves using a viral vector to deliver TAAs. The immune system has evolved to deal with viruses effectively, so a strong and durable response can be stimulated. A disadvantage, however, is that repeat vaccination is limited due to the anti-viral response neutralising the vector. To avoid this, different vector types can be used for repeat administrations. The PROSTVAC-VF/Tricom vaccine for prostate cancer involves using Prostate-Specific Antigen (PSA) first with a vaccinia virus, followed by booster vaccines

using a Fowlpox virus (47). In stage II trials the vaccine resulted in a 10 month increased overall survival time, however in a larger stage III trial this finding was not replicated (47, 48).

Another way that viruses can be used is through virus-like particles (VLPs). This involves using the capsid (outer layer) proteins of a virus as a form of vehicle to insert the desired TAA into the body where it can then be expressed and used to activate the immune system. Insect, yeast or mammalian cells are used to express the VLPs as they are able to perform post-translational modifications, unlike bacterial cells (49). As they do not contain any viral genetic material, VLPs are non-replicative and non-infectious, therefore enhancing their safety profile. Once injected, VLPs are taken up by APCs (mainly DCs), broken down and the tumour antigen is displayed on MHC-I and -II, where it can activate $CD4^+$ and $CD8^+$ T-cells, as well as B-cells. T_H1 responses are desired to get efficient activation of CTLs (49).

The Rabbit Haemorrhagic Disease Virus (RHDV) is a virus framework for VLPs used in the Young laboratory. This is a non-enveloped virus from the *Caliciviridae* family and causes rabbit haemorrhagic disease in European rabbits. As it is an animal virus, it has been selected for therapeutic use because humans will not have any pre-existing immunity against the virus, which would render the vaccine invalid and is one of the problems with viral vaccines (50). The capsid of this virus is made up of 90 arch-like dimers, forming 32 cup-shaped depressions in a T=3 icosahedron which is 35-40 nm in diameter. By using the viral capsid proteins (180 copies of viral protein (VP)60), the RHDV VLP spontaneously assembles devoid of ribonucleic acid (RNA) (51). TAAs can then either be incorporated into the virus via genetic engineering or be conjugated onto the capsid itself. Studies working to optimise this technique have found that the addition of a processing linker between the VP60 gene and the C-terminus of the epitope to

prevent the epitopes from hindering VLP assembly enhances T-cell activation (52). Furthermore, mannosylation with a dimannoside has been shown to provide around 270 mannose groups onto the surface of each VLP particle. This significantly increases uptake by providing a second route of internalisation mediated by a mannose receptor-mediated pathway, in murine DCs, macrophages and B-cells as well as human DCs and macrophages (53). Dimannosylation significantly decreases tumour growth and increases murine survival (52).

The RHDV VLP has been modified to contain the survivin epitope. Survivin is a member of the Inhibitor of Apoptosis protein family and is upregulated in a variety of cancers, playing an important role in inhibiting apoptosis and promoting angiogenesis (54). Furthermore, while present in embryological structures, it is absent in most normal tissues, which makes it a good target for cancer therapies (55). In this project, the survivin-VLP (surv.VLP) was used for models of colorectal cancer. For breast cancer models, the mucin-1 (MUC1) protein was conjugated onto the VLP surface via a double sulphide bond (surv.VLP-SS-MUC1), which corresponds to the MUC1 antigen on the C57mg.MUC1 cell line and is overexpressed in a variety of human cancers (56) (Figure 2). Cytosine-phosphate guanosine (CpG) was added to the VLP solution before injection. It has an affinity for the VLP and conjugates to it naturally, acting as a vaccine adjuvant by enhancing the function of professional APCs and boosting the immune response (57, 58).

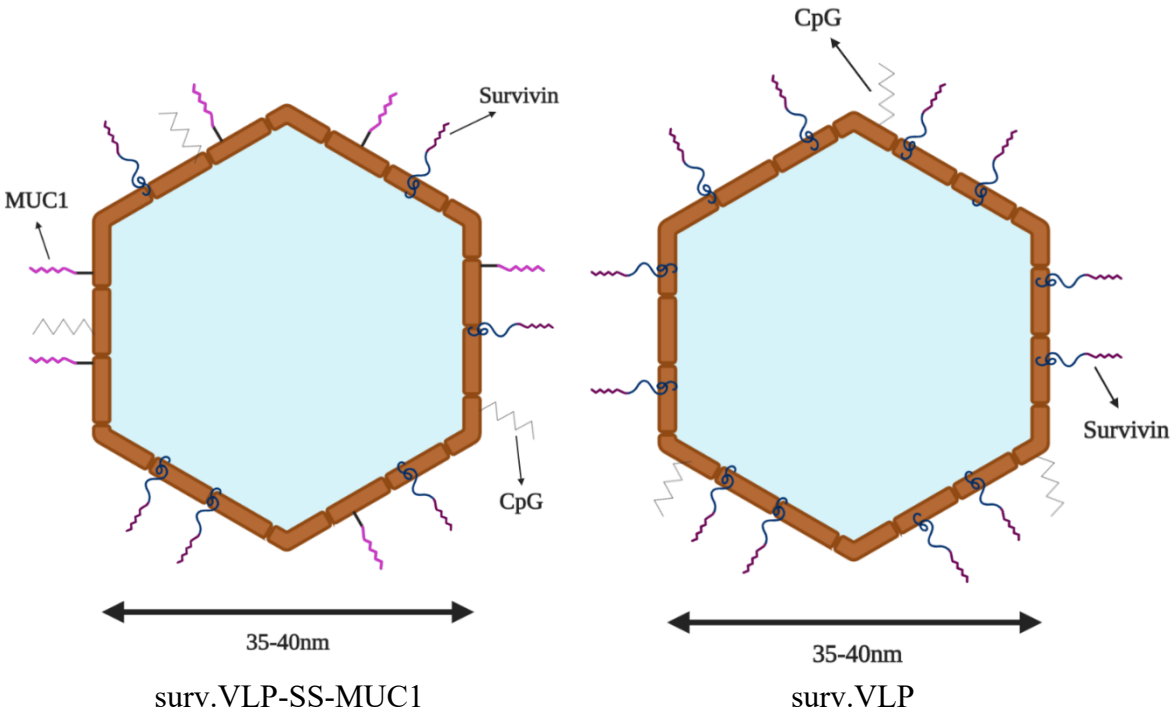

Figure 2: Simplified VLP construct

The RHDV VLP is formed from 180 copies of the capsid protein VP60 and has a diameter of 35-40nm. The survivin epitope is recombinantly inserted into the VP60 gene and is expressed on the outer surface of the VLP. The MUC1 peptide is then conjugated onto the surface of the VLP as well. Before injecting, CpG is added to the VLP solution and naturally conjugates onto the surface as well.

Diagram created with *biorender.com*

1.5.1.2 Autologous tumour cells

This method involves generating a vaccine using whole tumour cells obtained from the patient's tumour. These are used in combination with adjuvants, cytokines, chemokines or co-stimulatory molecules. This type of vaccine has the advantage of containing a wide spectrum of antigens and cells, maximising the amount of tumour cells that can be targeted and reducing the need to specify a target antigen for treatment (47). However, the patient's tumour may not be accessible or a sufficient amount may not be able to be taken in order to prepare the vaccine. Furthermore, it can be expensive and time-consuming to prepare these patient-specific vaccines (59). A variation of this is using allogeneic cells, which are derived from tumour cell lines instead of the patient's tumour. An example of a vaccine produced using this technique is the GVAX vaccine. This vaccine is composed of killed whole tumour cells that have been genetically modified to secrete granulocyte-macrophage colony-stimulating factor (GM-CSF). This acts as a potent immunostimulatory cytokine and promotes antigen presentation, and survival and activation of DCs. This vaccine was successful in murine models, however, it showed limited efficacy in clinical trials where it has been used against prostate cancer, melanoma, pancreatic cancer, and lung cancer (47).

1.5.1.3 Peptide and protein vaccines

This involves administering peptide sequences or whole proteins from TAAs. Adjuvants are also used to maximise the immune response. Examples of adjuvants used in this context are immune checkpoint inhibitors, costimulatory molecules activators, and TLR ligands (45). While preclinical studies have found that peptides are able to successfully stimulate specific T-cell responses, significant benefit has not been found in clinical trials (47). A problem with this technique is that often single, short peptides are used as

antigens, however, these do not activate $CD4^+$ T-cells as they can bind directly to MHC-I. This results in an incomplete CTL response (47).

1.5.1.4 DC vaccination

A greater understanding of DC biology has led to the development of this technique. Here, patient-derived DCs are either loaded or transfected with peptide antigen *ex vivo*. Sipuleucel-T (Provenge) was the first US Food and Drug Administration-approved cancer vaccine and is generated using patient-derived DCs and activating them with GM-CSF fused to the Prostatic Acid Phosphatase antigen. It is approved for use in castration-resistant prostate cancer. Unfortunately, the price and complexity of producing this vaccine have been major drawbacks for widespread use (60).

1.5.2 Immune checkpoint blockade

Advanced cancers can reduce the efficacy of cancer vaccines through inducing immunosuppression. Combination therapy with an immune checkpoint blockade has been shown to result in improved efficacy (61). As discussed previously, immune checkpoints are inhibitory signals which are important to prevent over-activation of the immune system resulting in an auto-immune response. It has been shown that tumours upregulate these molecules in order to evade immune recognition. The first immune checkpoint molecule targeted was CTLA-4, with two humanised antibodies being clinically tested in 2000. Ipilimumab was approved by the FDA in 2010 for the treatment of advanced melanoma. Another checkpoint inhibitor, PD-1, can be blocked enabling T-cells specific for the cancer antigen to be activated. This will enhance the anti-tumour response, resulting in tumour regression (62). Therapies against both PD-1 and PD-L1, as well as CTLA-4 against melanoma and non-small-cell lung carcinoma, have shown success, and trials for these treatments against other types of cancer are underway (63).

Another way that some immune checkpoint monoclonal antibodies mediate tumour killing is by activating antibody-dependent cellular cytotoxicity (ADCC). An example of a drug that works in this fashion is Avelumab, which is an Immunoglobulin (Ig)G1 anti-PD-L1 inhibitor (64). As well as blocking the interaction between the PD-1 and PD-L1, the IgG component of the antibody which binds to the PD-L1 receptor is able to be recognised by CD16 expressed on NK cells. This enables NK cells to bind to the tumour cells, resulting in the secretion of lytic granules. Similar to the effector function of CTLs, this involves the release of molecules such as perforins and granzymes, which results in tumour cell death (65).

1.5.3 Adoptive cell transfer therapy

This form of therapy involves isolating TILs from the tumour mass, expanding tumour-specific T-cells with the desired TCR *ex vivo* and then reintroducing them into the body (66). While there have been several significant breakthroughs in this technology, patients must be capable of preparative immune depletion beforehand via chemotherapy or total body irradiation, and some groups of patients do not respond to the therapy. Furthermore, a major challenge is identifying tumour-specific antigens and expanding the appropriate T-cells so as not to cause an autoimmune response (66).

1.6 Metabolic syndrome

Metabolic syndrome is a cluster of disorders which often occur together and put the individual at an increased risk of cardiovascular disease. The main criteria include obesity, hyperglycaemia, hypertension and dyslipidaemia. Hyperuricemia (elevated levels of uric acid) is often included in this list as it is an indicator for diseases such as diabetes mellitus, cardiovascular disease, and chronic renal disease (67).

1.6.1 Obesity

Obesity is caused by an energy imbalance that favours weight gain, resulting in metabolic disturbances causing stress to tissues and ultimately leads to dysfunction (68). A crude measure for obesity is a Body Mass Index (BMI) of 30 or more, however, this is intended to be used as a population measure for epidemiological studies rather than on an individual basis (69).

The New Zealand Health Survey (2017/2018) found that 32% of adults aged 15 and over are obese, which is an increase of 5% since the 2006/2007 survey. This is higher in Māori and Pacific adults, being 47% and 65% respectively (70). This health problem also affects the younger population, with 12% of children being obese, increasing to 17% of Māori children and 30% of Pacific children. For both adults and children, areas with greater rates of deprivation have higher rates of obesity (70).

The increasing prevalence of obesity has resulted in increased morbidity and years of life lost due to cardiovascular disease, type-2 diabetes mellitus, osteoarthritis, psychological problems and obesity-related cancers (71). Reports from the World Cancer Research Fund and the International Agency for Research into Cancer have found that several types of cancer are associated with obesity, specifically endometrial, oesophageal adenocarcinoma, colorectal, breast cancer in postmenopausal women, prostate and renal cancers. Overall, the number of cases of cancer estimated to be caused by obesity is 20% and obesity is the second highest risk factor for cancer, after tobacco smoking (72). Furthermore, studies have found that obesity leads to poorer cancer treatment efficacy and greater mortality from cancer (72-75).

1.6.2 Sarcopenia

While obesity has been strongly linked to many pathologies, muscle mass is another body composition factor which is important to consider. Sarcopenia is the reduction in muscle mass as well as the quality of muscle fibres, resulting in increased frailty as muscle function deteriorates (76). While it is mostly associated with ageing, sarcopenia has been linked to chronic diseases such as chronic obstructive pulmonary disease and cancer (77).

1.6.3 Hyperuricemia

Uric acid is derived in the body by the oxidation of xanthine by xanthine oxidase as part of the breakdown of purines (78). A systematic review published in 2015 reports the prevalence of hyperuricemia (generally described as uric acid levels equal to or above 7.0 mg/dL in men or 6.0 mg/dL in women) as 8% in non-Māori and 17-19% in Māori. Data on the prevalence of hyperuricemia in the Pacific population is not available, however, in Samoa, the rate is 33% (79, 80). Diet is not considered a significant factor for causing hyperuricemia directly, with a purine-rich diet (specifically meat and seafood) only resulting in a 1-2 mg/dL increase in uric acid (79, 81). However, high waist circumference and increased BMI are associated with higher leptin production and greater rates of insulin resistance. Both of these factors have been found to reduce renal uric acid excretion, therefore increasing the concentration of uric acid (79).

Hyperuricemia can lead to gout and nephrolithiasis. It is an independent risk factor for coronary heart disease, stroke and type-2 diabetes mellitus (80, 82). Data from multiple studies have found that elevated soluble uric acid levels are independently associated with an increased risk of all site cancer incidence (83). Furthermore, conditions associated with hyperuricemia such as gout, metabolic syndrome, type-2 diabetes mellitus, insulin resistance and obesity have all been found to result in increased risk and incidence of cancer in large epidemiological studies. Patients who are hyperuricemic at

the time of diagnosis of colorectal cancer may be more likely to lose weight and have liver metastases (84).

1.7 The link between metabolic syndrome and cancer

1.7.1 Insulin resistance

Excess caloric intake has been shown to promote cancer cell proliferation and tumour progression (73). Insulin resistance is common in cases of excess adiposity. To compensate for this and maintain homeostatic control, insulin secretion by pancreatic β-cells is upregulated, resulting in hyperinsulinemia. This state has been shown to increase the growth and aggressiveness of obesity-associated cancers (73). Insulin signalling via the insulin receptor is linked to the extracellular-signal-regulated kinase and phosphatidylinositol-3 kinase (PI-3K) pathways. Both of these pathways are involved in the control of motility, proliferation, and survival of cancer cells. It is conceivable that hyperinsulinemia activates these pathways, resulting in cancer progression.

The PI3K pathway is also dysregulated due to an increase in neutrophils in white adipose tissue in obesity, promoting the proliferation of epithelial cells which can then become cancerous. Neutrophils produce neutrophil elastase, which cleaves insulin receptor substrate 1 (IRS1). This prevents it from binding to PI3K, thus causing issues in insulin-mediated signalling downstream of the insulin receptor (IR). This leads to insulin resistance. Changes in this pathway are one of the most common oncogenic events causing cancer (85).

Another mechanism through which hyperinsulinemia facilitates oncogenesis is the similarities in shape of insulin and insulin-like growth factor (IGF)-1. As a result, they are both able to bind to the IR and the IGF-1 receptor (IGF-1R) (86). Cell migration

resulting in increased tumour invasion can be induced through the activation of IGF-1R kinase as it causes the loss of epithelial cell integrity (87).

Furthermore, the increase of insulin in the portal circulation due to hyperinsulinemia causes the upregulation of the growth hormone receptor (GHR). This results in increased GHR signalling, causing an increase in the synthesis of IGF-1 (88). Free IGF-1 is also more available as insulin decreases the hepatic expression of binding proteins of IGF-1 (89). Increased visceral adipose tissue causes the reduction of IGF binding protein 3, which is the most abundant of the IGF binding proteins. This protein also has an independent role in preventing cancer by inducing apoptosis via tumour protein p53 and Bcl-2 mechanisms (88). IGF-1 causes angiogenesis and induces the synthesis of hypoxia-inducible factor 1a (HIF-1a). Along with vascular endothelial growth factor (VEGF), this leads to neovascularisation and metastases. IGF-1 also inhibits p53 thus preventing apoptosis and inducing metastatic spread (73). IGF-2, which binds to IR and IGF-1R, is overexpressed in this state and leads to tumour development through similar mechanisms.

1.7.2 Sex hormones

Excess weight leads to an increase in endogenous sex hormones. Increased levels of circulating hormones such as dehydroepiandrosterone (DHEA), testosterone, oestrone and oestradiol is linked to increased risk of breast cancer in postmenopausal women (90). These hormones are active in tumour sites, particularly endometrial and breast tumours due to the hormone-dependent nature of these types of cancer. Evidence from several studies suggests that oestrogens are mitogenic, induce DNA damage via free radicals, cause genetic instability and mutations, and regulate the expression of IRS1 in breast

tissue (73). Furthermore, increased oestradiol concentration in the plasma causes endometrial proliferation, inhibits apoptosis, and promotes IGF-1 synthesis (91).

1.7.3 Adipokines

In an obese state, there is over-secretion of deleterious adipokines from adipose tissue such as IL-6, TNFα and leptin, and under-secretion of beneficial adipokines like adiponectin (92). High levels of leptin, which normally acts to suppress food intake, can promote mitosis and is pro-inflammatory, anti-apoptotic and pro-angiogenic by synergistically acting with VEGF (93, 94). Prostate, colon, and breast cancers have all been associated with an increase in leptin concentration (95). Leptin also upregulates oestrogen signalling and production and is therefore implicated in breast and endometrial cancer. (96)

Adiponectin, which is downregulated in the obese state, has a protective role in carcinogenesis and is negatively correlated with cancer development (97). Low levels of adiponectin are associated with high levels of soluble uric acid, and high levels of uric acid reduce levels of adiponectin (83). This protective effect occurs by preventing insulin resistance, as well as activating the 5'-AMP-activated protein kinase (AMPK) pathway, which inhibits the mammalian target of rapamycin (mTOR). Activation of mTOR is associated with cell growth and proliferation and has been associated with prostate, ovarian, colon, breast, lung and liver cancer progression (98). Furthermore, adiponectin induces p53 and Bax expression and decreases Bcl-2 expression, thus stimulating apoptosis. It also has an anti-inflammatory role and reduces tumour spread by downregulating vascular adhesion molecules, angiogenesis and cell migration (99, 100).

1.7.4 Upregulation of the PD-1/PD-L1 pathway

Obesity limits the anti-tumour immune response by upregulating the immune checkpoint molecule PD-1 (101). With elevated levels of leptin in obesity, signal transducer and activator of transcription (STAT)3, a major downstream transcription factor of the leptin receptor, is upregulated and binds to transcription sites in the promoter region of PD-1, increasing transcription and subsequent expression (101). It is hypothesised that this change is an attempt to keep inflammation in check during weight gain. However, in the context of a tumour, it impairs the ability of CTLs to effectively destroy cancer cells (see section 1.2.6), thus limiting the immune response and accelerating tumour onset and progression (85, 101).

1.7.5 The effect of body composition on cancer prognosis

When it comes to the effect of obesity on outcomes after the diagnosis of cancer, the literature is incomplete and conflicting. On the one hand, difficulties have been reported when treating obese patients. Many obese patients do not receive the appropriate dose intensity of chemotherapy, due to concerns about the risk of toxicity with increasing dosage (102). However, several analyses have shown that the risk of short-term or long-term adverse side effects does not increase when giving an obese person the correct dosing compared to a lean person (103). Considering that for most agents a reduction of 20% in dose makes tumour regrowth more likely and can cause decreased remission and cure rates, this is a potentially harmful practice (102). A review of radiation therapy has determined that obesity may have a high impact on how successful the surgery and subsequent radiation therapy is. This includes factors like an increased difficulty of performing the treatment, as well as having to increase the size of the margins due to possible malpositioning, which results in an increased risk of side effects (104).

Interestingly, patients who are classified as high-normal weight to overweight (BMI of 23-30) at the time of stage I-III colorectal cancer diagnosis have been shown to have reduced all-cause mortality, with overweight patients consistently having the best prognosis (105). Underweight (BMI <18.5) and significantly obese (BMI >35) patients have the highest risks. A separate study supports this, showing a trend towards overweight patients having increased survival six months after cancer diagnosis compared to normal-weight patients with stage II colorectal cancer. In stage III and IV colorectal cancer, underweight patients demonstrated a significant disadvantage (106).

However, although there have been many observations of what has been coined the 'obesity paradox', one review found several errors in these studies, including different forms of bias, confounding, and BMI being a crude measure of obesity (107).

When obesity was measured using Computed Tomography (CT) scans to calculate the cross-sectional area of fat, survival rates for non-metastatic breast cancer were decreased with increased adiposity and in patients with sarcopenia. Measurements using CT scans were also more correlated with survival than when using BMI (108). Overall, however, more studies need to be done to see if this effect on survival is consistent.

1.8 The effect of metabolic syndrome on the immune system

1.8.1 Chronic inflammation

A significant way in which obesity can cause cancer is through its effects on the immune system, creating a chronic state of inflammation. With the increased intake of nutrients as seen in obesity and metabolic syndrome, adipose tissue is required to expand to accommodate the influx (68). In adults, adipocyte hypertrophy is favoured over hyperplasia (109). However, these hypertrophic adipocytes induce shear mechanical stress on the extracellular environment and activate endoplasmic reticulum and

mitochondrial stress responses. Overall this results in a pro-inflammatory state within adipose tissue (110).

The persistent state of inflammation and stress in adipose tissue leads to apoptosis of adipocytes. This triggers an infiltration of inflammatory leukocytes, resulting in an increase in macrophage numbers within adipose tissue, which encircle the dead adipocytes to form crown-like structures (CLS) (85, 111). CLS have been found in 50% of patients with breast cancer, and are associated with higher BMI and other systemic markers of metabolic syndrome. The formation of CLS causes the activation of macrophage pattern recognition receptors, such as TLRs (85). As a result, macrophages are polarised towards a pro-inflammatory phenotype as opposed to an anti-inflammatory phenotype that macrophages in healthy adipose tissue have (112).

Both macrophages and hypertrophic adipocytes upregulate secretion of the pro-inflammatory mediators TNFα, IL-6, and monocyte chemoattractant protein-1 (113). These mediators further promote dysfunction, as well as block the production of adiponectin, which has anti-inflammatory effects and promotes insulin sensitivity. Molecules such as TNFα are also pro-angiogenic, and directly support the development of tumours (114). Overall, this results in the development of insulin resistance, increased lipolysis and impaired lipid storage (68). This change to a basal pro-inflammatory state has also been found to be the case in leukocytes circulating in the blood. Peripheral mononuclear cells display greater nuclear factor kappa-light-chain-enhancer of activated B cells (NF-κB) activation, which participates in the regulation of the inflammasome and upregulates pro-inflammatory genes such as those involved in cytokines and chemokines (115).

1.8.2 Lipid deposition in primary lymphoid tissue

Mobilisation of fat stores as a result of increased lipolysis and impaired lipid storage in adipose tissue causes an accumulation of lipids in non-adipose tissue, including lymphoid tissues like bone marrow and the thymus (116). Bone marrow-derived haematopoietic stem cells are continuously replicating in order to maintain lymphoid (T- and B-lymphocytes, NK cells) and myeloid-derived (monocytes, macrophages, dendritic cells, granulocytes, erythrocytes, megakaryocytes, mast cells) lineages of cells (117). Mature T-cells then travel to and undergo further development in the thymus. Both the thymus and bone marrow are considered to be primary lymphoid organs (118). Increased lipid deposits in these tissues disrupt their integrity, altering the environment in which leukocytes develop. In the bone marrow, this suppresses haematopoiesis and skews progenitor populations into producing a greater ratio of myeloid progenitor cells as opposed to lymphoid progenitor cells (119, 120).

In the thymus, changes occur which resemble the natural process of thymic involution that normally occurs with old age (118). This includes a loss of corticomedullary junctions, increased perithymic adiposity, and a reduction in populations of lymphocytic precursor cells (120). These changes result in a reduced thymic output of naïve T-cells, which is likely to negatively affect immune surveillance and therefore increase the likelihood of immune escape of pathogens or tumours (120).

1.8.3 Reduction of T-cell variation

Obesity has been linked to a reduced TCR repertoire of circulating T-cells (110). This reduces the amount of antigens that can be recognised and responded to. Obesity has also been shown to cause a reduction in lymph node size, impair lymphatic fluid transport and migration of DCs to peripheral lymph nodes, and reduce the number of T-cells in the lymph nodes. These changes reduce the ability of the immune system to recognise and

effectively deal with foreign antigens (110). Furthermore, the expansion of adipocytes caused by obesity suppresses anti-inflammatory pathways, enabling DCs and T-cells to become activated within visceral white adipose tissue. However, constant presentation of antigen by DCs may eventually lead to T-cell exhaustion and chronic inflammation, reducing the capability for T-cells to have a successful effector response (85).

1.8.4 Uric acid

Uric acid in its soluble state is not currently known to have any immunogenic properties. However, when crystallised, it can modulate the immune system by acting as a DAMP following cell death, although it is not involved in pathogen-related inflammation (121). The intracellular environment has a high concentration of soluble uric acid as a result of purine catabolism. Furthermore, after cell death, there is an increase in the production of uric acid via xanthine oxidase following DNA and RNA degradation. This results in a high concentration of uric acid being released into the extracellular fluid when a cell dies, often exceeding saturation point (higher than 6.8 mg/dL). The elevated concentration of sodium in the extracellular environment then promotes the crystallisation of soluble uric acid into monosodium urate (MSU) (121).

MSU can stimulate the immune system in different ways. Firstly, it can enhance the activation of DCs by upregulating the costimulatory molecules CD80/86. MSU has been used as an adjuvant in DC vaccinations to successfully increase the generation of CTLs (122). It is also known to stimulate monocytes to produce inflammatory mediators (123). Finally, MSU has been shown to trigger IL-1β mediated inflammation through activating the nucleotide-binding oligomerisation domain-like receptors (NOD)-like receptor protein (NLRP)3 inflammasome (124). IL-1β plays an important role in systemic

inflammation, promotes neutrophil infiltration, and supports tissue restructuring. It is also necessary for the efficient priming of T-cells (125).

1.9 The effect of metabolic syndrome on immunotherapies

The vast majority of studies trialling immunotherapy techniques use healthy, lean mice as models, and studies looking at the interaction between obesity and cancer immunotherapy are lacking. There are very few studies which use hyperuricemic mice as models. However, given the effects of obesity and hyperuricemia on the immune system, it is hypothesised that an immune-based therapy would not be as efficacious. One group has found that the administration of immunotherapy into *ob/ob* mice (which are obese due to being leptin-deficient) compared to lean mice resulted in high levels of TNFα, leading to multiorgan pathological responses and rapid lethality. This has been attributed to the baseline level of chronic inflammation found in obese mice (126).

A higher BMI has been shown to be correlated with a greater decline in influenza antibody titres 12 months following vaccination compared to healthy weight individuals. Furthermore, the obese individuals had decreased CTL activation as well as decreased expression of functional proteins, both contributing to a decreased immune response to the influenza virus (127). It has also been found that obesity increases the risk of failure of other types of vaccines, such as hepatitis B and tetanus (110). Furthermore, DC-based immunotherapy in mice with renal cell carcinoma showed regression in lean mice but was ineffective in diet-induced obese (DIO) mice. Further investigation found that there was an increase in regulatory DCs in the tumour-bearing kidneys and decreased local infiltration of CTLs (128).

While these are murine models, they demonstrate the impact of obesity on the immune system. This both reduces the efficacy of cancer vaccines, as well as increases the likelihood of adverse events.

Conversely, melanoma patients who are classified as overweight or obese have been shown to have a better response to anti-PD-1/PD-L1 immune checkpoint inhibitors (129). This finding was also replicated in studies where tumour-bearing mice had an increased response to anti-PD-L1 treatment if they were obese compared to lean. This phenomenon has been postulated to be due to leptin, as increased leptin levels (as seen in obesity) leads to greater expression of PD-1 (130).

Limited research has been performed into the effects of hyperuricemia on immunotherapy. However, one study found that melanoma tumour-bearing hyperuricemic mice ($Urah^{Plt2/Plt2}$ strain) had a reduced response to Poly I:C therapy compared to wild type mice (131). This may have been due to a reduction in the proportion of antigen-specific $CD8^+$ T-cells in these mice. However, they also had a greater number of proliferating antigen-specific T-cells in the lymph nodes compared to wild type mice. The authors of the study hypothesised that the high background rate of division might limit the ability of immunotherapeutic treatments to stimulate an anti-tumour response (131)

1.10 Aims and rationale

Metabolic syndrome is a prevalent and rising problem in our society today. Obesity is a known cause of cancer development and progression and has been shown to impair the treatment of cancer using traditional techniques. Furthermore, limited research has been performed in obese animal models investigating the effect of obesity on cancer

immunotherapy. From the studies that have been done, issues around increased toxicity and reduced efficacy have been highlighted.

A previous student in the Young laboratory found that there may be a more immunosuppressive environment in obese mice compared to lean mice. Hyperuricemia may also impair the activation of the vaccination itself. Following on from this study, it has been proposed to research a VLP-based treatment in lean, obese, and hyperuricemic mice with breast and colorectal cancer. Specifically, aims are to (i) test the efficacy of a standard RHDV VLP vaccine with survivin and MUC1 epitopes in obese and hyperuricemic mice compared to lean mice, and (ii) trial a combination with additional anti-PD-L1 treatment, which has been shown to increase the efficacy of cancer vaccines and may dampen the state of chronic inflammation shown in obesity. Anti-PD-L1 therapies have not previously been trialled in the Young laboratory. To identify any reasons for differences in treatment efficacy observed, TILs will be analysed for the frequency of infiltration into the tumours, as well as the expression of markers of exhaustion.

In order to translate results from the murine studies into the patient setting, a case series descriptive observational study within the Dunedin colorectal cancer cohort will be conducted. This will investigate how obesity and sarcopenia affects 5-year survival following cancer resection surgery, and how markers of inflammation vary between obesity statuses, something which will also be covered in the murine experiments. CT images from the time of diagnosis will be used to determine body composition status, rather than relying on BMI as previous studies have done due to the inaccuracies of this measure to correctly identify fat mass. Visceral adiposity, which is adipose tissue within the abdominal wall, is considered to be a more significant cause of pathologies such as cancer and cardiovascular disease (132). Fat in this compartment surrounds the viscera

and drains its blood supply via the portal system, and so free-fatty acids entering through this route have a more direct effect on the liver than other adipose types (133). Therefore, measuring this may give interesting results.

It is hypothesised that the VLP vaccine alone will be less effective in obese and hyperuricemic mice compared to lean mice, but that an increase in the efficacy of treatment will be observed when combined with an anti-PD-L1 antibody. Based on previous studies, obesity and sarcopenia may cause decreased survival, although overweight patients could have an increased survival rate. This study is important as it will identify any groups that immunotherapy may work differently in, which is especially significant as this technology becomes more widely available.

Chapter 2

Materials and Methods

2.1 Tumour trials

2.1.1 Mice

Male and female specific pathogen-free lean (C57BL/6), obese (C57BL/6NCrl-Leprdb-lb/Crl, referred to as POUND) and hyperuricemic (Urah$^{Plt2/Plt2}$) mice aged between 12-20 weeks old were obtained from the Hercus Taieri Research Unit (HTRU), University of Otago, New Zealand (131, 134). Approval for each experimental protocol was obtained by the University of Otago Animal Ethics Committee before commencement. Approval numbers were DET 17/17 for cell culture work and AUP 18-31 for animal work.

2.1.2 Cell culture

Breast cancer C57mg.MUC1 (Gendler Lab, Mayo Clinic, Phoenix, AZ, USA) or colorectal cancer MC-38 (Vile Lab, Mayo Clinic, MN, USA) cells were grown in large tissue culture flasks in Dulbecco's Modified Eagle Medium (DMEM) (Gibco, Thermo Fisher Scientific, Waltham, MA, USA) + 10% Foetal Calf Serum (FCS) (Moregate Biotech, Bulimba, QLD, Australia) + 150 µg/mL geneticin (G418) (Gibco) or DMEM + 10% FCS respectively (Appendix) (135). At 90% confluency, cells were harvested using a solution of 0.002% ethylenediaminetetraacetic acid (EDTA) (Appendix). The cells were then spun down with 50 mL sterile Dulbecco's phosphate-buffered saline (DPBS) (Appendix) for 5 minutes at 350 x g at 4ºC and washed with DPBS three times. Cells were counted using a 1/20 dilution of 0.4% trypan blue (Appendix) and resuspended in DPBS to attain a concentration of 5 x 10^6 cells/mL (C57mg.MUC1 cells to be injected into POUND and C57BL/6 mice), 5 x 10^7 cells/mL (C57mg.MUC1 cells to be injected into Urah$^{Plt2/Plt2}$ mice) or 6.7 x 10^5 cells/mL (MC-38 cells to be injected into all mouse types). Tumour growth kinetics were performed by a previous laboratory member, who

observed that higher concentrations of C57mg.MUC1 cells were needed in order for adequate tumour growth in Urah$^{Plt2/Plt2}$ mice (136). Molecular subtyping was not performed on the C57mg.MUC1 cells, although MC-38 cells have been shown to be microsatellite instability-high, BRAF^{+} and KRAS^{-} (137).

2.1.3 Tumour grafting

Aliquots of 1 x 10^5 C57mg.MUC1 cells in a volume of 20 µL were injected into the second left mammary fat pad (MFP) of thirty female POUND (in two trials with fifteen mice each due to the availability of mice) and C57BL/6 mice. Thirty female Urah$^{Plt2/Plt2}$ mice received 1 x 10^6 cells. Prior to this, C57BL/6 and Urah$^{Plt2/Plt2}$ mice were injected with a Ketamine/Domitor/Atropine mixture subcutaneously (s.c) for inducing anaesthesia, placed on heat pads and eye ointment applied. POUND mice were not anaesthetised due to safety concerns. Chests were shaved and Nair hair removal cream applied with a cotton bud around the nipple area, and then removed 3 minutes later. Mice were injected with Antisedan s.c for Domitor reversal and monitored until fully awake. Due to a high rate of ulceration in the original fifteen POUND mice, cells in subsequent trials were injected into the left fourth MFP as this was thought to rub along the ground less. Following suspected pathogen contamination of the C57BL/6 mice, the experiment was moved to the Microbiology animal facility and thirty new mice were injected with the same amount of cells in the left fourth MFP.

Aliquots of 1 x 10^5 MC-38 cells in a volume of 150 µL were injected s.c into the left flank of 30 male POUND (two trials of 15 mice each), C57BL/6 and Urah$^{Plt2/Plt2}$ mice. As this was a s.c injection, mice were not required to be anaesthetised.

After injections, mice were monitored daily until tumours were palpable. Mice were then monitored every second day until euthanised. Mice that achieved tumour remission for a

minimum of twenty days were regrafted with the same amount of tumour cells on the opposite side of the body.

2.1.4 Preparation of the virus-like particle (VLP)

The VLP expressing either the survivin and MUC1 epitopes (surv.VLP-SS-MUC1) or survivin alone (surv.VLP) has been described in the previous chapter. Katrin Kramer, a research fellow in the Young laboratory, manufactured the VLP using a previously validated method (138). Particles were checked via Philip CM100 BioTWIN Transmission Electron Microscopy (Philips/FEI Corporation, Eindhoven, Netherlands) and Mass Spectrometry (Centre for Protein Research, Dunedin, New Zealand) to ensure the presence of the relevant epitopes. Before injecting, the VLP concentration was confirmed using a NanoDrop 1000 Spectrophotometer, version 3.1 (Thermo Fisher Scientific) or a Qubit protein assay (Thermo Fisher Scientific). The VLP was diluted in complete PBS (cPBS) (Appendix) to reach a concentration of 0.67 mg/mL (corresponding to 100 µg in 150 µL). CpG ODN 1826 (Integrated DNA Technologies, Coralville, IA, USA) was added at 0.166 mg/mL (corresponding to 25 µg in 150 µL).

2.1.5 Treatment injections during tumour challenges

Once tumours were palpable in all or the majority of mice, mice were distributed into three groups with an average approximately equal tumour size. Group one (PBS control) was injected with 150 µL cPBS s.c + 10 mg/kg anti-PD-L1 isotype control (Bio X Cell, West Lebanon, NH, USA) intraperitoneally (i.p). Group two (VLP only) was injected with 150 µL s.c containing 100 µg surv.VLP-SS-MUC1 (breast cancer) or surv.VLP (colorectal cancer) + 25 µg CpG, + 10 mg/kg anti-PD-L1 isotype control i.p. Group three (VLP + anti-PD-L1) was injected with 150 µL s.c containing 100 µg surv.VLP-SS-MUC1 or surv.VLP + 25 µg CpG, + 10 mg/kg anti-PD-L1 (Bio X Cell) i.p. Mice were

then injected with either the anti-PD-L1 isotype control or anti-PD-L1 at 10 mg/kg i.p three days and six days later. Once tumours had reached 150 mm^2 or ulcerated, mice were euthanised via cervical dislocation and tumours were either preserved for histological staining or tumour-draining lymphocytes (TILs) were prepared for flow cytometric analysis.

2.2 Investigating tumour-infiltrating lymphocytes

2.2.1 Immunohistochemical analysis of tumours

Mice were euthanised, secured on a dissection stage and heavily sprayed with 70% ethanol. Tumours were removed using sterile scissors and tweezers and preserved in formalin (Sigma-Aldrich, St Louis, MO, USA) for 24 hours. Tumours were then kept in 70% absolute ethanol (Lab Supply Ltd, Dunedin, New Zealand) until prepared and stained with Gill's haematoxylin and alcoholic eosin (H&E) (Surgipath, Leica Biosystems, Wetzlar, Germany), and cluster of differentiation (CD)3 antibody (Abcam, Cambridge, UK) at a 1 in 150 dilution, which contained a 3,3′-Diaminobenzidine (DAB) substrate. This was performed by a Medical Laboratory Scientist within the Otago Histology Services Unit. Slides were scanned using Aperio ScanScope slide scanner (Leica Biosystems) and Scanner Console, version 102.0.7.5. Images were loaded onto Aperio ImageScope, version 12.4.0, and exported into TIFF format. Images were further analysed using ImageJ (National Institutes of Health, USA), version 1.52a.

To measure the area of each cross-section, a freehand selection line was drawn around the border of each tumour. Tumours were then split into inner and outer tumour regions, defined by a 250 μm width margin from the outer border. Area measurements were taken at this point. The different components of the histological stain were then separated and the DAB component selected. The image was converted to black-and-white and individual cells defined in order to be able to be read and counted by the software (Figure 3). This process was repeated for whole tumour, inner tumour and outer tumour images.

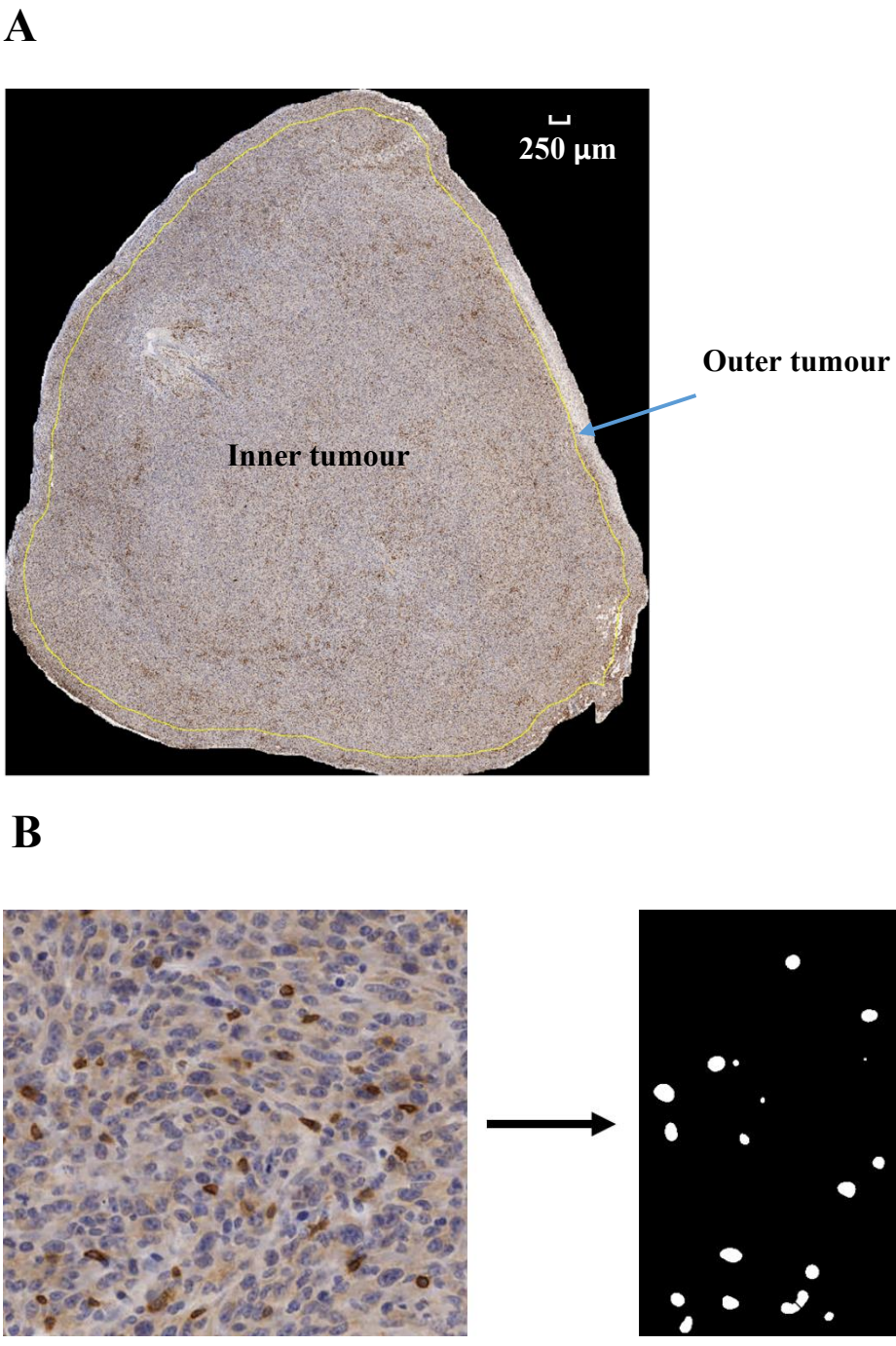

Figure 3: Analysis of CD3 immunohistochemical staining

A) Tumour isolated from the background and split into whole tumour, inner tumour and outer tumour regions

B) $CD3^+$ cells identified and converted into a binary form, allowing for automatic cell counting.

2.2.2 Isolation of Tumour Infiltrating Lymphocytes (TILs)

Mice were euthanised, secured on a dissection stage and heavily sprayed with 70% ethanol. Tumours, spleens and lymph nodes (tumour draining and non-tumour draining) if possible were removed using sterile scissors and tweezers and placed in cold Roswell Park Memorial Institute (RPMI) 1640 + GlutaMAX™ (Gibco) media. To create single-cell suspensions, samples were processed using the plunger from a 5 mL syringe and filtered through a 100 µm strainer followed by a 70 µm strainer. Single-cell suspensions were layered onto Ficoll-Paque™ PLUS (GE Healthcare Bio-Sciences AB, Uppsala, Sweden) using a transfer pipette to isolate the white blood cells and centrifuged for 20 minutes at 800 x g, acceleration 3, brake 0, at 20°C. This technique causes white blood cells to become suspended in an intermediate layer known as the buffy coat, which was transferred into a falcon tube and washed with DPBS. An aliquot of 3 mL warm red blood cell (RBC) lysis buffer (Appendix) was added to the isolated splenocytes for 3 minutes in order to lyse RBCs. Cells were washed with DPBS.

To stain for live cells, samples were stained with 50 µL Zombie Yellow™ viability dye (Table 1) diluted 1/200 in DPBS for 15 minutes in the dark at room temperature. Cells were then washed in 2 mL Fluorescence-Activated Cell Sorting (FACS) buffer (Appendix) and centrifuged for 3 minutes at 350 x g at 4°C. To prevent non-specific staining of antibodies, 50 µL Fc block (Table 1) diluted 1/200 in FACS buffer was added to each sample and incubated for 5 minutes at 4°C. Antibodies against T-cell lineages (CD3, CD4, CD8) and markers of T-cell exhaustion, PD-1, LAG-3, Tim-3, CD127, and CD39 (Table 1) were used to phenotype T-cells. Antibodies diluted in 50 µL FACS buffer were added to the cells and incubated for 15 minutes at 4°C. Cells were then washed with 1 mL FACS buffer and centrifuged for 3 minutes at 350 x g at 4°C. Cells were resuspended in 200 µL FACS buffer and analysed by flow cytometry.

If samples were not to be analysed the same day, cells were incubated in 200 µL 2% paraformaldehyde (Appendix) and incubated for 15 minutes in the dark at room temperature. Samples were washed with 1 mL FACS buffer and centrifuged for 3 minutes at 350 x g at 4°C. Cells were resuspended in 200 µL FACS buffer, covered in Parafilm (Bemis, Neenah, WI, USA) and stored at 4°C.

2.3 Isolation of immune cell populations from the blood of tumour-bearing mice

In order to examine how the immune cell populations in the blood changed over time during treatment, blood from C57BL/6 and POUND mice injected with MC-38 cells was collected. Tails of five mice were tipped and 4-5 drops of blood collected into 1 mL Alsever's solution (to prevent clotting) (Appendix) before injection of tumour cells and before initiation of treatment. The blood of five mice per treatment group was then collected weekly until the end of the trial. Samples were centrifuged for 5 minutes at 350 x g at 4°C. An aliquot of 3 mL RBC lysis buffer was added to the samples and incubated for 2 minutes. Samples were washed two times with DPBS before commencing standard FACS staining procedures as described previously (section 2.2.2). Antibodies against Ly6G, Ly6C, CD11c, B220, CD8, CD4 and CD3 were used (Table 1).

2.4 Flow cytometric analysis

All samples were analysed by flow cytometry using a Gallios™ flow cytometer (Beckman Coulter, Brea, CA, USA). 100,000 events per sample were collected for TIL staining, and at least 10,000 events per sample for blood staining. Data was analysed using Kaluza analysis software (Beckman Coulter, Brea, CA, USA), version 2.1.

Table 1: antibodies used in flow cytometry

Anti-mouse antibodies	Fluorophore	Concentration	Dilution	Clone	Supplier
CD11b	APC	0.2mg/mL	1:400	M1/70	Biolegend
CD11c	PE	0.2mg/mL	1:100	N418	Biolegend
CD127	PE-CF594	0.2mg/mL	1:100	5B/199	BD Biosciences
CD16/32 (FcR Block™)	None	0.5mg/mL	1:200	2.4G2	BD Biosciences
CD223	PE	0.2mg/mL	1:100	C9B7W	BD Biosciences
CD279 (PD-1)	FITC	0.5mg/mL	1:100	29F.1A12	Biolegend
CD279 (PD-1)	PerCP/Cy5.5	0.2mg/mL	1:100	29F.1A12	Biolegend
CD3	BV421	0.2mg/mL	1:200	17A2	Biolegend
CD366	APC	0.2mg/mL	1:100	RMT3-23	Biolegend
CD39	PE/Cy7	0.2mg/mL	1:100	Duha59	Biolegend
CD4	APC-H7	0.2mg/mL	1:200	GK1/5	BD Biosciences
CD45R/B220	PE/Dazzle™594	0.2mg/mL	1:100	RA3-GB2	Biolegend
CD45R/B220	PerCP/Cy5.5	0.2mg/mL	1:100	RA3-6B2	Biolegend
CD8a	AF700	0.5mg/mL	1:200	53-6.7	Biolegend
Live/Dead	Zombie Yellow™		1:200		Biolegend
Ly-6C	PE/Cy7	0.2mg/mL	1:400	HK1.4	Biolegend
Ly-6G	FITC	0.5mg/mL	1:200	1A8	BD Biosciences

2.5 Descriptive observational study: the effect of body composition on cancer outcomes

2.5.1 Inclusion criteria

Patients enrolled in the Dunedin colorectal cancer cohort were identified using the Health Research Council Colorectal Cancer (HRC CRC) database. Patients that had surgeries between January 2008 and June 2014 were selected to maximise the likelihood of having a computerised tomography (CT) scan at diagnosis being available as well as allowing at least five years of follow-up time. Those diagnosed with stage I or II colorectal cancer were chosen as their body compositions were less likely to have been modified by cancer. Finally, patients in the Southern District Health Board electronic record system Health Connect South database with National Health Index (NHI) numbers that were no longer registered, those who were duplicated, or those without a CT scan around the time of diagnosis were excluded (Figure 4).

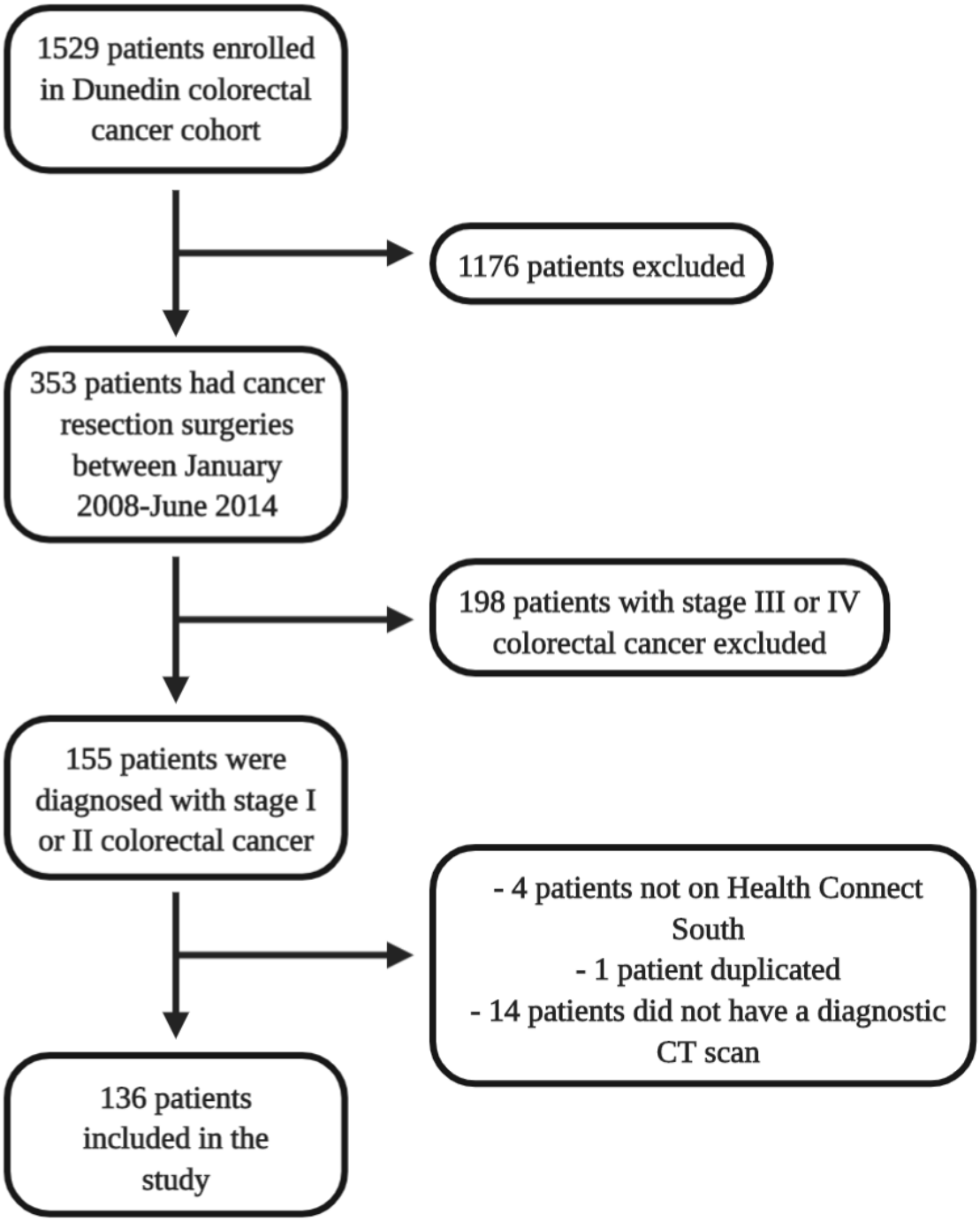

Figure 4: Inclusion criteria

Out of the 1529 patients enrolled in the study, 353 patients had their cancer resection surgeries between January 2008 and June 2014. Of these, 155 patients had stage I or II colorectal cancer. After removing patients either not on the database, duplicates, or those without a diagnostic CT scan, 136 patients were included in the study.

2.5.2 CT analysis

The body composition factors fat mass and muscle mass were investigated as these are significant for the health outcomes of a variety of diseases (139). To split the data into groups based on obesity status, height and weight were recorded and BMI calculated. However, as many patients did not have online records of these measurements, and due to the inaccuracy of BMI to accurately reflect obesity status, pre-operative CT scans performed at the time of diagnosis were used to calculate fat mass and waist circumference. Abdominal CT scans (field of view of 368 mm, slice thickness of 5 mm, 120 kVp, 425 mAs) were selected and the intervertebral disc between the level of the third and fourth lumbar vertebra (L3/4) was identified using a pre-programmed spinal level tool as well as using the anatomical landmarks of the iliac crest and aortic bifurcation which occur at the level of L4. This level has been shown to be a good representation of overall fat mass (140). To calculate the total fat area, a line was drawn around the skin using the software Syngo.via (Siemens Healthineers, Erlangen, Germany). The Anatomy Visualiser tool was used to measure the cross-sectional area of fat, thresholded by the Hounsfield values of -150 to -50. To determine visceral fat area this process was repeated, however, the line was drawn around the inner layer of abdominal wall muscles (Figure 5A).

CT scans were used at the level of L3 to measure waist circumference (141). Using the distance polyline tool, a freehand line was drawn around the skin, giving the waist circumference in centimetres (Figure 5B). Waist circumferences measured on CT have been shown to be equivalent to those measured by a health professional while the patient is standing (142).

To measure skeletal muscle mass, CT scans were used at the level of L3 (143). Rectus abdominis, transverse adbominis, external and internal oblique muscles, psoas, quadratus

lumborum and erector spinae were identified and a line drawn around them. A Hounsfield threshold of -29 to 150 was used. This was normalised by dividing by height (in m^2) (144).

Both skeletal muscle and fat mass calculations were measured as a volume with the units of cm^3. In order to convert this to the surface area, measurements were divided by slice thickness (145).

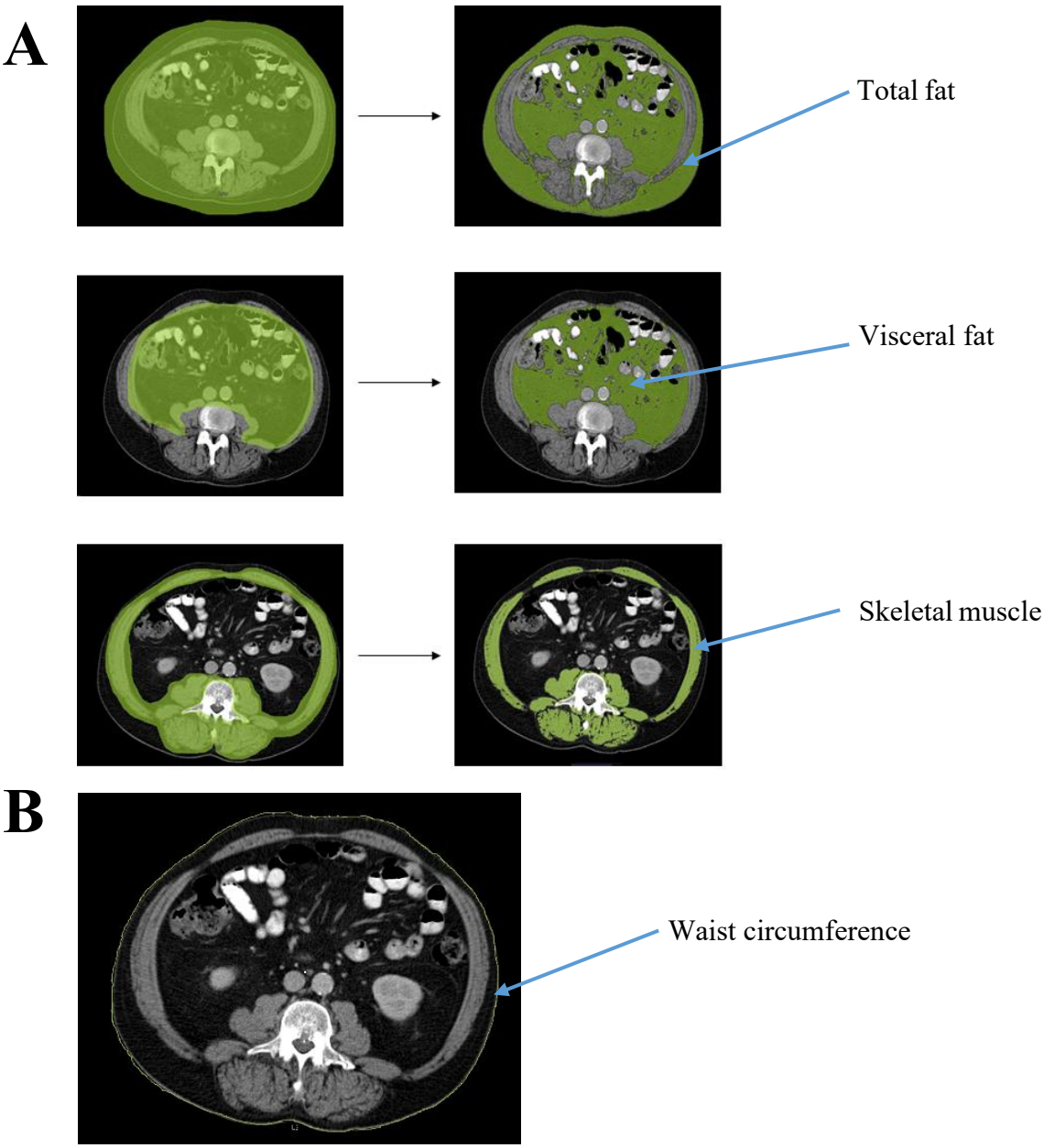

Figure 5: Measuring body composition using CT

A) Using the Anatomy Visualiser tool on Syngo.via, freehand lines were drawn around the skin and abdominal muscle wall at the intervertebral disc between L3/4, and around the abdominal muscles at L3. Hounsfield values of -150 to -50 for fat, and -29 to 150 for muscles were then used as a threshold to identify either fat or muscle. Volumetric measurements were taken, which were divided by the slice thickness in order to get the cross-sectional area for total fat, visceral fat, and lumbar skeletal muscle mass.

B) Using the distance polyline tool, a freehand line was drawn around the skin at the level of L3 in order to calculate the waist circumference.

2.5.3 Patient data collection

Data was collected using Health Connect South. NHI numbers were used to identify blood tests performed up to three months before tumour resection date. The following parameters were collected from the patient where possible: complete blood count (including haemoglobin, platelets, white blood cell (WBC), neutrophil, lymphocyte, monocyte, eosinophil and basophil levels), albumin and total protein, C-reactive protein (CRP), erythrocyte sedimentation rate (ESR), and carcinoembryonic antigen (CEA) levels. Sex, smoking status, age and 5-year survival from the date of surgical resection were also recorded. This study comes under that of the Dunedin colorectal cancer cohort, ethics number 14/NTA/33.

2.6 Statistical analysis for all data

Five mice per group were used for TIL phenotyping and blood immune cell isolation and then pooled in one graph to show the consistency of the results. Two mice per group were used for TIL frequency due to the time-consuming nature of the analysis. Data was expressed as mean ± standard error of the mean (SEM). All data was tested for normality using the Shapiro-Wilks test. Normally distributed means were compared using unpaired student's t-test or one-way analysis of variance (ANOVA) followed by post hoc Tukey's pairwise comparison. If data was not normally distributed, a Kruskal-Wallis test was performed followed by post hoc Dunn's pairwise comparison. Kaplan-Meier survival curves were analysed using the Mantel-Cox test.

Appropriate sample sizes were determined using a power analysis with a signal-to-noise statistic of 1.35. Using 5% significance at 80% power, this confirmed that a sample size of n=10 mice per group for the tumour trials was required. Power calculations were unable to be performed prior to starting the colorectal cancer patient cohort research as the number of patients possible to use was unknown. Therefore, the intent of the research

in this section was to general hypotheses and determine whether this type of analysis was possible in this cohort.

Chapter 3

Results (Murine)

3.1 Tumour growth and survival rates in lean, obese and hyperuricemic mice

3.1.1 Immunotherapeutic treatment of cancer in obese mice

3.1.1.1 Breast cancer

To see if obesity had an impact on the efficacy of VLP treatment of breast cancer, thirty female POUND +/+ mice were injected with 1 x 10^5 C57mg.MUC1 cells in two individual experiments. The trial was split in half (fifteen mice per experiment) due to the availability of POUND mice. The first fifteen mice had cells injected into the second left MFP. After significant ulceration problems (3/4, 4/5 and 3/5 tumours in the PBS, VLP and VLP + anti-PD-L1 groups respectively), it was decided that further experiments would involve injecting cells into the fourth left MFP as tumours in this area would rub against the ground less. Tumours were palpable on day 7 for the first trial and day 6 for the second. At this time, mice were treated with either PBS + an isotype control of anti-PD-L1, surv.VLP-SS-MUC1 + isotype control, or surv.VLP-SS-MUC1 + anti-PD-L1.

Results from the two trials differed. In the first trial, compared to control, treatment with VLP alone did not result in tumour remission although survival was increased. While tumour growth curves were similar, the median survival for the VLP group was 59 days as opposed to 47.5 days in the PBS group. The combination therapy of VLP + anti-PD-L1 resulted in tumour remission for 2/5 mice. One mouse remained tumour free for over 50 days and did not show tumour growth after rechallenge with the same cancer cells. Median survival for this group was 145 days (Figure 6A).

Due to the high number of ulcerations in this trial, data from ten mice had to be censored, so these observations were only in a limited number of mice. This also resulted in the large standard error as shown in the tumour growth graph (Figure 6A).

In the second trial, there was no difference in tumour growth rates between treatment groups. Survival curves show that the VLP and VLP + anti-PD-L1 groups survived longer than the PBS control group, however median survivals times for PBS and VLP + anti-PD-L1 groups were 46 and 50 days respectively. The median survival for the VLP group was extended compared to the other two groups at 70 days (Figure 6B). 1/5 tumours from the PBS group, and 1/5 tumours from the VLP group, ulcerated.

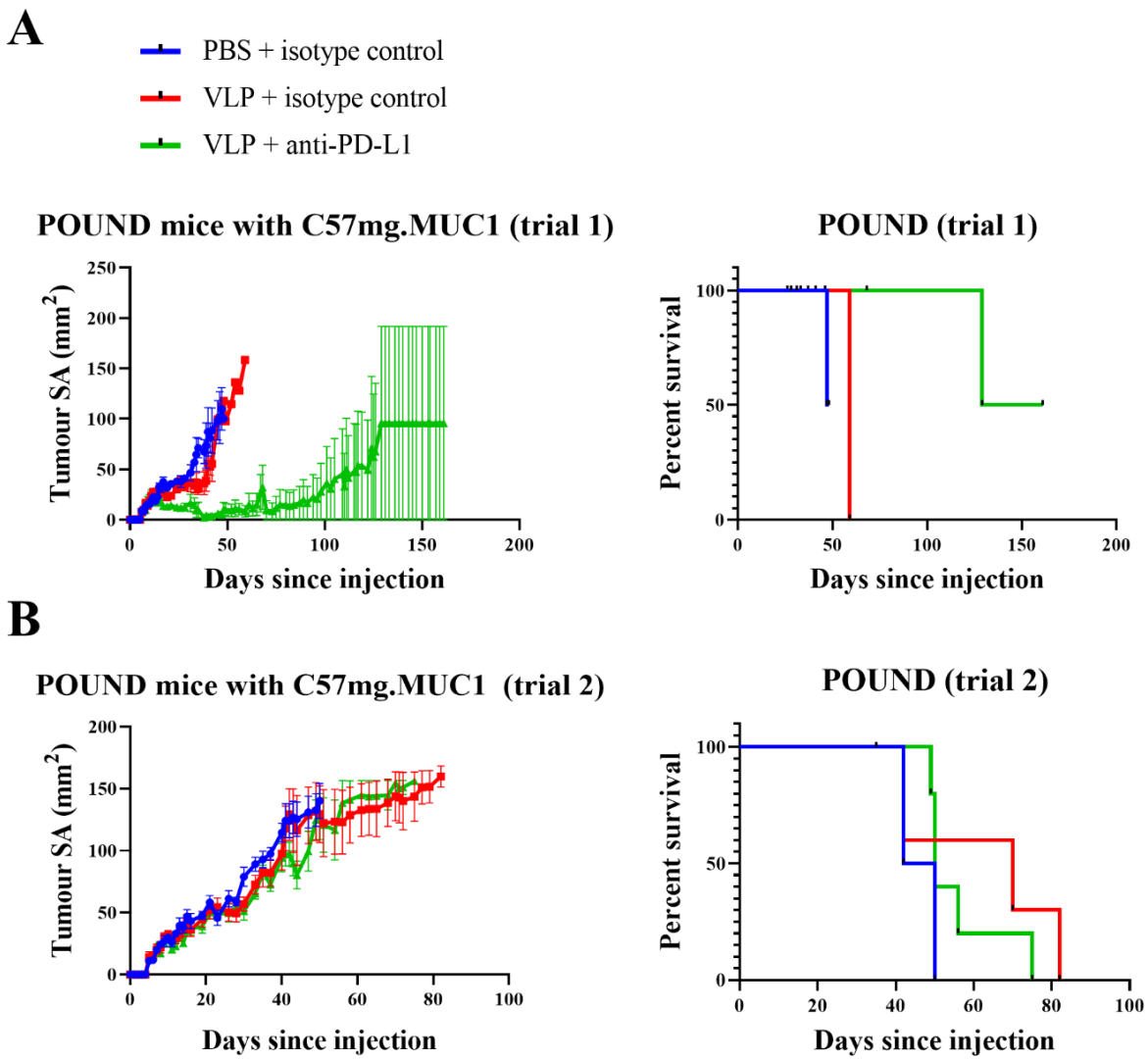

Figure 6: Tumour growth and survival curves for obese mice injected with C57mg.MUC1 cells

Mice aged between 12-20 weeks were injected with 1 x 10^5 C57mg.MUC1 cells and given a treatment of either PBS s.c + isotype control i.p, VLP s.c + isotype control, or VLP + anti-PD-L1 i.p once tumours became palpable. Mice were weighed and tumours measured every two days until tumours reached 150 mm^2 or ulcerated, after which they were culled. **A)** trial one involving fifteen POUND +/+ mice, **B)** trial two involving fifteen POUND +/+ mice.

The results for tumour growth rates represent the mean (± SEM) of five mice per treatment group. Mice with ulcerated tumours were censored at the date of termination. Statistical differences were determined using a Mantel-Cox test.

3.1.1.2 Colorectal cancer

In order to investigate the effects of obesity on the efficacy of VLP vaccine treatment of colorectal cancer, fifteen male POUND +/+ mice were injected with 1 x 10^5 MC-38 cells s.c into the left flank. Once tumours were palpable (day 8 for the first trial and day 7 for the second trial), mice were divided into three groups with approximately equal tumour size. Mice were treated with either PBS + an isotype control of anti-PD-L1, surv.VLP + isotype control, or surv.VLP + anti-PD-L1.

There was no difference in growth rates or survival time in any of the treatment groups, and by day 30 all mice had been culled due to reaching the specified surface area (150 mm^2), with a small number of tumours ulcerating (Figure 7A). Median survival for the PBS and VLP + anti-PD-L1 groups was 25 days, and for the VLP only group was 27 days. 2/5 and 2/5 tumours in the VLP and VLP + anti-PD-L1 groups respectively ulcerated.

In the second trial, fifteen male POUND mice were injected with 1 x 10^5 MC-38 cells. Tumours grew slower in the VLP and VLP + anti-PD-L1 groups compared to the PBS group, although tumours in the two treatment groups grew at a similar rate (Figure 7B). Survival rates for the three groups showed a difference between each, with a median survival of 25 days for PBS, 34 days for VLP and 39 days for VLP + anti-PD-L1, which was statistically significant between the PBS and VLP + anti-PD-L1 groups ($p = 0.0014$). Respectively, 1/5, 2/5 and 1/5 tumours in the PBS, VLP and VLP + anti-PD-L1 groups ulcerated.

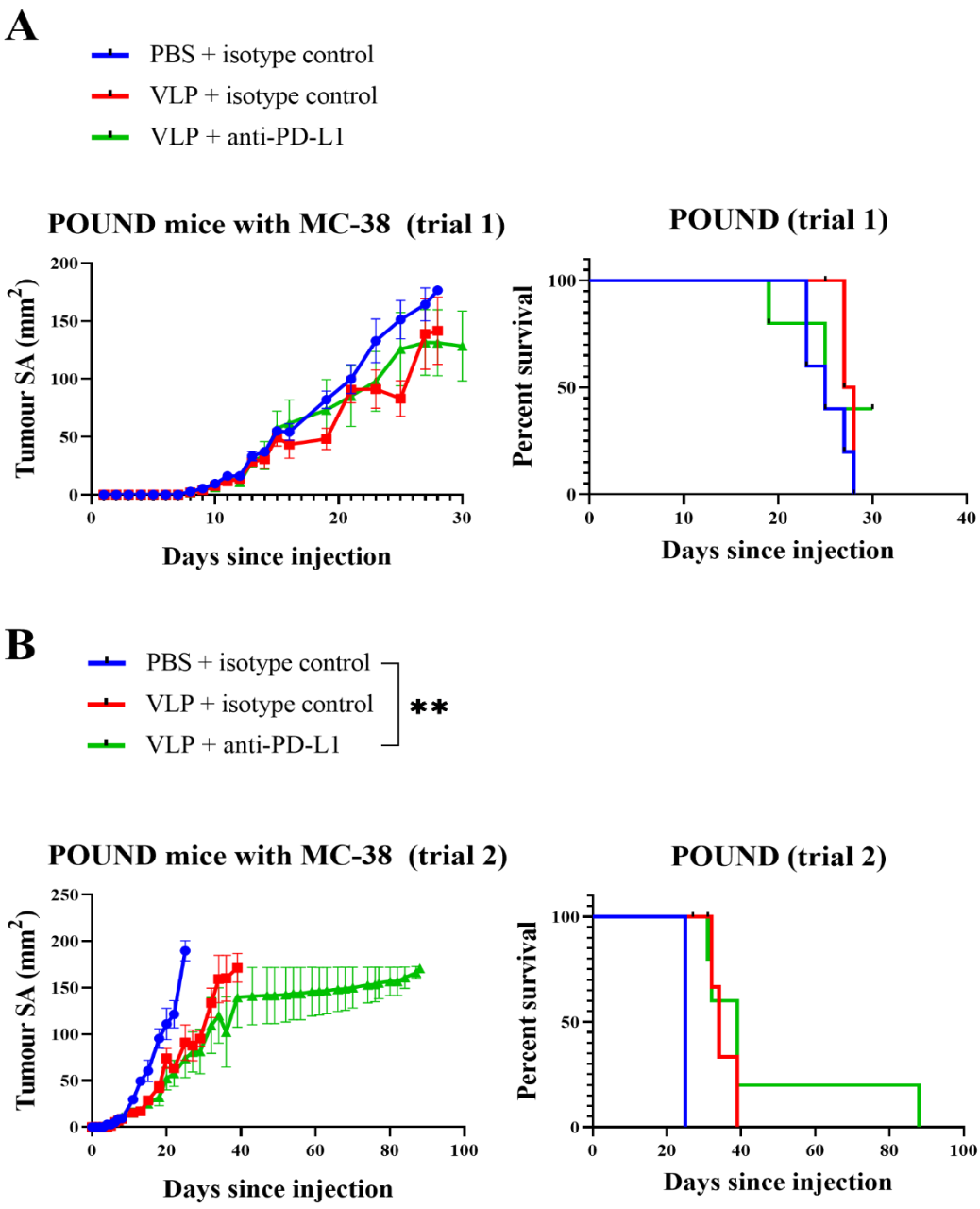

Figure 7: Tumour growth and survival curves for obese mice injected with MC-38 cells

Mice aged between 12-20 weeks were injected with 1 x 10^5 MC-38 cells and given a treatment of either PBS s.c + isotype control i.p, VLP s.c + isotype control, or VLP + anti-PD-L1 i.p once tumours became palpable. Mice were weighed and tumours measured every two days until tumours reached 150 mm^2 or ulcerated, after which they were culled. **A)** trial one involving fifteen POUND +/+ mice, **B)** trial two involving fifteen POUND +/+ mice.

The tumour growth results represent the mean (± SEM) of five mice per treatment group. Mice with ulcerated tumours were censored at the date of termination. Statistical differences were determined using a Mantel-Cox test. ** $p \leq 0.01$

3.1.2 Immunotherapeutic treatment of cancer in hyperuricemic mice

3.1.2.1 Breast cancer

To investigate the effects of hyperuricemia on the efficacy of VLP vaccine treatment of breast cancer, thirty female Urah$^{Plt2/Plt2}$ mice were injected with 1 x 10^6 C57mg.MUC1 cells into the second left MFP. Tumours became palpable on day 5, and mice were treated as described previously.

Tumours in all three groups grew at the same rate and no tumour remission was observed. Mice treated with VLP and VLP + anti-PD-L1 had a superior median survival of 55 and 53 days respectively, with the PBS group having a median survival of 46 days (Figure 8). However, this difference was not statistically significant. Ulcerations occurred in 3/10, 6/10 and 4/10 tumours in the PBS, VLP and VLP + anti-PD-L1 groups respectively.

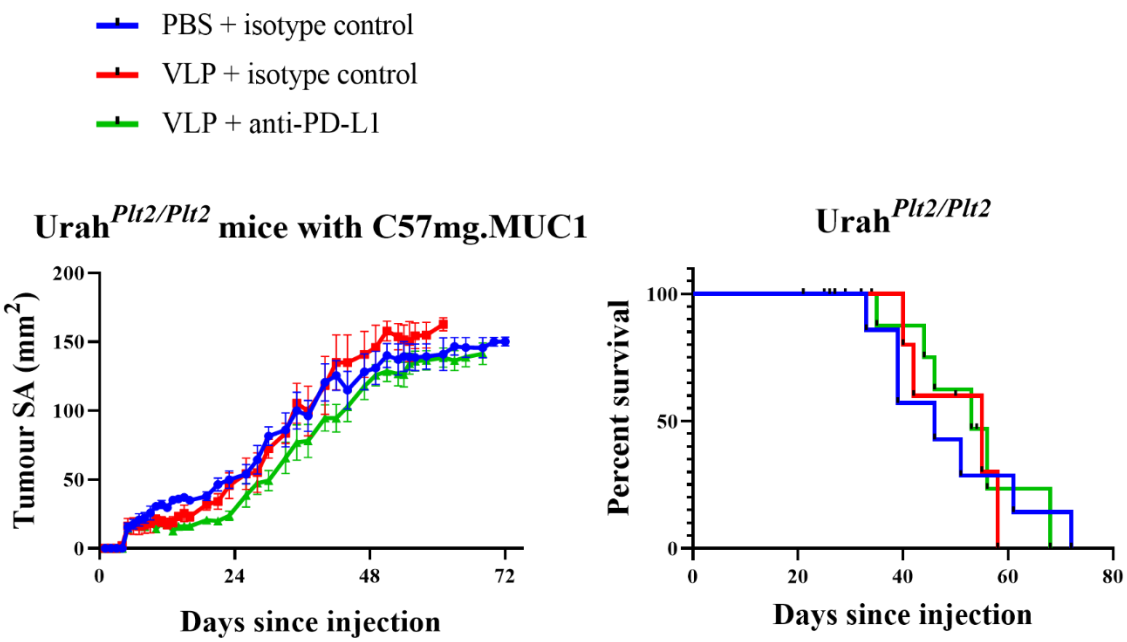

Figure 8: Tumour growth and survival curves for hyperuricemic mice injected with C57mg.MUC1 cells

Mice aged between 12-20 weeks were injected with 1 x 10^6 C57mg.MUC1 cells and given a treatment of either PBS s.c + isotype control i.p, VLP s.c + isotype control, or VLP + anti-PD-L1 i.p once tumours became palpable. Mice were weighed and tumours measured every two days until tumours reached 150mm^2 or ulcerated, after which they were culled.

The tumour growth results represent the mean (± SEM) of ten mice per treatment group. Mice with ulcerated tumours were censored at the date of termination. Statistical differences were determined using a Mantel-Cox test.

3.1.2.2 Colorectal cancer

Investigation into the effects of hyperuricemia on the efficacy of VLP vaccine treatment on colorectal cancer involved injecting 30 male Urah$^{Plt2/Plt2}$ mice with 1 x 10^5 MC-38 cells s.c into the left flank. Treatment on day 8 with either VLP alone or in combination with anti-PD-L1 did not result in a regression of tumour sizes (Figure 9). Survival was reduced in the PBS group, with a median survival of 30 days respectively. Mice in the VLP and VLP + anti-PD-L1 groups survived slightly longer, with a median survival of 35 days, although this was not statistically significant (Figure 9). After excluding mice that did not develop tumours, 2/8 and 3/9 tumours from the PBS and VLP groups respectively ulcerated.

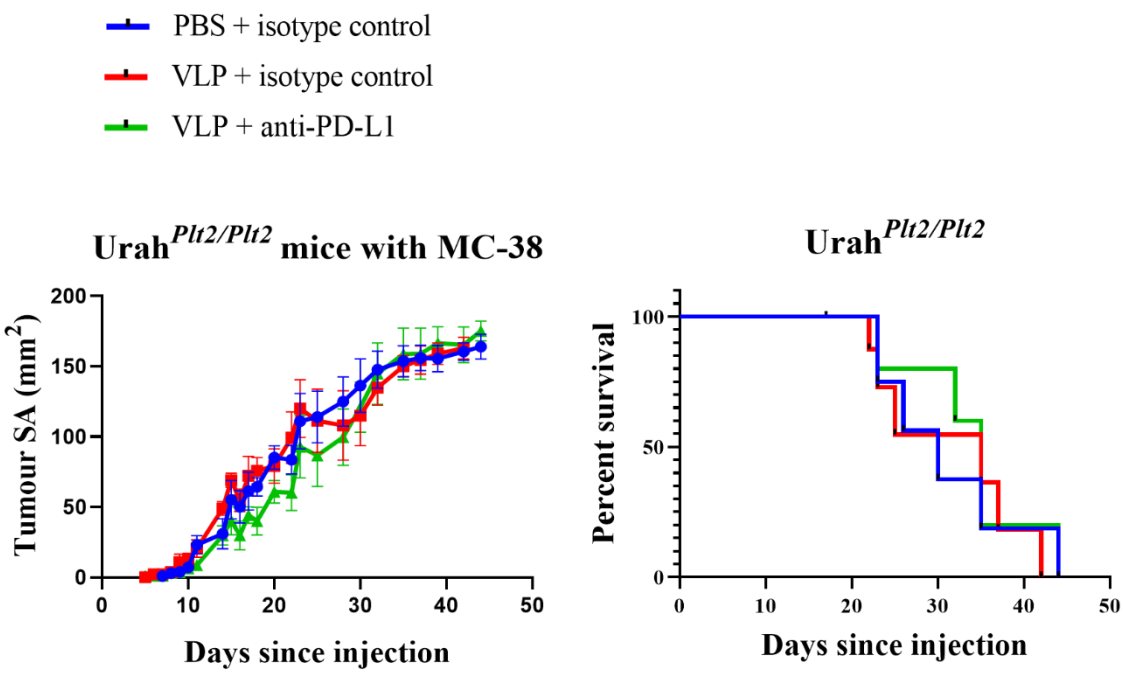

Figure 9: Tumour growth and survival curves for hyperuricemic mice injected with MC-38 cells

Mice aged between 12-20 weeks were injected with 1 x 10^5 MC-38 cells and given a treatment of either PBS s.c + isotype control i.p, VLP s.c + isotype control, or VLP + anti-PD-L1 i.p once tumours became palpable. Mice were weighed and tumours measured every two days until tumours reached 150 mm^2 or ulcerated, after which they were culled.

The tumour growth results represent the mean (± SEM) of 10 mice per treatment group. Mice with ulcerated tumours were censored at the date of termination. Statistical differences were determined using a Mantel-Cox test.

3.1.3 Immunotherapeutic treatment of cancer in lean mice

3.1.3.1 Breast cancer

To compare the efficacy of the VLP or VLP + anti-PD-L1 treatment in obese and hyperuricemic mice, lean mice were used as a positive control as they have previously shown to respond to the VLP treatment. Thirty female POUND -/- mice were injected with 1 x 10^5 C57mg.MUC1 cells into the second left MFP. Tumours were palpable on day 6 and mice were treated as before.

Initially, tumours grew at a linear rate and mice injected with either VLP or VLP + anti-PD-L1 diverged with slower-growing tumours from the PBS control group at approximately day 14. However, for reasons unknown, between days 14 and 36 tumour growth in the control group plateaued, after which all groups grew at a similar rate (Figure 10A).

Survival during this time was the same for all groups. Tumours from the control group did not grow in a linear fashion, which was not expected and had not previously been observed. Therefore, we were unable to make a comparison of treatment efficacy between groups, and it was decided that all mice would be culled, and the trial repeated.

At this time, the Young laboratory had several other tumour trials housed in the Hercus Taieri Animal Facility that experienced similar issues. It was decided to shift all trials to the Microbiology animal facility.

In the repeat trial, C57BL/6 mice were used instead of POUND -/- mice as this strain could not be transferred between buildings. POUND mice come from the same genetic background, so the two strains of mice were considered to be synonymous with each other. Cells were injected into the fourth left MFP.

Tumours were palpable at day 8 and treatment injections were given at this time. Growth curves were similar for the PBS and VLP groups, with a median survival of 77 days for both. Mice injected with VLP + anti-PD-L1 had a slowed tumour growth, with a significantly prolonged median survival of 128 days ($p = 0.0004$) (Figure 10B). Three mice in this group achieved tumour remission. After 50 days of tumour-free survival, the mice were rechallenged with the same amount of tumour cells. Tumour remission was sustained following this, and no mice grew new tumours. After 50 more days, the mice were culled. Tumour growth in all groups was slower than in previous trials investigating C57mg.MUC1 cell growth rates in C57BL/6 mice, with the first mouse reaching 150 mm^2 at day 65 (Figure 10B). Ulcerations occurred in 2/10, 4/10 and 5/10 tumours in the PBS, VLP, and VLP + anti-PD-L1 groups respectively. These mice were censored from the survival curve at the date of termination.

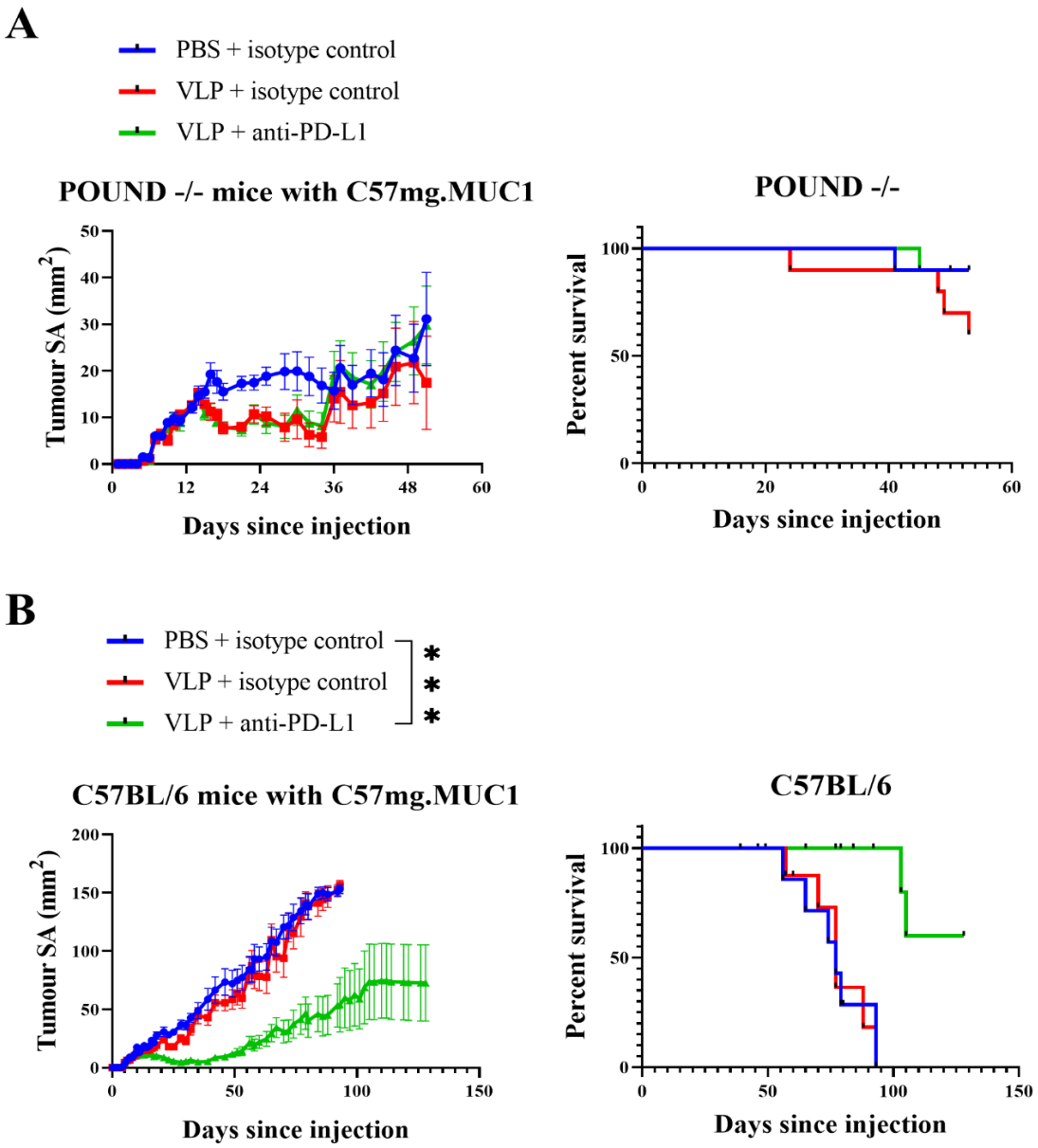

Figure 10: Tumour growth and survival curves for lean mice injected with C57mg.MUC1 cells

Mice aged between 12-20 weeks were injected with 1 x 10^5 C57mg.MUC1 cells and given a treatment of either PBS s.c + isotype control i.p, VLP s.c + isotype control, or VLP + anti-PD-L1 i.p once tumours became palpable. Mice were weighed and tumours measured every two days until tumours reached 150 mm^2 or ulcerated, after which they were culled. **A)** trial one involving thirty female POUND -/- mice which were terminated after PBS-treated tumours failed to grow, **B)** trial two involving thirty female C57BL/6 mice.

The tumour growth results represent the mean (± SEM) of ten mice per treatment group. Mice with ulcerated tumours were censored at the date of termination. Statistical differences were determined using a Mantel-Cox test. *** $p \leq 0.001$

3.1.3.2 Colorectal cancer

To assess the efficacy of VLP vaccine treatment against colorectal cancer in lean mice, thirty male C57BL/6 mice were injected with 1 x 10^5 MC-38 cells s.c into the left flank. Tumours were palpable on day 7 and treatments were given as before. Tumour growth rates in all groups were the same and median survival was 31 days for all groups. 1/10 mice in the VLP group and 1/10 mice in the VLP + anti-PD-L1 group were able to achieve remission which was sustained following tumour rechallenge (Figure 11). Only one tumour, in the VLP + anti-PD-L1 group, ulcerated.

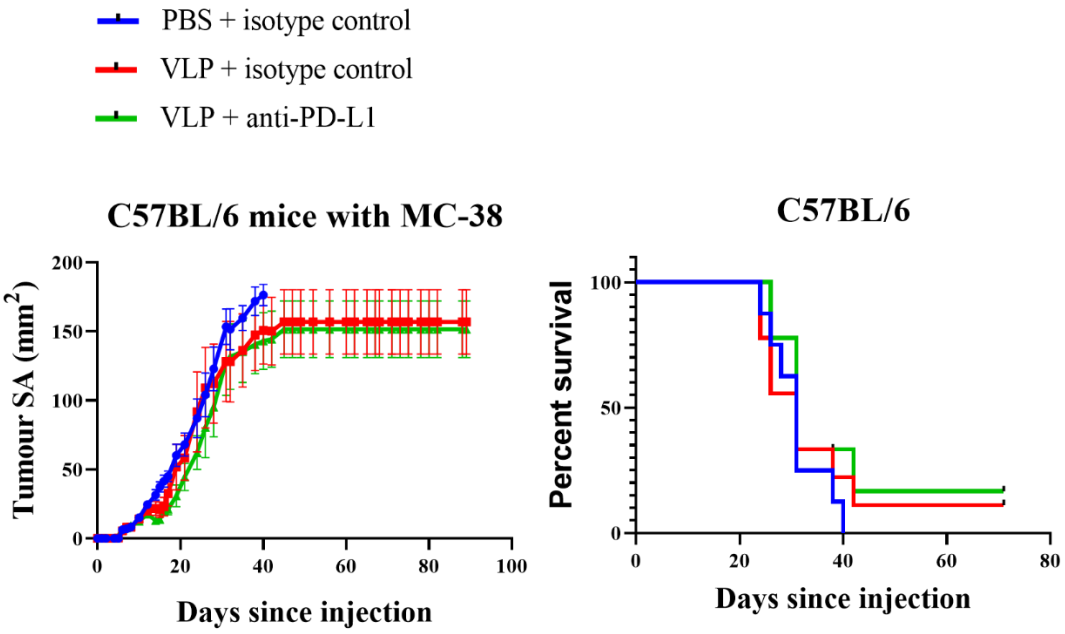

Figure 11: Tumour growth and survival curves for lean mice injected with MC-38 cells

Mice aged between 12-20 weeks were injected with 1 x 10^5 MC-38 cells and given a treatment of either PBS s.c + isotype control i.p, VLP s.c + isotype control, or VLP + anti-PD-L1 i.p once tumours became palpable. Mice were weighed and tumours measured every two days until tumours reached 150 mm^2 or ulcerated, after which they were culled.

The tumour growth results represent the mean (± SEM) of ten mice per treatment group. Mice with ulcerated tumours were censored at the date of termination. Statistical differences were determined using a Mantel-Cox test.

3.2 Analysis of tumour-infiltrating lymphocytes

3.2.1 Analysis of immunohistochemical staining of tumours

In order to determine why many of the tumour trials had unexpected results, a preliminary study to investigate the infiltration frequency of TILs in the tumours was undertaken. Half of the tumours from all tumour trials were preserved in formalin and stained for $CD3^+$ cells, allowing us to see the distribution and frequency of TILs. Slides were analysed using ImageJ and tumours divided into outer tumour and inner tumour regions. Only two tumours per group were analysed, so this low sample number meant that statistical analysis was not performed.

3.2.1.1 Breast cancer

In all mouse breeds, there was a trend of no difference in TIL frequency between PBS, VLP or VLP + anti-PD-L1 treatment groups. This was the same for the outer part of the tumour and the inner segment, as well as the tumour as a whole.

However, there were trends of differences between mouse breeds. In all treatment groups, there appears to be greater infiltration of both the inner and outer tumour by T-cells in lean mice, with obese mice having the smallest frequency. Hyperuricemic mice had a frequency that is in between that of obese and lean mice in all parts of the tumour (Figure 12A). The exception for these findings was in hyperuricemic mice treated with VLP only, where there was an increase in the frequency of TILs in the outer tumour.

3.2.1.2 Colorectal cancer

All mice grafted with colorectal cancer and treated with VLP had an increase in the number of TILs in the outer part of the tumours. This difference was most pronounced in

hyperuricemic and obese mice. There were no other differences in TIL frequency between treatment groups in any mouse type.

When comparing TIL frequency between mice breeds, the trend observed was that obese and lean mice treated with PBS and VLP + anti-PD-L1 had similar levels of TILs, while hyperuricemic mice had a lower frequency. When treated with VLP, obese mice had the greatest numbers of TILs, with hyperuricemic mice also having an increase in TIL frequency compared to the PBS-treated mice. Lean mice had the lowest frequency of the three mouse types (Figure 12B).

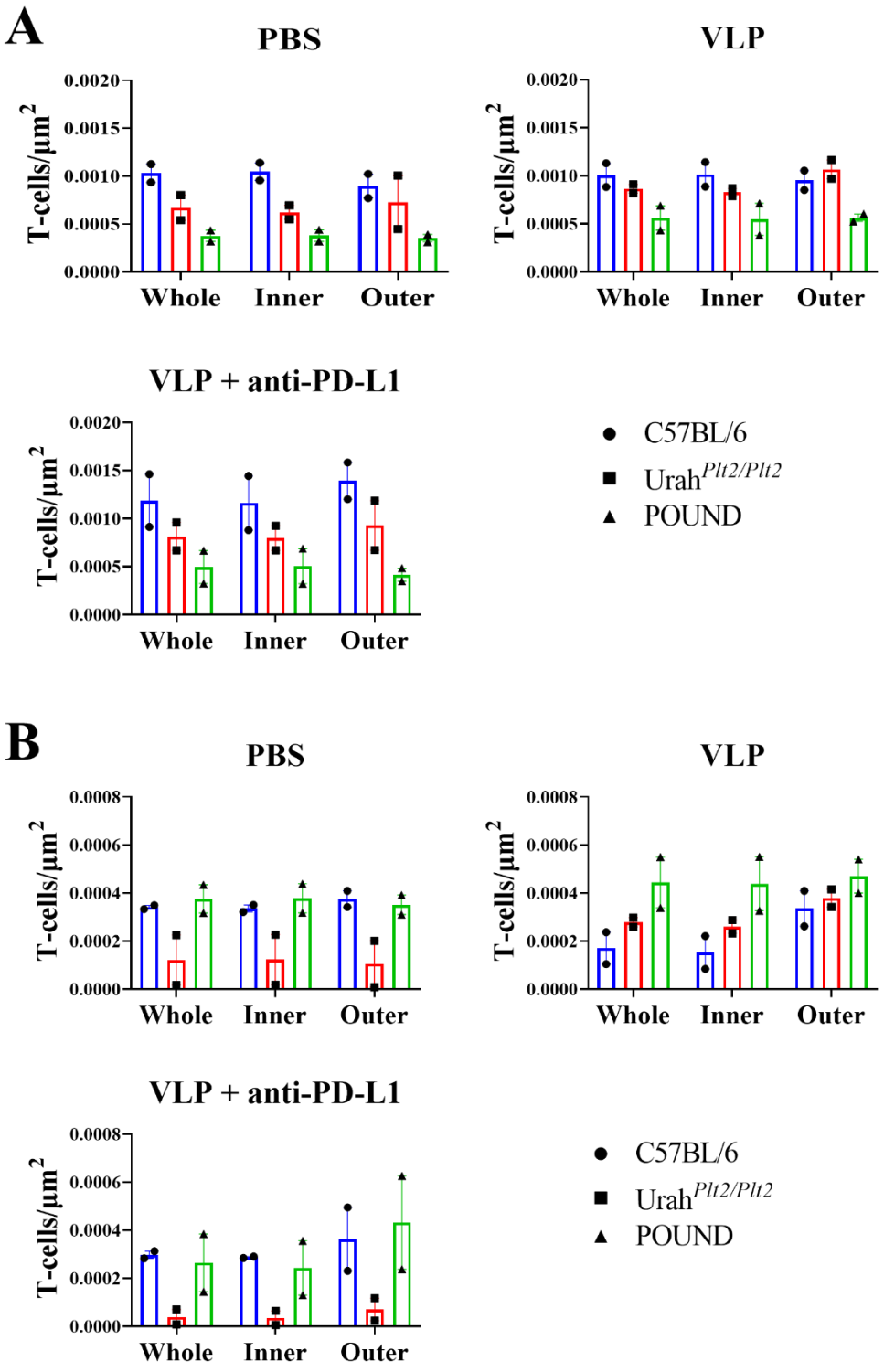

Figure 12: Frequency of TILs in C57mg.MUC1 and MC-38 tumours based on treatment group

Two tumours per mice were preserved in formalin per treatment group per mouse strain and stained for CD3. Images were then analysed using ImageJ and cell number divided by the area of the tumour in microns^2. **A)** C57mg.MUC1 tumours, **B)** MC-38 tumours. The results represent the individual values (± SEM) of two mice per treatment group. Due to the low sample number, statistical analysis was not performed.

3.2.2 Phenotyping TILs for markers of exhaustion

To phenotype the TILs, tumours, spleens, tumour-draining lymph nodes and non-tumour-draining lymph nodes were removed from half of the lean and obese mice and processed. Samples were stained and analysed by flow cytometry. CD3 was used to detect the T-cells, which were further divided into $CD4^+$ and $CD8^+$ T-cells. Surface markers PD-1, LAG-3, Tim-3, CD127, and CD39 were used to phenotype T-cells for exhaustion. Figure 13 shows the gating strategy used to isolate specific cell populations. This was performed for C57BL/6 and POUND mice.

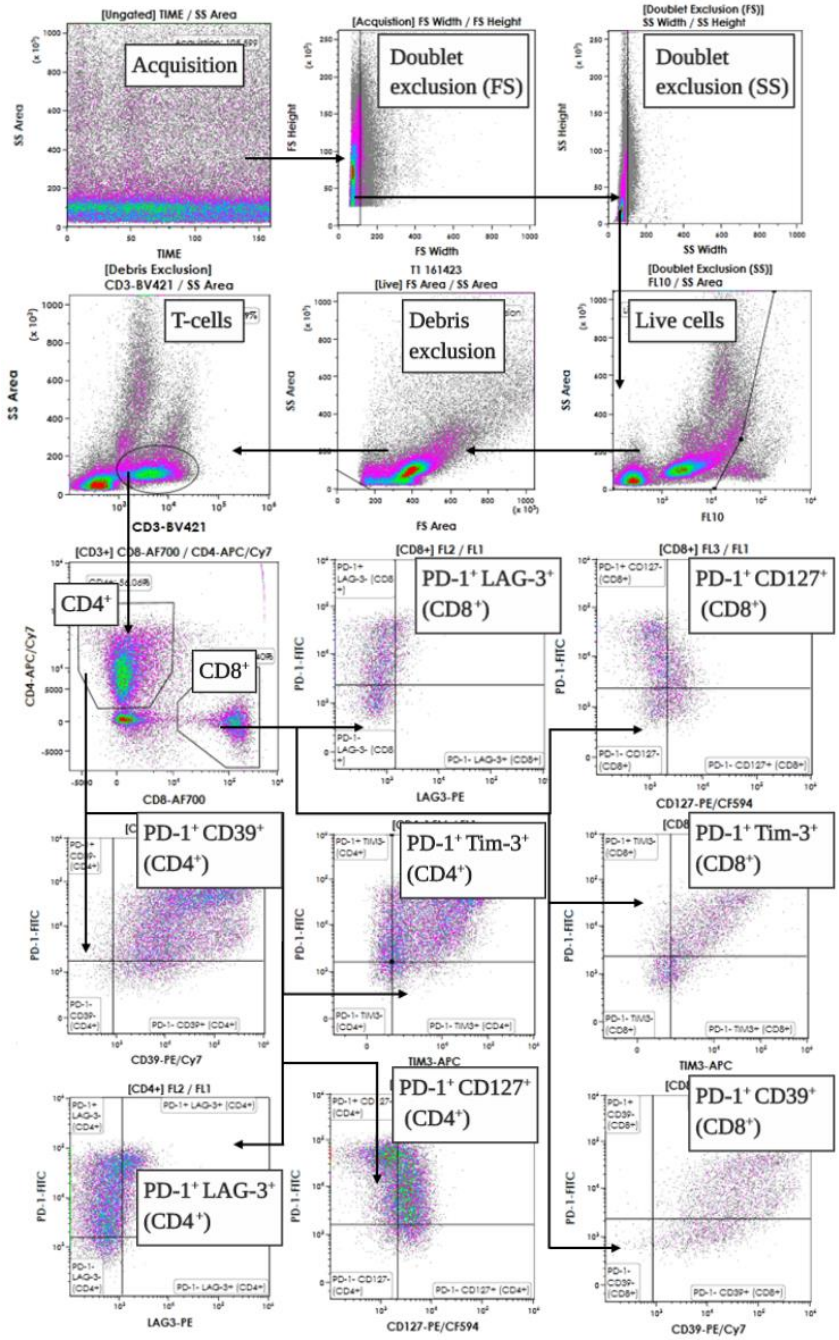

Figure 13: Gating strategy for phenotyping of tumour-infiltrating lymphocytes

POUND and C57BL/6 mice were injected with 1 x 10^5 MC-38 or C57mg.MUC1 cells and then treated with either PBS, VLP, or VLP + anti-PD-L1. Once tumours reached the defined endpoint (150 mm^2 or ulceration), mice were culled and tumours, spleens, tumour-draining lymph nodes and non-tumour-draining lymph nodes were harvested and stained with fluorophore-conjugated antibodies against different receptors. Cells were gated based on size (forward scatter) and granularity (side scatter) in order to exclude doublet cells, and with Zombie Yellow Live/Dead viability staining to exclude dead cells. Cells were labelled with fluorophore-conjugated antibodies against PD-1, LAG-3, CD127, CD39, Tim-3, CD8, CD4 and CD3.

3.2.2.1 Breast cancer

Overall PD-1 expression in tumour-bearing lean and obese mice was high, indicating that there was some level of exhaustion in both $CD8^+$ and $CD4^+$ T-cells (Figure 14A, F). In lean mice, the frequency of $CD4^+$ $PD\text{-}1^+$ T-cells was reduced in the VLP compared to the PBS group, and in the VLP + anti-PD-L1 group compared to the VLP group. This was not statistically significant (Figure 14A). $CD8^+$ T-cells in the PBS and VLP groups expressed similar levels of PD-1, however, mice treated with VLP + anti-PD-L1 had lower levels (Figure 14F). Levels did not differ between treatment groups in the obese mice. There was a trend towards a higher expression of PD-1 in obese mice compared to lean mice, with there being significantly higher levels of $PD\text{-}1^+$ $CD8^+$ T-cells in the obese mice compared to the lean mice treated with VLP + anti-PD-L1 ($p = 0.0314$).

Tumour specific but terminally exhausted T-cells can be characterised by being $PD\text{-}1^+$ $CD39^+$ (146). The frequencies of $CD8^+$ T-cells expressing these markers were similar in all obese treatment groups and similar for lean mice in the PBS and VLP groups (Figure 14B, G). Lower frequencies of tumour-specific $CD4^+$ and $CD8^+$ T-cells were detected in the VLP + anti-PD-L1 treated lean mice. Differences between mice strains were not statistically significant.

CD127, which is the α-chain of the IL-7 receptor and is important in long term persistence of T-cells in the absence of antigen, has reduced expression in exhausted T-cells (32). Differences between treatment groups and mouse strains were not significant except between $CD8^+$ T-cells in the VLP and VLP + anti-PD-L1 groups in lean mice (Figure 14C, H). In this group, VLP-treated mice had significantly higher numbers ($p = 0.0387$), indicating a lower level of exhaustion.

T-cells which are terminally exhausted are PD-1$^+$ as well as Tim-3$^+$ or LAG-3$^+$. There were statistically significantly more PD-1$^+$ LAG-3$^+$ CD4$^+$ T-cells in obese mice compared to lean mice ($p = 0.0331$), and there was the same trend in CD8$^+$ T-cells (Figure 14D, I). Differences between treatment groups were not significant. The frequencies of PD-1$^+$ Tim-3$^+$ T-cells were the opposite, whereby there were greater numbers of these cells for all treatments groups in the lean mice than the obese mice, which was statistically significant in CD4$^+$ T-cells ($p = 0.0308$) (Figure 14E, J). Differences between treatment groups were not significant.

When comparing the expression of PD-1, CD39, LAG-3 and Tim-3 in TILs, as opposed to those located in the spleen, expression in the splenocytes was reduced in all cases. Expression of CD127 was increased in splenocytes for the majority of treatment groups. There was no significant difference between treatment groups or mouse strains, although there was a trend of an increase in the overall expression of PD-1, LAG3 and Tim-3 in obese mice compared to lean mice (Supplementary Figure 1, Appendix).

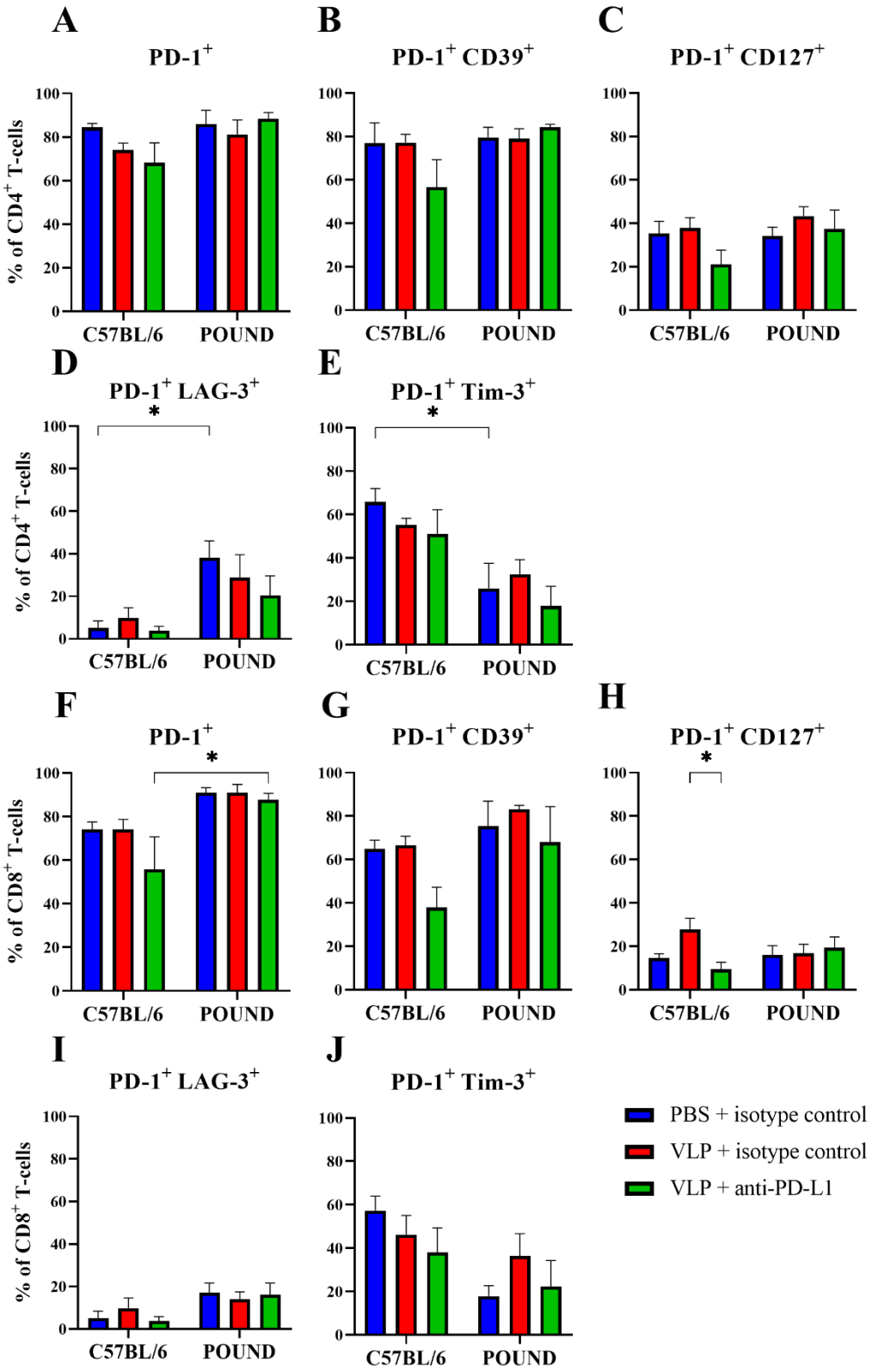

Figure 14: Markers of T-cell exhaustion in C57mg.MUC1 tumours

The results represent the mean (± SEM) of five mice per treatment group. Statistical differences were determined by using a one-way ANOVA. * $p \leq 0.05$.

3.2.2.2 Colorectal cancer

Analysis of the results from MC-38 tumours showed no statistically significant differences between treatment groups or mouse strains. The majority of TILs in MC-38 tumours expressed PD-1, indicating some level of exhaustion in most T-cells. PD-1 expression in $CD4^+$ T-cells was the same between obese and lean mice and between treatment groups (Figure 15A). PD-1 expression in $CD8^+$ T-cells was the same between mouse types, however, there was a trend of PD-1 expression being lower in the PBS groups (Figure 15F).

Differences in the frequencies of $PD\text{-}1^+$ $CD39^+$ (tumour specific, terminally exhausted) T-cells were not significant between obese and lean mice for both $CD4^+$ and $CD8^+$ T-cells (Figure 15B, G). For both subsets of T-cells, expression of these markers tended to be higher in the VLP and VLP + anti-PD-L1 treatment groups.

CD127 expression, which is reduced in exhausted T-cells, had no difference in frequency between treatment groups in obese mice. However, in lean mice the VLP treated group trended towards a higher amount of these cells than the PBS and VLP + anti-PD-L1 groups for both $CD4^+$ and $CD8^+$ T-cells (Figure 15C, H).

The frequency of terminally exhausted $CD4^+$ T-cells which are $PD\text{-}1^+$ $LAG\text{-}3^+$ did not differ in lean mice across treatment groups (Figure 15D). Obese mice treated with VLP alone showed a trend towards slightly reduced numbers of $PD\text{-}1^+$ $LAG\text{-}3^+$ $CD4^+$ T-cells. In general, obese mice had a higher frequency of $PD\text{-}1^+$ $LAG\text{-}3^+$ $CD4^+$ T-cells.

In the $CD8^+$ T-cell population, both obese and lean mice had similar levels of $PD\text{-}1^+$ $LAG\text{-}3^+$ cells (Figure 15I). VLP and VLP + anti-PD-L1 treated groups had a trend of higher frequencies of these cells in lean mice, and the VLP + anti-PD-L1 treated group had a trend of a higher frequency in the obese mice.

PD-1^{+} Tim-3^{+} CD4^{+} and CD8^{+} T-cells had similar frequencies in both mouse types (Figure 15E, J). The two treatment groups tended to have higher frequencies of these cells compared to the PBS group in both lean and obese mice.

These markers highlight a trend that in MC-38 tumours, groups treated with VLP or VLP + anti-PD-L1 tended to have a higher level of exhausted TILs compared to the control.

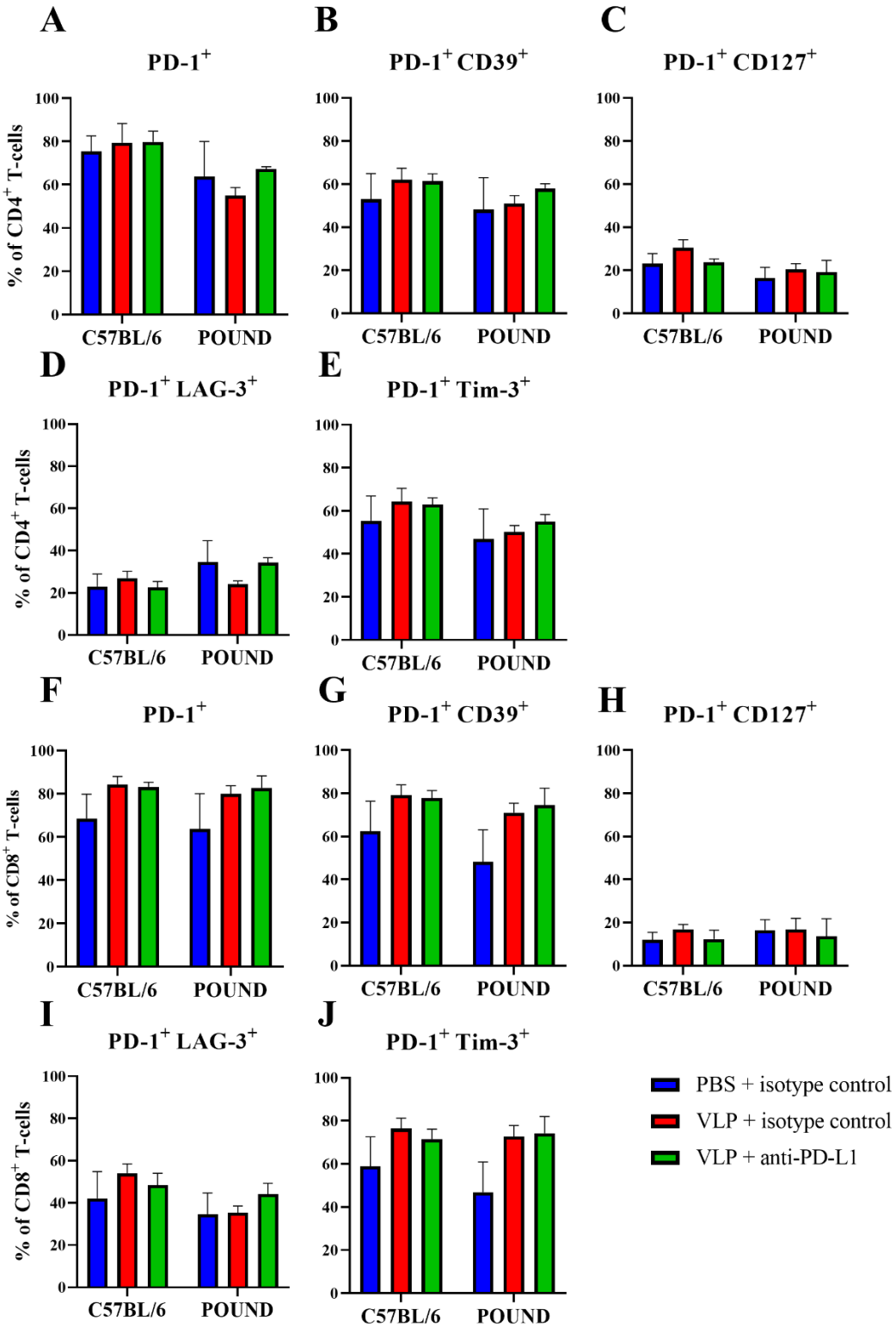

Figure 15: Markers of T-cell exhaustion in MC-38 tumours

The results represent the mean (± SEM) of four mice per treatment group, except for C57BL/6 mice treated with PBS and VLP + anti-PD-L1, which had five mice. Statistical differences were determined by using a one-way ANOVA.

3.3 Frequencies of circulating immune cells in lean and obese mice

To follow the expansion of immune cell populations in the blood during immunotherapy treatment, C57BL/6 and POUND mice grafted with MC-38 cells were tail bled every 7 days. Treatments (PBS, VLP or VLP + anti-PD-L1) were injected on days 7-13. Samples were then FACS stained and analysed via flow cytometry. Cell populations stained for were T-cells ($CD4^+$ and $CD8^+$), B-cells ($CD3^-$ $B220^+$), inflammatory monocytes ($CD3^-$ $B220^-$ $CD11b^+$ $Ly6C^+$ $Ly6G^-$), neutrophils ($CD3^-$ $B220^-$ $CD11b^+$ $Ly6C^+$ $Ly6G^+$), and myeloid- and lymphoid-derived DCs ($CD3^-$ $B220^-$ $CD11c^+$ $CD11b^+$ or $CD11b^-$ respectively). Figure 16 shows the gating strategy used to identify these cell types. Samples were taken until the majority of mice per group were culled, until day 28 in POUND mice (except for the PBS group which was until day 21), and day 35 in C57BL/6 mice.

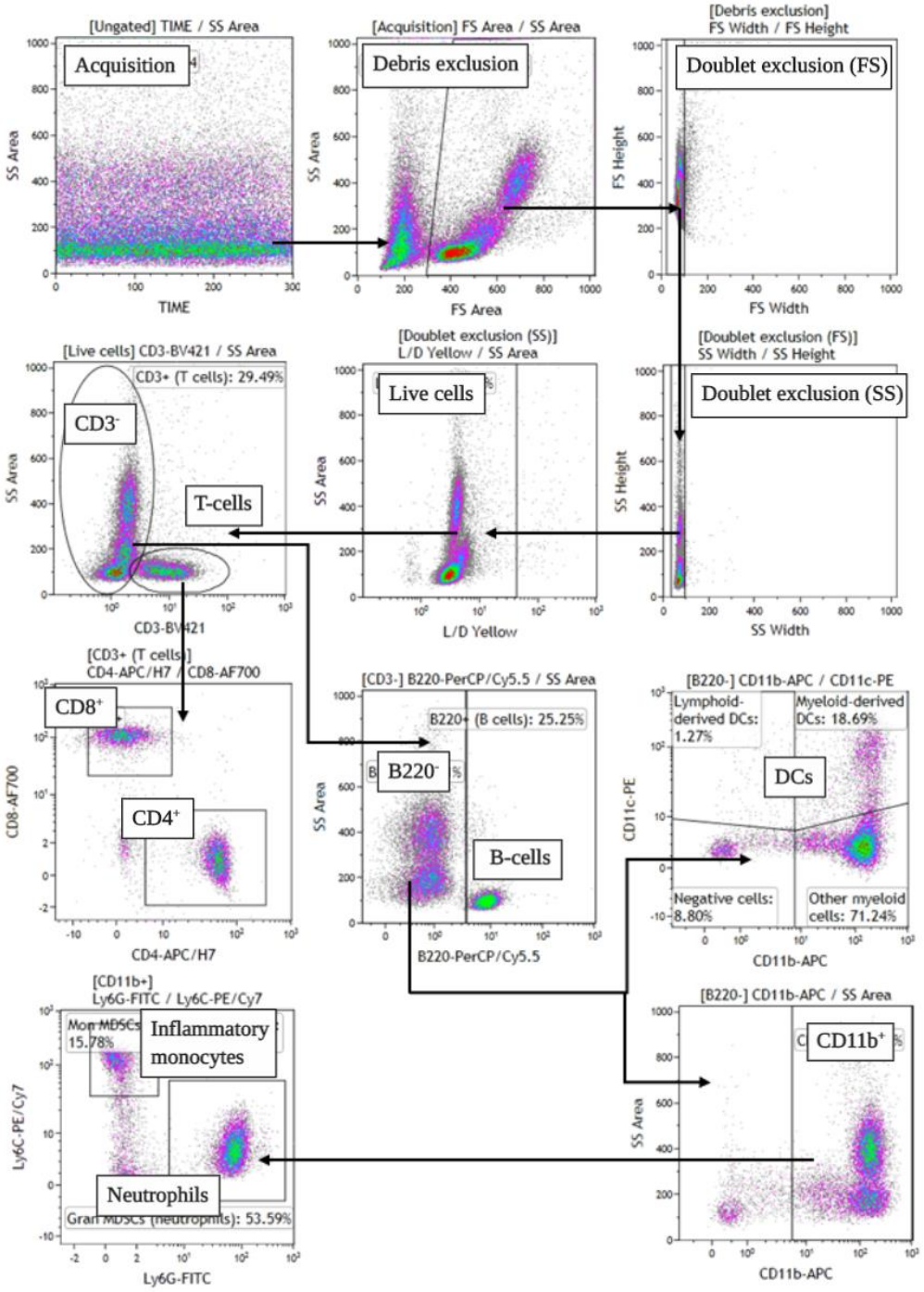

Figure 16: Gating strategy to identify immune cell populations in the blood

POUND and C57BL/6 mice were injected with 1 x 10^5 MC-38 cells and then treated with either PBS, VLP, or VLP + anti-PD-L1. Every 7 days mice were tail bled and stained with fluorophore-conjugated antibodies against different immune cell markers. After exclusion of debris, cells were gated based on size (forward scatter) and granularity (side scatter) to exclude doublet cells, and with Zombie Yellow Live/Dead viability staining to exclude dead cells. Cells were labelled with fluorophore-conjugated antibodies against Ly6G, CD11c, B220, Ly6C, CD11b, CD8, CD4 and CD3.

Differences in several cell populations were detected in lean and obese mice types. The frequency of $CD8^+$ T-cells increased in both mouse types from baseline up to seven days post tumour cell grafting and remained steady at ~10% of live cells after this (Figure 17A). On day 14, seven days post-VLP treatment, lean mice had statistically higher levels of $CD8^+$ T-cells ($p = 0.0463$) however levels were similar at all other time points. Frequencies of $CD8^+$ T-cells in both of the mouse types were comparable.

$CD4^+$ T-cells were initially significantly higher in obese mice ($p < 0.0001$), however, this dropped slightly while in lean mice the population increased at day 7 (Figure 17B). After this, frequencies of $CD4^+$ T-cells remained stable and were slightly higher in the obese mice than the lean mice at day 7, at around 15% of live cells compared to 10% although this was not statistically significant (Figure 17B).

Lean mice initially had significantly higher amounts of neutrophils at day 0 ($p = 0.0050$), however this decreased by day 7 so that obese mice had a trend of increased frequency (Figure 17C). Obese mice had higher levels of inflammatory monocytes than lean mice, which was significant at day 14 ($p = 0.0098$) (Figure 17D).

Lean mice had significantly higher frequencies of lymphoid-derived DCs initially ($p = 0.0051$ on day 7 and 0.0143 on day 14), however this population decreased on day 28 to be the same as in the obese mice (Figure 17E). Myeloid-derived DCs had similar frequencies in both lean and obese mice and did not fluctuate significantly throughout the experiment (Figure 17F).

Frequencies of B-cells were significantly higher in obese mice at day 0 ($p < 0.0001$), however after seven days since tumour grafting this changed to lean mice having a significantly higher amount ($p = 0.0293$) (Figure 17G). This was because as the tumours

grew, levels remained stable in obese mice, while the frequency in lean mice increased to statistically significant levels (day 21 $p < 0.0001$, day 28 $p = 0.0002$).

No differences in cell populations between treatment groups in either lean or obese mice could be detected.

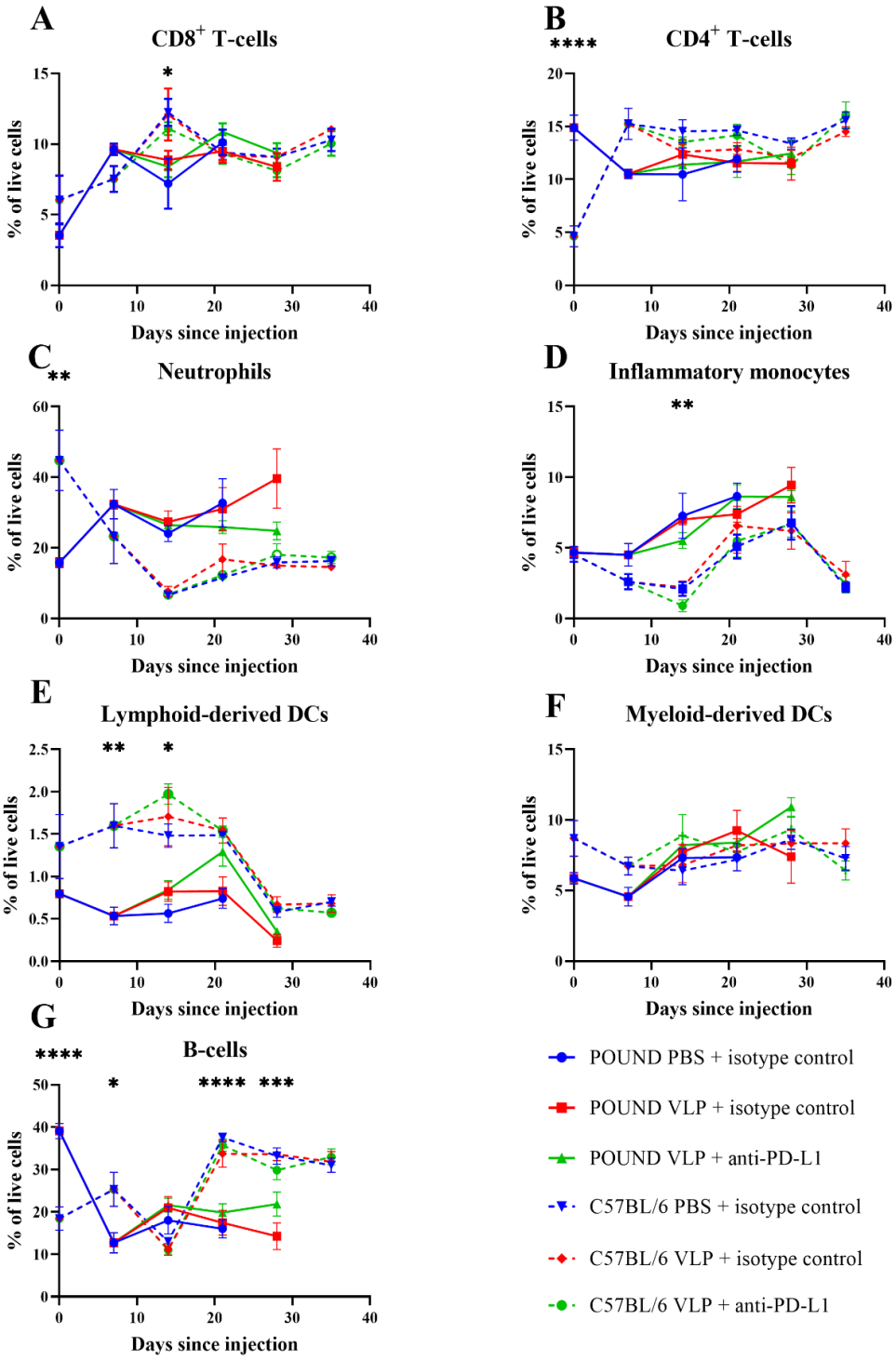

Figure 17: Analysis of immune cell populations in the blood of tumour-bearing mice

Lean and obese mice were tail-tipped every 7 days in order to follow the expansion of immune cells during immunotherapy treatment. The results represent the mean (± SEM) of five mice per treatment group. Statistically significant differences were determined by using a one-way ANOVA. * $p \leq 0.05$, ** $p \leq 0.01$, *** $p \leq 0.001$, **** $p \leq 0.0001$

Chapter 4

Results (Human)

4.1 The effect of body composition on 5-year survival of colorectal cancer patients

4.1.1 Overall patient survival

To determine whether the data from the murine studies is translatable into clinical findings, the effects of obesity on 5-year survival following surgery for the resection of colorectal cancer were investigated. Historical patient data was gathered from patients enrolled in the Dunedin colorectal cancer cohort. Patients who were diagnosed with stage I or II colorectal cancer in 2008-2014 were selected for analysis. From these patients, a variety of parameters were able to be considered for survival analysis. This is useful not only for investigating the relationship between body composition and overall survival (OS), but also to identify any factors that could be confounding the results.

Measures of obesity used were body mass index (BMI), waist circumference (WC), and visceral fat area (VFA). Muscle mass was determined based on the skeletal muscle index at the third lumbar vertebra (L3SMI). Ranges for body composition status are displayed in Table 2.

Table 2: Ranges for determining body composition status

BMI: Body mass index, WC: waist circumference, VFA: visceral fat area, L3SMI: skeletal muscle index at the third lumbar vertebra

	Underweight	**Normal**	**Overweight**	**Obese**
BMI (kg/m^2)	< 18.5	18.5-24.9	25-29.9	> 30 (147)
WC (cm)		< 93 (females) < 100 (males) (148)		> 93 (females) > 100 (males)
VFA (cm^2)		< 80.1 (females) < 163.8 (males) (140)		> 80.1 (females) > 163.8 (males)
	Sarcopenic	**Normopenic**		
L3SMI (cm^2/m^2)	≤ 38.5 (females) ≤ 52.4 (males)	> 38.5 (females) > 52.4 (males) (149)		

The number of patients defined as obese was different depending on the measure. Overall, 40.4% of patients with stage I or II colorectal cancer who underwent surgery between January 2008 – June 2014 were classified as obese when looking at VFA. When looking at BMI, 36.0% of patients were obese, and when considering waist circumference, 54.4% of patients were obese. In terms of muscle mass, 52.2% of patients were defined as sarcopenic.

The baseline characteristics for each body composition group are displayed in Table 3. Tumour stage, sex, age and smoking status were the only attainable sets of information that could be gathered from Health Connect South.

Table 3: Baseline characteristics

Patients were divided into groups based on VFA, L3SMI, BMI, and WC. Proportions of the tumour stage, sex, age, and smoking status of patients in each group were calculated.

		VFA		L3SMI	
		Non-obese *n=81 (%)*	**Obese** *n=55 (%)*	**Sarcopenic** *n=48 (%)*	**Normopenic** *n=44 (%)*
Stage	**I**	33 (40.7)	13 (23.6)	16 (33.3)	17 (38.6)
	II	48 (59.3)	42 (76.4)	32 (66.6)	27 (61.4)
Sex	**f**	41 (50.6)	33 (60)	19 (39.6)	29 (65.9)
	m	40 (49.4)	22 (40)	29 (60.4)	15 (34)
Age	**<50**	3 (3.7)	3 (5.5)	3 (6.3)	1 (2.3)
	50-59	11 (13.6)	3 (5.5)	4 (14.6)	6 (13.6)
	60-69	18 (22.2)	9 (16.4)	9 (18.8)	10 (22.7)
	70-79	30 (37.0)	31 (56.4)	24 (50)	23 (52.3)
	80-89	19 (23.4)	9 (16.4)	4 (8.3)	8 (18.2)
Smoker	**current**	10 (12.3)	5 (9.1)	6 (12.5)	8 (18.2)
	never	38 (46.9)	16 (29.1)	17 (35.4)	23 (52.3)
	past	20 (24.7)	18 (32.7)	13 (27.1)	14 (31.8)
	unknown	13 (16.0)	16 (29.1)	8 (16.7)	3 (38.0)

		BMI				WC	
		Under *n=2 (%)*	**Normal** *n=23 (%)*	**Over** *n=32 (%)*	**Obese** *n=32 (%)*	**Non-obese** *n=62 (%)*	**Obese** *n=74 (%)*
Stage	**I**	1 (50)	8 (34.8)	14 (43.8)	8 (25)	20 (32.3)	26 (35.1)
	II	1 (50)	15 (65.2)	18 (56.3)	24 (75)	42 (67.7)	48 (64.9)
Sex	**f**	2 (100)	15 (65.2)	14 (43.8)	15 (46.9)	39 (62.9)	35 (47.3)
	m	0 (0)	8 (34.8)	18 (56.3)	17 (53.1)	23 (37.1)	39 (52.7)
Age	**<50**	0 (0)	2 (8.7)	0 (0)	2 (6.3)	3 (4.8)	3 (4.1)
	50-59	0 (0)	2 (8.7)	5 (15.6)	2 (6.3)	8 (12.9)	6 (8.1)
	60-69	0 (0)	2 (8.7)	8 (25)	8 (25)	9 (14.5)	18 (24.3)
	70-79	2 (100)	14 (60.9)	14 (43.8)	16 (50)	29 (46.8)	32 (43.2)
	80-89	0 (0)	3 (13.0)	5 (15.6)	4 (12.5)	13 (21.0)	15 (20.3)
Smoker	**current**	0 (0)	5 (21.7)	6 (28.1)	3 (9.4)	10 (16.1)	5 (6.8)
	never	1 (50)	10 (43.5)	17 (53.1)	10 (31.3)	27 (43.5)	27 (36.5)
	past	1 (50)	5 (21.7)	8 (25)	13 (40.6)	12 (19.4)	26 (35.1)
	unknown	0 (0)	3 (26.1)	1 (6.3)	6 (18.8)	13 (21.0)	16 (21.6)

4.1.3 Survival when obesity is defined by VFA and WC

Overall, 31/136 patients did not reach the 5-year survival point (22.8%). Based on VFA, nine patients were non-obese females, six were non-obese males, twelve were obese females and four were obese males (22.0%, 15%, 36.4% and 18.2% of the respective groups) (Figure 18A). This showed a decrease in OS in obese females, with non-obese patients and obese males having similar rates of survival. Based on WC, thirteen patients were non-obese females, two were non-obese males, eight were obese females and eight were obese males (representing 46%, 8.7%, 22.9% and 20%) (Figure 18B). This demonstrated a decrease in OS in non-obese females compared to obese females, but no large difference in survival in male patients. None of these groups were statistically significantly different.

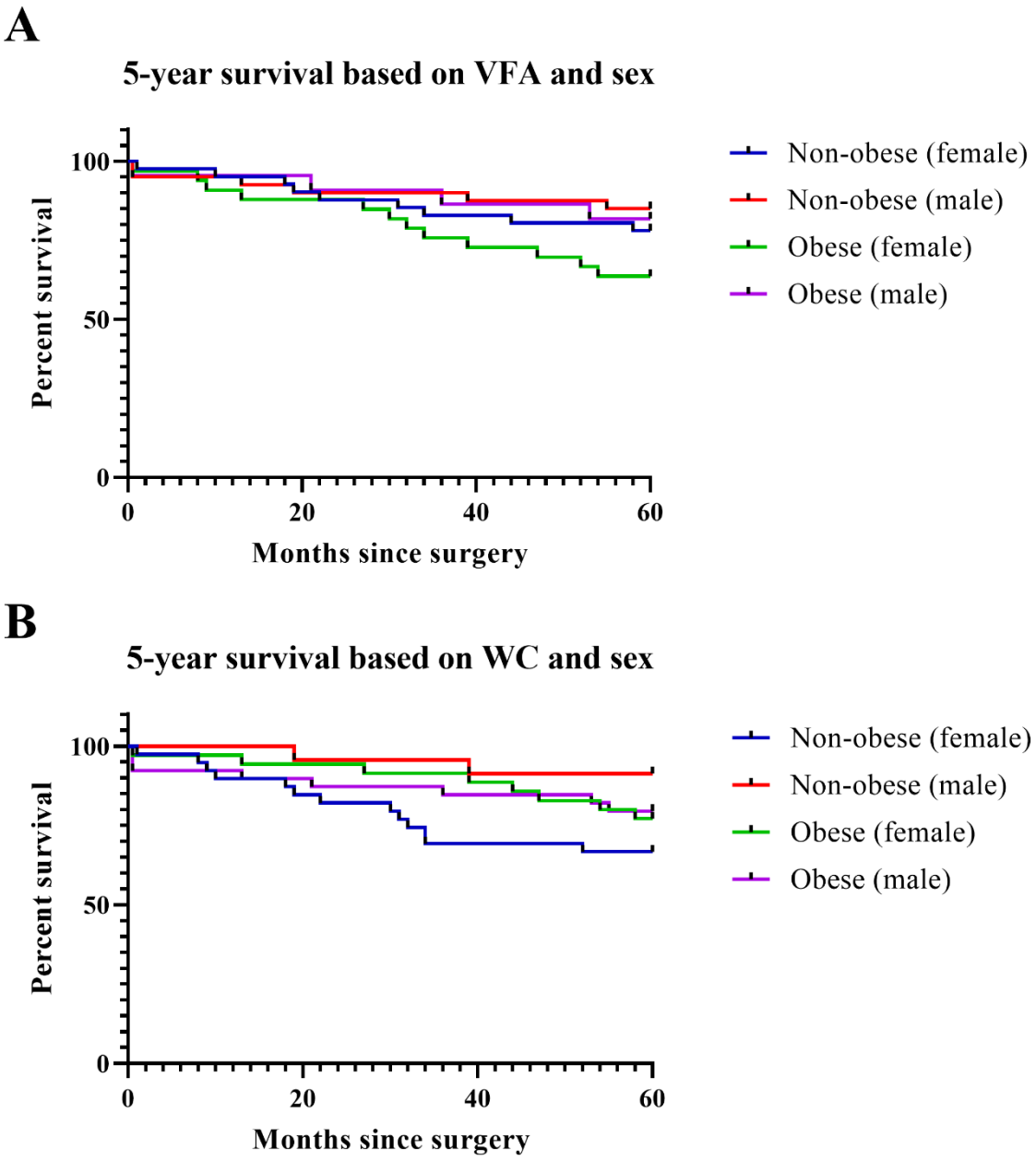

Figure 18: 5-year survival of stage I and II colorectal cancer patients based on VFA and WC defined obesity

A) Obesity based on VFA (visceral fat area) was defined as > 80.1 cm^2 for females and > 163.8 cm^2 for males. Obese females *n*=33, obese males *n*=22, non-obese females *n*=41, non-obese males *n*=40.

B) Based on WC (waist circumference), obesity was defined as > 93 cm for females and > 100 cm for males. Obese females *n*=35, obese males *n*=39, non-obese females *n*=39, non-obese males *n*=23.

Statistical differences were determined using a Mantel-Cox test.

4.1.4 Survival when obesity is defined by BMI, and skeletal muscle index

BMIs were calculated for 89/136 patients (65.4%), with documented height and weight measurements. As there were no sex-specific cut-offs for BMI ranges, and as this would reduce group sizes, groups were not split into male and female patients. Of patients who had their BMI documented and died after surgery before the 5-year follow up period was reached, one was underweight, six were of normal-weight, six were overweight, and five were obese (representing 50%, 26.1%, 18.8% and 15.6% of their groups). This showed that 5-year survival was similar in overweight and obese patients, and increased compared to normal weight patients (Figure 19A) although this was not statistically significant. OS was worse in underweight patients, however, this outcome is misleading as the cohort was n=2, with one patient surviving past 5 years.

L3SMIs were determined for 92/136 (67.6%) of patients as height was required for this calculation. From this cohort nineteen patients died, of which four were sarcopenic females and three were sarcopenic males (representing 21.1% and 11.5%), while nine were normopenic females and three were normopenic males (31.0% and 20%). This indicated that those who were defined as sarcopenic had a trend of an increased OS compared to those with normal muscle mass (Figure 19B).

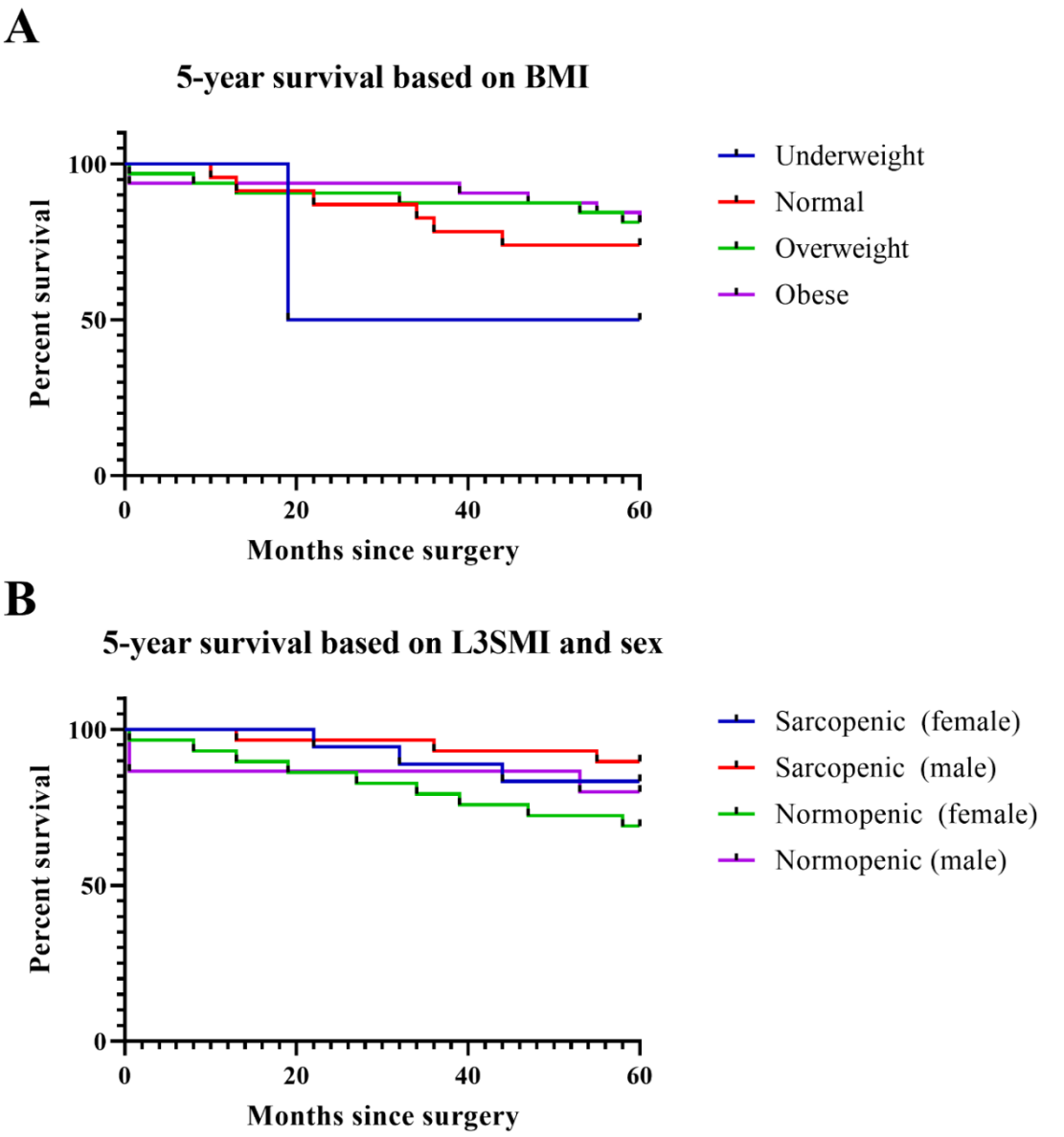

Figure 19: 5-year survival of stage I and II colorectal cancer patients stratified based on BMI and L3SMI

A) Obesity based on BMI (Body Mass Index), definitions were the following: underweight (< 18.5 kg/m^2), *n*=2, normal weight (18.5-24.9 kg/m^2), *n*=23, overweight (25-29.9 kg/m^2), *n*=32, and obese (> 30 kg/m^2), *n*=32.

B) Sarcopenia defined by L3SMI (skeletal muscle index at the third lumbar vertebra) is < 38.5cm^2/m^2 for females and < 52.4 cm^2/m^2 for males. Sarcopenic females *n*=19, sarcopenic males *n*=29, normopenic females *n*=15, normopenic females *n*=29.

Statistical differences were determined using a Mantel-Cox test.

4.1.5 Survival based on tumour stage and sex of patient

The four parameters identified as possibly affecting the above results were tumour stage, age at the time of surgery, sex, and cigarette smoking status. Out of 136 patients, forty-six (33.8%) had stage I while ninety (66.2%) patients had stage II colorectal cancer. 11/46 (23.9%) stage I patients did not reach the 5-year survival point while 20/90 (22.2%) stage II patients died, indicating that there is no difference in OS between stage I and II colorectal cancer patients (Figure 20A).

From the cohort, seventy-four (54%) patients were female while sixty-two (45.6%) were male. 21/74 (28.4%) of females died and 10/62 (16.1%) of males died, however, this was not statistically significant. Overall this shows that males have a trend of increased 5-year survival compared with females (Figure 20B).

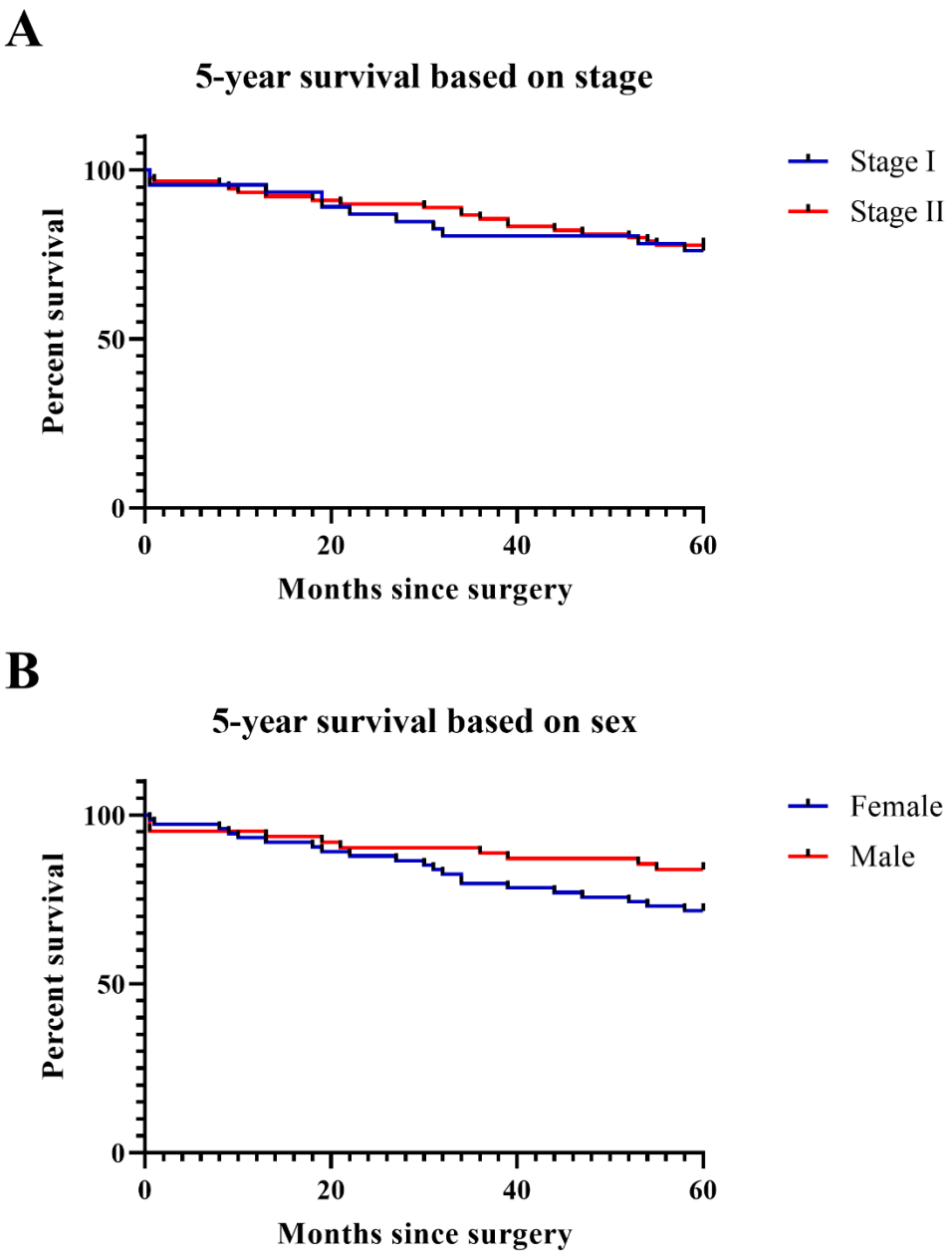

Figure 20: 5-year survival of stage I and II colorectal cancer patients based on tumour stage and sex

Numbers of patients from the cohort in each group:

A) stage I *n*=46, stage II *n*=90.

B) female *n*=74, male *n*=62.

Statistical differences were determined using a Mantel-Cox test.

4.1.6 Survival based on the age and smoking status of patients

Based on age, 6/136 patients were < 50 years old at the time of surgery, 14/136 were between 50-59, 27/136 were between 60-69, 61/136 were between 70-79 and 28/136 were between 80-89 years old. No patients were aged 90 or above. All patients < 50 and between 50-59 years reached the 5-year survival point. 3/27 (11.1%) patients between 60-69, 16/61 (26.2%) of patients between 70-79, and 12/28 (42.9%) patients between 80-89 years old died. This showed that patients with colorectal cancer were less likely to survive beyond 5 years past surgery over the age of 60 years (Figure 21A). This was statistically significant between the ages of 50-59 and 70-79 ($p = 0.040$), 50-59 and 80-89 ($p = 0.0057$), and 60-69 and 80-89 ($p = 0.0059$).

Finally, 54/136 patients had never smoked, 15/136 patients smoked at the time of surgery, and 38/136 patients were ex-smokers. Information about the smoking status of thirty-two patients was not able to be obtained. 7/54 patients (13.0%) who had never smoked, 3/15 (20%) of current smokers, and 12/38 (31.6%) of ex-smokers died within 5-years post-surgery. There was a trend that current smokers were at greater risk of dying than people who have never smoked. In this cohort, patients who had previously smoked but had quit by the time of surgery were at a statistically significantly higher risk of dying than those who had never smoked ($p = 0.0316$) (Figure 21B).

Overall, this information indicates that differences in body composition groups, such as sex, age, and smoking status, but not tumour stage, may be acting as confounding factors in this data.

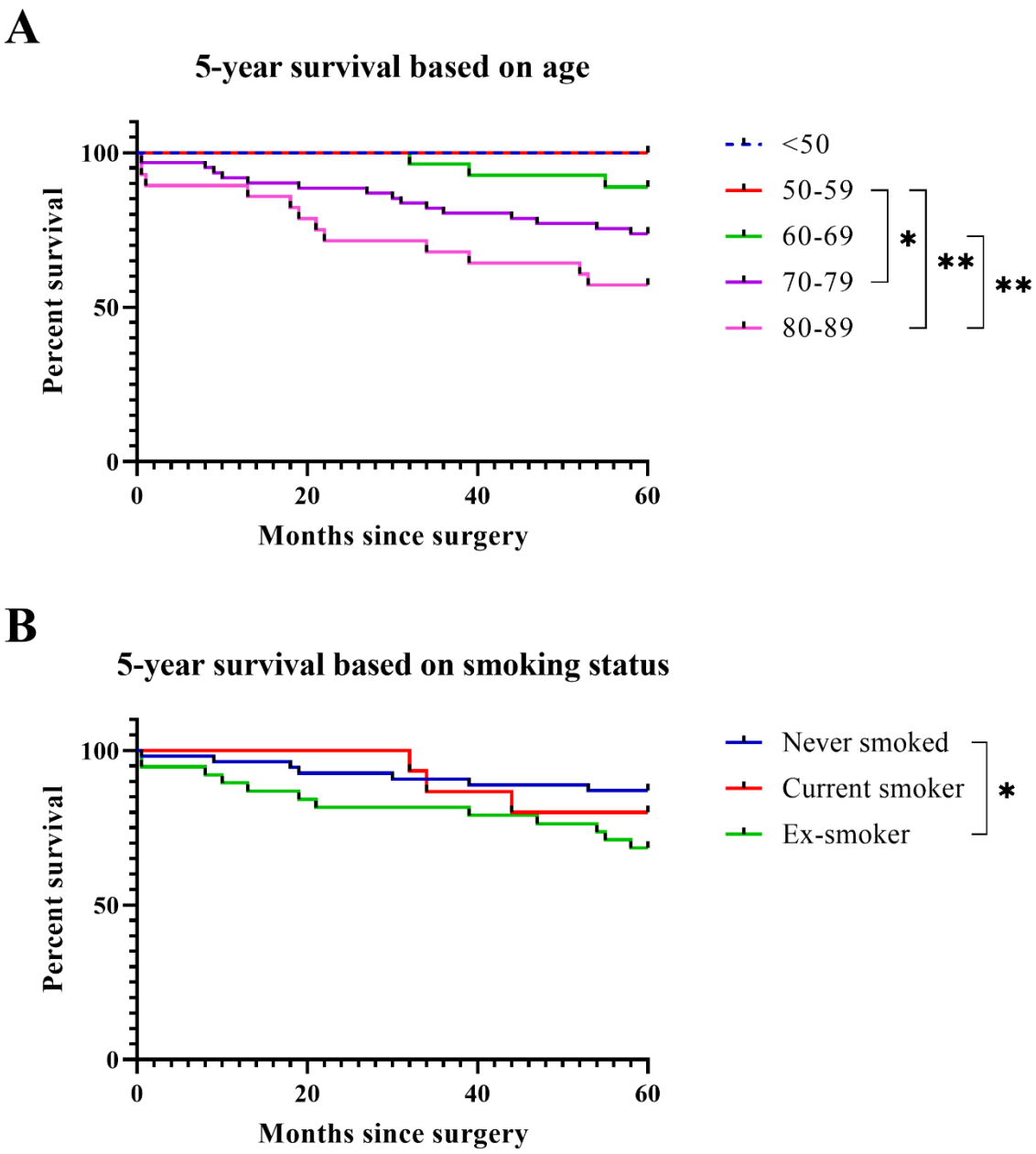

Figure 21: 5-year survival of stage I and II colorectal cancer patients based on age and smoking status

Numbers of patients in the cohort in each group:

A) < 50 years *n*=6, 50-59 years *n*=14, 60-69 years *n*=27, 70-79 years *n*=61, 80-89 years *n*=28.

B) never smoked *n*=54, current smoker *n*=15, ex-smoker *n*=38.

Statistical differences were determined using a Mantel-Cox test. * $p \leq 0.05$, ** $p \leq 0.01$

4.2 Differences in markers of inflammation in obesity and sarcopenia

To examine any differences in immune cell numbers between body composition types, patients were stratified based on visceral obesity and muscle mass based on L3SMI. Data was obtained from blood tests performed up to 3 months prior to surgery.

When comparing non-obese and obese patients, there were no statistically significant differences however several trends were observed. Eosinophil, monocyte, CEA and haemoglobin levels (Figure 22B, D, H, I) were similar in both obese and non-obese patients. Basophils, neutrophils and platelet numbers were decreased in obese patients (Figure 22A, E, F), while lymphocyte and albumin levels were increased (Figure 22C, J). The neutrophil to lymphocyte ratio (NLR), which is a marker of systemic inflammation and is the total neutrophil count divided by the total lymphocyte count, was decreased in obese patients (Figure 22G) (150).

Comparing sarcopenic and normopenic patients showed that eosinophil, monocyte, and haemoglobin levels were similar (Figure 23B, D, I). Basophils, neutrophils, platelets, CEA and albumin levels were raised in sarcopenic patients (Figure 23A, E, F, H, J). Lymphocytes were decreased in sarcopenia (Figure 23C). The NLR was raised in sarcopenic patients (Figure 23G).

CEA, which is used clinically as a biomarker for colorectal cancer, is known to be increased in patients who smoke cigarettes (151). However, only 11.1% of non-obese patients, 9.1% of obese patients, 16.7% of sarcopenic patients and 13.6% of normopenic patients smoked at the time of surgery, so this is unlikely to have affected the results greatly.

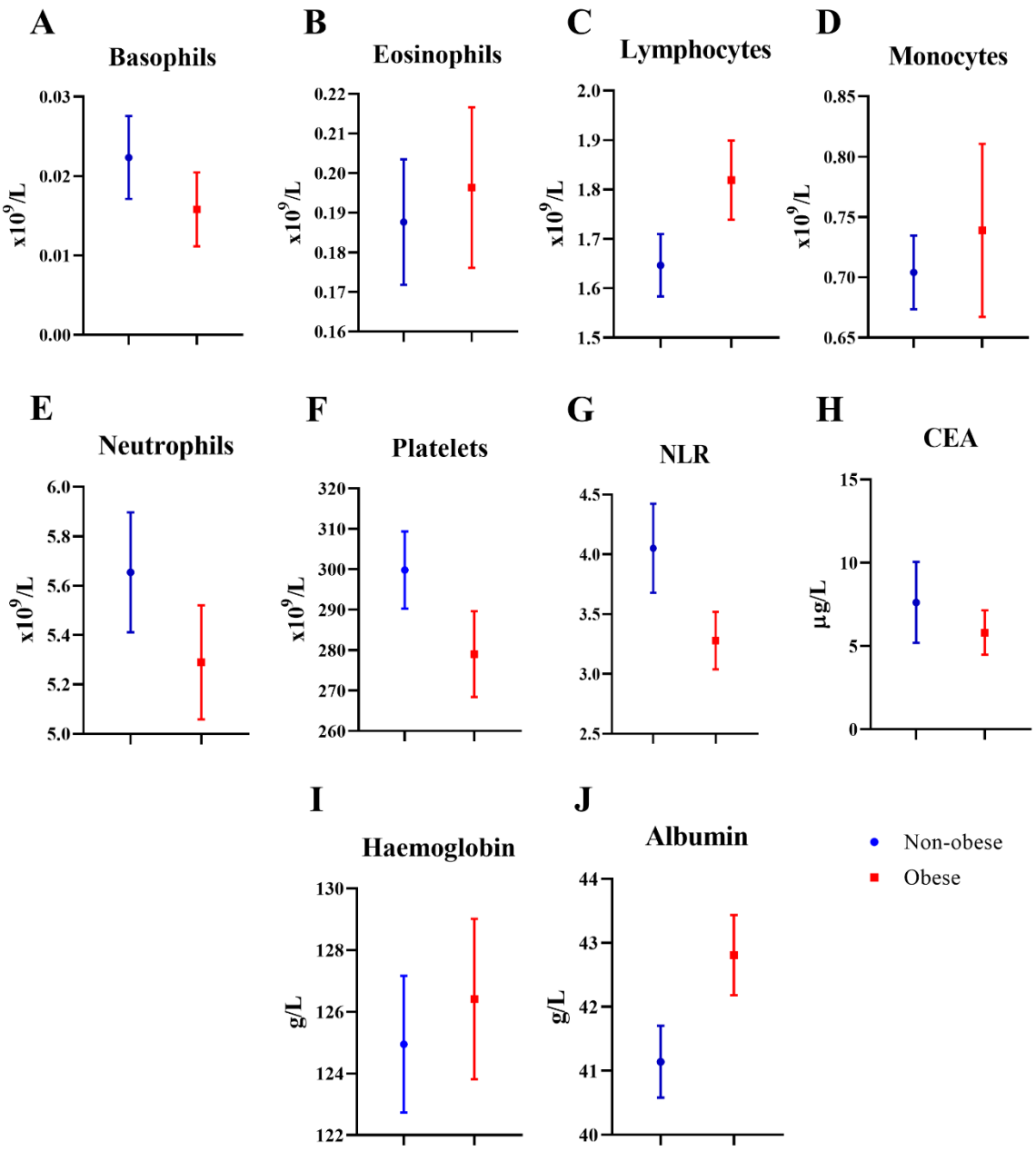

Figure 22: Immune cell populations in the blood of colorectal cancer patients stratified based on obesity

The results represent the mean (± SEM) of 136 patients grouped based on visceral fat area-classified obesity. An unpaired student's t-test was used to assess significance.

CEA: carcinoembryonic antigen, NLR: Neutrophil/lymphocyte ratio.

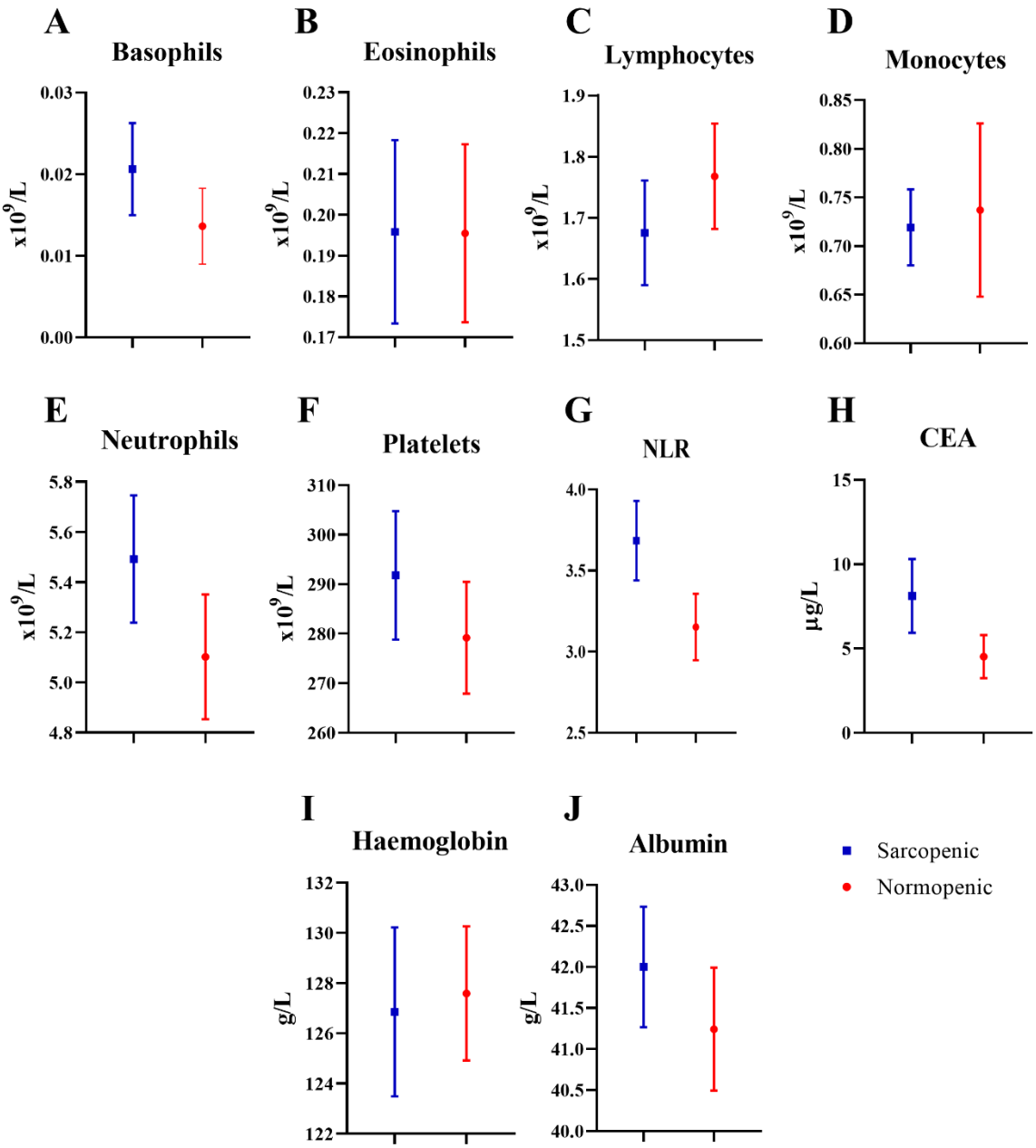

Figure 23: Immune cell populations in the blood of colorectal cancer patients stratified based on muscle mass

The results represent the mean (± SEM) of ninety-two patients grouped based on skeletal muscle index at the third lumbar vertebra classified sarcopenia. An unpaired student's t-test was used to assess significance.

Chapter 5

Discussion

Over a third of New Zealanders are overweight, obese, or suffer from other metabolic disorders, and this rate increases in Māori and Pacific populations (70, 80). Therefore, understanding how therapies should be adapted in this setting is an important issue. Obesity has been linked to reduced responses to immunotherapies and vaccines, although there is some evidence that overweight and obese patients with melanoma respond better to immune checkpoint inhibitors (129). Conditions associated with hyperuricemia have been found to cause an increase in the risk of developing cancer, and patients who are hyperuricemic at the time of cancer diagnosis are more likely to have poorer outcomes (84). However, little is known about the effects of uric acid on cancer and cancer therapy.

Previous experiments in the Young laboratory have demonstrated the efficacy of the surv.VLP-SS-MUC1 and surv.VLP vaccines in models of breast and colorectal cancer (52, 53, 58, 138, 152). However, these trials only used lean mice. Obesity creates a state of chronic inflammation, increases thymic destruction resulting in a reduced number of naïve T-cells, and impairs the ability of T-cells to circulate efficiently (110). This underlying inflammatory state is important to address when considering the success of immunotherapies. Furthermore, clinical trials have seen significant benefits of immunotherapies in some patients but not in others, and it would be useful to understand possible reasons why there is such a variation in outcome (153). Therefore, the VLP treatments previously proven to be efficacious by the Young laboratory were tested in mouse models of obesity and hyperuricemia.

Building on preliminary experiments, this project was centred on a series of tumour trials performed in lean, obese, and hyperuricemic mice in order to determine if tumour-bearing mice responded differently to VLP or VLP in combination with the immune checkpoint inhibitor anti-PD-L1. It was hypothesised that combination therapy may be beneficial to overcome the effects of these co-morbidities on the immune system.

Finally, while murine models are useful, human data is more relevant to medical practice. Colorectal cancer patient data was accessed via the Dunedin colorectal cancer cohort. This data was used to stratify the cohort based on obesity and muscle mass status and assess whether these factors influenced survival up to five years post-surgery. Furthermore, cell populations in the blood were analysed for changes potentially influenced by these body composition factors.

5.1 Tumour growth and survival following immunotherapeutic treatment

Treatment with VLP alone caused a very slight increase in survival in obese and hyperuricemic mice compared to lean mice with breast cancer. Conversely, VLP combined with anti-PD-L1 treatment resulted in a statistically significant increase in survival in lean mice, however, this was not the case in obese and hyperuricemic mice. This initial evidence suggests that the underlying metabolic disorders of obesity and hyperuricemia cause a diminished response to therapy with checkpoint inhibitors, and so treating patients with this kind of therapy who suffer from these conditions may not be efficacious.

In a colorectal cancer setting, VLP treatment resulted in an improvement in survival for obese mice, although this was not the case in lean and hyperuricemic mice. The same trend was observed in mice treated with VLP + anti-PD-L1. However, these results need to be interpreted with some caution as the lean mice grafted with both types of cancer did not respond to the treatment as has previously been shown.

Interestingly, the overall benefit of anti-PD-L1 treatment was decreased in colorectal cancer compared to breast cancer. This shows that even at a mouse model level, there is a difference between the types of cancers, even though both tumour models expressed PD-L1 (136).

Other studies have found a significant increase in the efficacy of anti-PD-L1 treatment in obese mice and humans (101). This was not the case in the obese mice with breast cancer in this study, although it did have increased efficacy in some obese mice in the colorectal cancer model. One reason why this benefit was not observed in high amounts in the study may have been due to the model of obesity used. In diet-induced obese (DIO) mice, leptin levels are increased compared to lean mice, which is positively correlated with an increase in PD-1 expression (101). However, leptin receptor-deficient (POUND) mice do not have this upregulation (101). While the POUND mice mimic obesity in many ways, the changes to the PD-1/PD-L1 pathway may be missing. There are other mechanisms which can result in the upregulation of PD-1/PD-L1 expression, however, it is likely that this was the reason why an increase in the efficacy of this checkpoint inhibitor was not observed in the obese mice.

An issue encountered during these trials were a significant amount of tumour ulceration. This particularly affected the breast cancer trials for all mouse types, and the colorectal cancer trial in Urah$^{Plt2/Plt2}$ mice. Possible reasons for ulcerations include self-induced trauma, mechanical trauma (such as tumours rubbing against the bedding), rapid tumour growth, or contamination of the tumour (154). Attempts to reduce ulcerations were made by ensuring that cages contained only the softest bedding available. The location of the breast cancer grafting site was also changed from the second to the fourth MFP to reduce rubbing.

When it became apparent that this issue had affected several different tumour trials conducted by different members of the Young laboratory, those involved compared data around ulcerations. It was observed that a higher frequency of ulcerations than normal started occurring from the end of 2018. Possible reasons were identified as (i) the mice may have already been contaminated with a pathogen that was not screened for, (ii) the

environment they were housed in, or (iii) the mice may have been inoculated with a pathogen at the time of the injection of tumour cells.

The mice and cell lines were sent to the Cerberus Sciences lab in Australia to be tested for possible contamination, however, the results from this are still not available. Recent experiments which cultured cells with penicillin and streptomycin saw no ulcerations in the mice inoculated with cells grown in the presence of an anti-fungal agent as well, but several ulcerations in the mice inoculated with cells not cultured in this. These findings further strengthen the hypothesis that a fungal infection was the reason behind the ulcerations. As to where this infection was being introduced is currently unknown. As the mice that had tumours ulcerate were censored from the data, this reduced the size of the groups of mice analysed. In doing so, this affected the power of the statistical analysis.

The other major issue was the unexpected decrease in efficacy of the VLP to reduce tumour growth and increase survival in both breast and colorectal cancer. There are several reasons why this may have occurred, considering that an improvement in survival had been observed in lean mice using the same VLP treatments previously. The most likely reason was that the measured concentration of VLP was incorrect. Before treatments were given, the concentration of the VLP was measured using a NanoDrop, which measures the amount of protein in a particular sample. Unfortunately, other people working in the same laboratory noticed increasingly varied results from this piece of equipment, indicating that it may not have been producing reliable results. When compared to the Qubit protein assay, the NanoDrop was giving higher readings. This may have led to the mice receiving a reduced dose of VLP, hence the treatment not working as before. Backing this up is that the only mice who had VLP measured using the Qubit assay were the obese mice grafted with colorectal cancer. These mice had the greatest improvement in survival when treated by VLP alone.

5.2 Frequencies of TILs in breast and colorectal cancer

To understand why the VLP wasn't protecting the mice against tumour growth, a small number of tumours from lean, obese, and hyperuricemic mice with either breast or colorectal cancer were preserved in formalin and stained for lymphocyte infiltration. As only two tumours per treatment group were able to be analysed, this meant that statistical analysis could not be performed, so all observations made were described as trends. However, we were still able to do some basic assessment of T-cell infiltration.

Previous unpublished work in the Young lab has shown that smaller tumours have a greater number of T-cells migrating to the centre of the tumour, but with tumour progression T-cells accumulate in the periphery of the tumour. As tumours were only removed once they had grown to the maximum size of 150 mm^2, fewer T-cells were expected to be observed in the centre of the tumours.

In the breast cancer models, obese and hyperuricemic mice had a diminished frequency of TILs compared to lean mice. This pattern was the same in all treatment groups in both the centre and peripheral parts of the tumours, except for hyperuricemic mice treated with VLP where there was an increase in the amount of T-cells in the periphery. This suggests that T-cells in metabolically compromised mice have a reduced ability to invade tumours regardless of the treatment, and therefore immunotherapies are less likely to be successful. This may have played a role in why these mouse types were not as successful as the lean mice in reducing tumour growth when treated with the combination therapy.

In colorectal cancer tumours, there was no change in the frequency of TILs in obese mice treated with PBS or the combination therapy compared to lean mice, with hyperuricemic mice having a reduced amount. Interestingly, when treated with VLP the number of TILs increased in all areas of the tumour in obese and hyperuricemic mice but decreased

slightly in lean mice. This may suggest that the T-cells in the obese and hyperuricemic mice had an increased ability to infiltrate the colorectal tumour tissue when stimulated compared to lean mice. An increase in TIL frequency is generally thought to be linked to greater survival, which was observed in the obese mice (155).

In the obese mice with colorectal cancer, the VLP group had an increase in median survival compared to the PBS group. This can perhaps be explained by the increase in TIL frequency in these tumours, whereas survival was not improved by VLP in the lean mice, hence a lower frequency of TILs. However, the increase in the frequency of TILs in the VLP group in hyperuricemic mice did not result in any improvement in survival, suggesting that these lymphocytes may not have been as effective at invoking an effector response. A study comparing C57BL/6 mice to Urah$^{Plt2/Plt2}$ mice found that hyperuricemic mice were less capable of causing a reduction in tumour growth when given immunotherapeutic treatment against melanoma (131). This difference was attributed to a reduction in the proportion of antigen-specific $CD8^+$ T-cells (characterised as $CD39^+$, as discussed in section 5.3) (131). However, while hyperuricemic mouse tumours underwent immunohistochemical staining, flow cytometric analysis was not performed so it cannot be confirmed if this was the case in these mice. This decision was made due to the high number of ulcerations in the tumour trials, so in order to reduce the numbers of mice used in this project, only lean and obese mice were used for further TIL analysis.

Overall, there was reduced T-cell infiltration in MC-38 tumours compared to C57mg.MUC1 tumours. PD-L1 is expressed by MC-38 cells once stimulated by IFNγ, while it is present on unstimulated C57mg.MUC1 cells (136). This is likely to have caused diminished expression of PD-L1 receptors as CTLs are a source of IFNγ. This

may have caused the reduced response to anti-PD-L1 treatment compared to the C57mg.MUC1 tumours.

A higher frequency of $CD3^+$ TILs in the centre of the tumour has been associated with an improved response to neoadjuvant chemotherapy in breast cancer (156). The type, density, and location of lymphocytes within human colorectal cancers has also been shown to be a good predictor of patient survival (157). Therefore, analysing TIL distribution and frequency may be important in predicting the outcome of treatment. There is not a large number of studies comparing the frequency of TILs in tumours based on obesity status, although one study looking at prostatectomy tissue did not find a correlation between TIL number and BMI status (158). Evidence from these tumour trials has shown a trend towards a difference in TIL frequency between lean, obese, and hyperuricemic mice. Interestingly, differences between mouse strains were not consistent between breast and colorectal cancer models. This implies that there are more complex interactions occurring between the metabolic differences, the types of tumour cells, and the TME.

5.3 Characterisation of TILs in mice grafted with breast or colorectal cancer tumours

An important consideration when looking at TILs is whether they are tumour-specific (and so capable of making an effector response against the tumour cells), characterised by co-expression of PD-1 and CD39. In the breast cancer model, obesity did not result in a difference in the frequency of tumour-specific $CD4^+$ T-cells. $CD8^+$ T-cells, however, which are important for tumour cell killing, tended to be more tumour specific in the obese mice than the lean mice. Immunotherapeutic treatment did not modulate this pattern.

It is worth noting that tumours were only stained once they had reached the 150 mm^2 endpoint and hence achieved immune escape. It is possible that the reason there was no difference observed in the mice that had immunotherapeutic treatment was that the T-cells were not phenotyped when they had their greatest effect. Previous unpublished data from the Young laboratory stained TILs taken from lean and obese mice as tumours grew and showed that there is an increase in tumour-specific T-cells as tumour burden increases, however, these cells also become more exhausted. This showed that lean mice initially had a higher frequency of antigen-specific $CD4^+$ T-cells. However, by day 21, the obese mice had higher numbers. Equal levels of antigen-specific $CD8^+$ T-cells were observed at this time point. More research needs to be done into this field to confirm these initial findings but this evidence suggests that obese mice may be able to generate a stronger antigen-specific T-cell response as tumours burden increases.

When T-cells are continuously stimulated by antigen, such as in the TME, they are known to convert to an exhausted form. Once exhausted, the effector response becomes reduced and the numbers of antigen-specific T-cells are depleted (32). This is an important reason why cancers are poorly controlled by the immune system. Exhausted T-cells have upregulated expression of several inhibitory immune checkpoint receptors such as PD-1 once initially exhausted, and Tim-3 and LAG-3 when terminally exhausted (32).

When TILs from breast cancer tissue were stained for these markers, there were differences in co-expression of PD-1 and Tim-3, and PD-1 and LAG-3 on T-cells between obese and lean mice. LAG-3 expression, which was more common in $CD4^+$ T-cells than $CD8^+$ T-cells, was raised in obese mice compared to lean mice. Conversely, $PD\text{-}1^+$ $Tim\text{-}3^+$ T-cells, which were at similar levels for both T-cell subtypes, were reduced in obese mice. As both receptors are upregulated in terminally exhausted T-cells, it was expected that if obesity caused an increase in T-cell exhaustion there would have been

an increase in the expression of both markers in these mice. One study found that $CD8^+$ TILs in DIO mice expressed higher levels of PD-1, Tim-3 and LAG-3 compared to lean mice (101). It was unclear as to why Tim-3 was downregulated in the TILs of obese mice in this study.

T-cells were also isolated from the spleens of mice with breast cancer in each treatment group. As the cells were located within tumour-free tissue, they can be used to compare the functionality of T-cells in the periphery versus those localised in the tumour (159). Expression of all markers of exhaustion were downregulated in splenocytes compared to TILs, so the high rate of exhaustion in the TILs was most likely due to the tumour tissue as opposed to being a baseline characteristic of the T-cells. There were trends of an increase in expression of all markers of exhaustion in the obese mice compared to lean mice. This could mean that in this study, obesity resulted in a higher level of T-cell exhaustion. This would mean that the T-cells were less capable of making a meaningful response against the tumour cells in the first place.

In the colorectal cancer model, both lean and obese mice had similar frequencies of tumour-specific T-cells, which increased in both treatment groups. In conjunction with the information about the frequency of TILs inside the tumour tissue, it shows that while there was no difference in total T-cell numbers, the percentage of cells which were tumour specific increased with treatment.

The frequency of terminally exhausted $CD8^+$ T-cells in mice grafted with colorectal cancer showed a trend of generally increasing in the VLP and VLP + anti-PD-L1 treatment groups compared to the PBS group. This observation was similar in both lean and obese mice.

It is interesting that obesity did not cause a difference in either T-cell infiltration frequency or the rate of T-cell exhaustion in mice grafted with colorectal cancer, while in the breast cancer models obese mice had both a reduction in T-cell infiltration and a general trend of increased exhaustion. MC-38 tumours also had a much lower rate of T-cell invasion than C57mg.MUC1 tumours. As the TME varies between tumour types, this is plausible. The importance of this is that when modulating VLP-based immunotherapies for different types of cancers, it may not be just a matter of changing epitopes. If certain environments are more difficult or hostile to infiltrate, this will also have to be mediated.

As detailed earlier, there was a reduced response to the VLP treatment in both cancer types compared to what had been shown in previous studies. Therefore, T-cell exhaustion may be different in mice with tumours that had successfully reduced growth as a result of the treatment. Once the problem with the VLP has been resolved, it would be beneficial to repeat this staining, because there may be other factors at play causing the T-cell exhaustion.

As will be discussed in section 5.8, analysis of TILs in tumours of non-obese and obese humans could be investigated in the future. However, from this data, obese patients may have increased benefit from anti-LAG-3 treatment against breast cancer compared to lean patients, while lean patients may benefit from treatment with anti-Tim-3. Both lean and obese patients with colorectal cancer may benefit equally from these treatments. Anti-LAG-3 therapies are currently in clinical trials, while anti-Tim-3 is a less desirable target due to being expressed on a variety of immune cells (160).

5.4 Changes to immune populations in the blood following MC-38 tumour challenge

As this project was being undertaken, it was decided that it would be beneficial to see if there were any changes to the frequencies of different types of immune cells in the blood. Along with T-cells and DCs, other immune cells measured were B-cells (which produce antibody in response to a foreign antigen), neutrophils (one of the most common white blood cells to respond to an injury or infection), and inflammatory monocytes (contribute to inflammation by secreting cytokines into the blood, and can differentiate into macrophages in tissue) (161). This was only performed for the colorectal cancer models, but differences observed in the breast cancer model would be useful to elucidate at a later date.

Following tumour-grafting, neutrophils and inflammatory monocyte counts were raised in obese mice, which also had reduced frequencies of lymphoid-derived DCs and B-cells compared to lean mice. Neutrophils and inflammatory monocytes have previously been shown to be increased in obesity, and an increase in these innate immune cells correspond to the chronic level of inflammation seen in this disease state (162). DCs are crucial for the presentation of antigens to cells of the adaptive immune system. If obesity causes a reduction in the levels of these cells, it may result in a reduced ability of the immune system to respond to immunotherapies. The secretion of antibody by B-cells, while not studied in this context, is important for the function of most vaccines and so this data also backs up previous research surrounding a reduced long-term efficacy of vaccines in obese patients (127).

Obese mice had higher levels of $CD4^+$ T-cells before therapy was initiated compared to lean mice, although the level of $CD8^+$ T-cells was similar in both mouse types. This is consistent with clinical findings, where obesity has been linked to a higher total

lymphocyte count (163, 164). However, after tumour-grafting the frequency of $CD4^+$ T-cells in lean mice increases to be similar to that of the obese mice. Similarly, $CD8^+$ T-cells were higher in lean mice compared to obese mice a week. This could mean that the underlying inflammation brought about by obesity meant that these mice were unable to create as strong a T-cell response against the tumour cells. No differences in the frequency of any of the immune cells measured were found between the treatment groups.

Clinical trials have found that an increased lymphocyte count following immunotherapeutic treatment is positively correlated with prognosis (165). There were no difference in circulating T-cell frequency between treatment groups in either mouse type, which could help to explain the low overall response rate in the mice.

In July 2019 a paper was published which outlines a comprehensive method to monitor a variety of immune populations using flow cytometry (166). It is yet to be seen if this will be taken on board in clinical trials, and whether information from this correlates with the data found here.

5.5 The role of body composition in the survival of patients with colorectal cancer

There have been very few studies performed which look at how obesity affects the survival of cancer patients, and those that do use BMI as an index of obesity. There are currently several different ways that obesity can be measured, with growing consensus that measuring visceral adipose tissue may look more specifically at the pathological effects of fat (132).

In this project, data from stage I and II colorectal cancer patients were analysed for the impact of obesity on cancer outcomes. These patients were chosen because they were less likely to be cachexic than those with more advanced disease. Cachexia causes severe

weight loss and muscle wasting, and strongly influences the body composition status of patients, hence acting as a confounding factor (167). Limiting the cohort to only stage I and II patients aimed to reduce the effect of this. Furthermore, because it was unknown from the outset of the project how many patients would have obtainable data, only stage I and II patients were used in order to make data extraction feasible in the time frame allowed for this project.

BMI is a frequently used measure of obesity in the clinic. Similar to observations in other studies, overweight and obese patients classified by BMI had a trend of slightly higher rates of survival than normal-weight patients (105, 106). WC is also commonly used, however, interestingly the effect of obesity differed by sex. When measuring WC, female obese patients had a higher rate of survival than their non-obese counterparts. In male patients, obesity had the opposite effect. Female patients had lower survival rates than males.

As mentioned, visceral adiposity has a greater pathology associated with it and may prove to be more useful when looking at the effects of obesity on disease outcome. Compared to BMI and WC, it takes longer to obtain this measurement as a CT scan is required. However, if a scan is already available then it only takes a few minutes to measure that fat mass and interpret the results. Furthermore, once trained correctly a radiologist would not be required to perform this task.

Obesity measured in this way gave different outcomes than when measured by BMI or WC. Females (both non-obese and obese) had a trend towards worse survival than males, with obese females having lower survival rates than non-obese females. Obese males, non-obese males, and non-obese females had similar survival rates. This is interesting for several reasons. Firstly, when taking the measurements, it was noticed that many of the patients had significant fat mass in the subcutaneous fat layer however they had

minimal fat within the abdominal wall. This resulted in these patients being defined as obese by waist circumference (and most likely by BMI) but non-obese by VFA. This shows that there is a group of patients who would normally be defined as obese but have a low amount of fat in the abdominal cavity, which is more pathological. Secondly, measuring obesity by VFA accounts for differences in the distribution of fat between men and women. Men store up to 30% of their total body fat in the abdominal compartment regardless of obesity status whereas women collect adipose tissue peripherally and only attain significant visceral fat once some level of obesity has been reached (140). By measuring VFA using sex-specific thresholds, this difference can be accounted for.

The differences observed in overall survival between men and women is likely due to the differences in fat deposition. Compared to men, women have a higher body fat percentage however more of this is in the subcutaneous and gluteo-femoral regions than the intra-abdominal region (168). This distribution has been linked to a decreased risk of diabetes, cardiovascular disease, and overall morbidity and mortality. Furthermore, women who have higher rates of fat deposition in the abdomen suffer from the same metabolic issues as men (168). Studies have also found that increase visceral adipose tissue is an independent risk factor for colorectal adenoma, whereas an increase in subcutaneous adipose tissue can be beneficial (169, 170). This may explain why an increase in survival in obese women was observed when obesity was determined by waist circumference. This will largely be considering subcutaneous tissue, as opposed to VFA, which only focuses on the disadvantageous visceral adipose tissue. Men have a higher amount of visceral adipose tissue to start with, so more of the waist circumference measurement will be related to the amount of visceral fat the male patients have. This may explain why obese males have worse survival rates when classified by waist

circumference. It is currently unclear why there was no difference in males based on VFA.

The other aspect of body composition is muscle mass, which is decreased in the elderly and associated with several chronic conditions (77). When split into groups based on sarcopenia, surprisingly the normopenic patients had a trend of a lower survival rate than the sarcopenic patients. This was the same for both females and males, with both groups of females having reduced survival rates when compared to the male groups. This data conflicts with currently available evidence, which has shown that sarcopenia is correlated with increased mortality in a variety of cancer types, including head and neck cancer, non-small cell lung cancer, breast cancer, and colorectal cancer (108, 171-173).

One reason why this outcome may be different is that only patients with stage I and II colorectal cancer were investigated, so the majority of these patients would not have had follow-up chemotherapy or radiotherapy after their cancer resection surgery. Most studies performed in this area have expanded to all stages, with muscle mass affecting the outcome of additional treatments. The measurements for obesity were defined in European cohorts. 30% of people living in New Zealand identify as being an ethnicity other than of European origin, with the largest group being Māori (174). It is known that fat distribution differs by ethnicity, however, this was not accounted for in this study (175).

There are also limitations with using a skeletal muscle index for classifying sarcopenia. Firstly, the diagnosis of sarcopenia is usually multi-faceted, involving both assessment of muscle mass (e.g. CT scans) as well as physical performance measures (176). As the latter was not available, CT scans alone were used to classify the population. Secondly, normalising the muscle cross-sectional area to create a skeletal muscle index involved

the patient's height. Only 67.6% of patients had this information recorded, which limited the sample size.

Patient sex, age and smoking status at the time of cancer resection surgery were identified as influencing 5-year survival in this cohort. When looking at the baseline characteristics of the different groups, age was fairly evenly distributed. However, because there were statistically significant differences between the groups it would be important to account for this. There were differences in the smoking status and sex of patients in different groups. These were therefore likely to be acting as confounders and would need to be accounted for in further analysis.

5.6 Changes in immune cells frequencies based on body composition

Given the difference in outcomes observed for obese patients when using VFA as a measure, markers of inflammation in the blood were analysed to see if any changes here could explain this finding. Using results from the full blood count and other blood tests that patients had before surgery, trends were able to be observed between patients based on obesity (defined by VFA) and sarcopenia (defined by skeletal muscle index).

Obesity causes a state of chronic inflammation, with several studies finding an increase in the total lymphocyte, $CD4^+$ and $CD8^+$ T-cell count (163, 164). Our data confirms this finding, with the lymphocyte count being raised in obese patients. Information on specific types of lymphocytes was not able to be gathered, although this would be interesting to investigate. Other cell populations such as neutrophils and platelets have also been reported to be elevated in obesity, such as were reported in section 5.4 (162). Interestingly, data from this project does not corroborate with this, having found that cell counts for neutrophils and platelets were decreased in obesity. NLR is not thought to be correlated with increased BMI, however, in the patients analysed here, this was decreased

(177). The reduction in NLR indicates an increase in lymphocyte count but a decrease in neutrophil count.

Albumin is the most abundant protein in the plasma, making up approximately 52% of the total plasma protein content. Studies have found that albumin levels are reduced in obese states, with a negative correlation between BMI and albumin levels (178). This is likely due to albumin being a negative acute-phase protein, which decreases in response to inflammatory cytokines (179). As obesity stimulates an increase in pro-inflammatory cytokines such as TNFα, albumin levels would decrease (113). However, the results from this project show an increase in albumin levels in the obese group. Colorectal cancer itself may have had an impact on the findings. While patients with colorectal cancer in the ascending colon or rectum have not been correlated with a variation in albumin levels, those with cancer in the descending colon have been shown to have increased levels of albumin (180). Information on the location of tumours was not able to be gathered for this study.

Research into levels of immune cells as well as other markers of inflammation in sarcopenia is considerably lacking. One study found that sarcopenic patients have lower levels of haemoglobin and albumin (181). However, in this project, there was no change in haemoglobin levels and some increase in albumin levels. Lymphocyte counts have been found to be decreased and NLR increased in sarcopenic patients with small cell lung cancer (182, 183). Results from this project are in agreement with this. As lymphocytes make up the majority of the adaptive wing of the immune system, a decrease in these cells would result in a decreased ability to protect the body against foreign invaders or tumours, and may contribute to why sarcopenic patients have reduced cancer survival rates in most studies.

5.7 Limitations

Several issues occurred in this project, which are likely to have affected our results. Problems around a high frequency of ulcerations, and the VLP not working as observed in other trials previously have been explained in section 5.1.

Another limitation was the strain of mice used. The model used for obesity was the POUND mice, which have a deletion mutation in exon two of the leptin receptor gene on chromosome four, resulting in it lacking the leptin receptor (134). Leptin causes satiety, so this mutation renders mice unable to control the urge to eat. They quickly display features of metabolic syndrome from 8 weeks of age. This makes it an easy model to study obesity as opposed to DIO mice. However, as discussed earlier there was no consistently significant increase in efficacy of anti-PD-L1 treatment in the obese mice that other studies have shown and this may be due to the mutation itself. DIO mice may, therefore, be a better model to use in future work.

5.8 Future directions

Due to the change in the efficacy of the VLP observed in this project, many of the tumour trials will have to be repeated. Before this is done, the underlying issues of protein concentration measurements, tumour ulceration, and possible contamination of either the tumour cell lines or mice, need to be resolved.

A different assay (Qubit) was used for the final VLP injections to double-check concentrations and will continue to be used in future tumour trials. Changes in technique such as loading syringes with tumour cells in a sterile hood before going to the animal facility instead of loading there will reduce the chance of contamination. Tumours that ulcerated have also been tested for bacteria by swabbing a small amount and allowing to

grow on a Luria-Bertani agar plate. An overgrowth of *Staphlococcus xylosus* was found in one of the ulcerated tumours.

Due to the high amount of ulcerations in these trials, tumours from the Urah$^{Plt2/Plt2}$ mice were unable to be analysed via flow cytometry. Running the exhaustion panel on these tumours would allow for a more complete story and would complement the data on TIL frequency.

The tumour trials were designed based on the assumption that the VLP was an efficacious treatment and that combination therapy with anti-PD-L1 would increase the benefit. However, due to the VLP not working, and with the VLP + anti-PD-L1 groups showing some reduced growth and increased survival, it may be useful to have a group of mice treated with just anti-PD-L1 in order to see the effect of this drug alone.

Finally, only stage I and II colorectal cancer patients have been investigated in the Dunedin cohort. This project will be continued next year, expanding to stage III and IV patients. These patients are more likely to have had chemotherapy and will more closely resemble the mouse work undertaken. Once the data from this has been analysed, it will provide a more complete picture of the differences already observed between groups based on muscle and fat mass. Stage III and IV patients are expected to have a reduced rate of survival, and studies tend to show that obesity has a greater effect in the more advanced stages of cancer (105).

Possible confounders, such as sex, age and smoking status, have been outlined. However, the results have not been adjusted for them yet as this was outside the scope of this project. This will be performed by a biostatistician before publishing. Ethnicity should also be accounted for when moving forward with this project.

As these patients are enrolled in the Dunedin colorectal cancer cohort, samples of the tumours are preserved and can be accessed. In this project, immune cell populations in the blood of these patients have been looked at. It would be interesting to look at the types of immune cells within the tumours or see the level of T-cell exhaustion. This could be done via immunohistochemical staining and would help further link this study to the murine component of the research.

5.9 Conclusion

Cancer is a disease which causes significant global morbidity and mortality. Especially in more advanced stages, it is complex to treat due to its ability to metastasise and adapt to current therapies. Immunotherapies are a promising new technology which are likely to become the future of cancer treatment. However, many of these treatments are still in novel stages and there are major discrepancies around who will benefit as many patients do not respond favourably. Metabolic syndrome, primarily obesity, has been identified as a possible influencer of immunotherapeutic treatment outcome due to its effect on the immune system. Among other things, the state of chronic inflammation induced by obesity both works to encourage tumour growth and may make it harder for treatments to stimulate the immune system, impeding success.

Previous work on this project found that obese mice may have a more immunosuppressive environment, while hyperuricemic mice may have impaired activation of certain immune cells. Due to the issues highlighted previously, it is difficult to make conclusions from this data. However, breast cancer tumour-bearing lean mice responded more favourably to anti-PD-L1 compared to obese and hyperuricemic mice. A higher frequency of TILs in the tumours of lean mice compared to obese and hyperuricemic mice may be responsible for this, although, in the colorectal cancer

tumours, lean and obese mice had similar levels of TILs while hyperuricemic mice were reduced.

It was found that classifying obesity by visceral fat gives a different pattern of 5-year survival in stage I and II colorectal cancer patients compared to classifying it by waist circumference or BMI. This is important as it means that current clinical methods for classifying obesity may not be accurately reflecting the effect of specific types of fat on health outcomes. More work needs to be done to expand this study to stage III and IV patients to complete the picture.

Overall, metabolic syndrome has a role to play in the efficacy of cancer treatment, and this may be cancer type and sex specific. Rates of obesity are increasing globally, which comes with a raft of different health problems. It is therefore important to tailor current and future cancer treatments, in order to obtain the best health outcomes for all populations of patients.

References

1. Cooper GM. The Development and Causes of Cancer. 2000. In: The Cell: A Molecular Approach 2nd edition [Internet]. Sunderland (MA): Sinauer Associates. Available from: https://www.ncbi.nlm.nih.gov/books/NBK9963/.

2. Mortality 2016: Data tables. Wellington: Ministry of Health; 2019.

3. Cancer 2018 Fact Sheet: World Health Organisation; 2018 [Available from: https://www.who.int/en/news-room/fact-sheets/detail/cancer.

4. Horton S, Gauvreau CL. Cancer in Low- and Middle-Income Countries: An Economic Overview. In: Gelband H, Jha P, Sankaranarayanan R, Horton S, editors. Cancer: Disease Control Priorities, Third Edition (Volume 3). Washington (DC)2015.

5. New cancer registrations 2016: Ministry of Health; 2018 [Available from: https://www.health.govt.nz/publication/new-cancer-registrations-2016.

6. Danciu M, Dima A, Cucu C, Mihailovici M. Invasive carcinoma of the breast. 2016. In: Atlas of Pathology [Internet]. Romania. 3. Available from: http://www.pathologyatlas.ro/invasive-ductal-carcinoma-breast-pathology.php.

7. Shah R, Rosso K, Nathanson SD. Pathogenesis, prevention, diagnosis and treatment of breast cancer. World Journal of Clinical Oncology. 2014;5(3):283-98.

8. Colorectal cancer types: Cancer Treatment Centre of America; 2019 [Available from: https://www.cancercenter.com/cancer-types/colorectal-cancer/types.

9. Grady WM, Markowitz SD. The molecular pathogenesis of colorectal cancer and its potential application to colorectal cancer screening. Digestive Diseases and Sciences. 2015;60(3):762-72.

10. Johnson CM, Wei C, Ensor JE, Smolenski DJ, Amos CI, Levin B, et al. Meta-analyses of colorectal cancer risk factors. Cancer Causes & Control. 2013;24(6):1207-22.

11. Alatrash G, Molldrem JJ. CH 7 - Tumor-associated antigens. In: Socié G, Blazar BR, editors. Immune Biology of Allogeneic Hematopoietic Stem Cell Transplantation. San Diego: Academic Press; 2013. p. 143-64.

12. Lotze MT, Demarco RA. Dying dangerously: Necrotic cell death and chronic inflammation promote tumor growth. Discovery medicine. 2004;4(24):448-56.

13. Mantegazza AR, Magalhaes JG, Amigorena S, Marks MS. Presentation of phagocytosed antigens by MHC class I and II. Traffic. 2013;14(2):135-52.

14. Kroemer G, Galluzzi L, Kepp O, Zitvogel L. Immunogenic cell death in cancer therapy. Annual review of immunology. 2013;31:51-72.

15. Andersen MH, Schrama D, thor Straten P, Becker JC. Cytotoxic T Cells. Journal of Investigative Dermatology. 2006;126(1):32-41.

16. Chandrasekaran S, King MR. Microenvironment of tumor-draining lymph nodes: opportunities for liposome-based targeted therapy. International Journal of Molecular Sciences. 2014;15(11):20209-39.

17. Tai Y, Wang Q, Korner H, Zhang L, Wei W. Molecular Mechanisms of T Cells Activation by Dendritic Cells in Autoimmune Diseases. Frontiers in Pharmacology. 2018;9:642.

18. Cavenagh M, Findlay EG. T-cell activation: British Society for Immunology; [Available from: https://www.immunology.org/public-information/bitesized-immunology/systems-and-processes/t-cell-activation.

19. Hadrup S, Donia M, Thor Straten P. Effector CD4 and CD8 T cells and their role in the tumor microenvironment. Cancer Microenvironment. 2013;6(2):123-33.

20. Ahrends T, Borst J. The opposing roles of CD4(+) T cells in anti-tumour immunity. Immunology. 2018.

21. Buferne M, Chasson L, Grange M, Mas A, Arnoux F, Bertuzzi M, et al. IFNγ producing $CD8^+$ T cells modified to resist major immune checkpoints induce regression of MHC class I-deficient melanomas. Oncoimmunology. 2015;4(2):e974959.

22. Groom JR, Luster AD. CXCR3 in T cell function. Experimental Cell Research. 2011;317(5):620-31.

23. Wissinger E. $CD8^+$ T cells: British Society for Immunology; [Available from: https://www.immunology.org/public-information/bitesized-immunology/cells/cd8-t-cells.

24. Krummel MF, Bartumeus F, Gerard A. T cell migration, search strategies and mechanisms. Nature Reviews Immunology. 2016;16(3):193-201.

25. Bhat P, Leggatt G, Waterhouse N, Frazer IH. Interferon-gamma derived from cytotoxic lymphocytes directly enhances their motility and cytotoxicity. Cell Death & Disease. 2017;8(6):e2836.

26. Cantaert T, Baeten D, Tak PP, van Baarsen LG. Type I IFN and TNFalpha cross-regulation in immune-mediated inflammatory disease: basic concepts and clinical relevance. Arthritis Research & Therapy. 2010;12(5):219.

27. Obar JJ, Lefrancois L. Memory CD8+ T cell differentiation. Annals of the New York Academy of Sciences. 2010;1183:251-66.

28. Kim HR, Hwang KA, Park SH, Kang I. IL-7 and IL-15: biology and roles in T-Cell immunity in health and disease. Critical reviews in immunology. 2008;28(4):325-39.

29. Kennedy R, Celis E. Multiple roles for CD4+ T cells in anti-tumor immune responses. Nature Reviews Immunology. 2008;222:129-44.

30. Buchbinder EI, Desai A. CTLA-4 and PD-1 Pathways: Similarities, Differences, and Implications of Their Inhibition. American Journal of Clinical Oncology. 2016;39(1):98-106.

31. Das M, Zhu C, Kuchroo VK. Tim-3 and its role in regulating anti-tumor immunity. Nature Reviews Immunology. 2017;276(1):97-111.

32. Wherry EJ. T cell exhaustion. Nature Immunology. 2011;12(6):492-9.

33. Scolyer RA, Busam KJ. Prognosis, Staging, and Reporting of Melanomas. In: Busam KJ, Gerami P, Scolyer RA, editors. Pathology of Melanocytic Tumors. Philadelphia: Elsevier; 2019. p. 386-96.

34. Stanton SE, Disis ML. Clinical significance of tumor-infiltrating lymphocytes in breast cancer. Journal for ImmunoTherapy of Cancer. 2016;4:59.

35. Yi JS, Cox MA, Zajac AJ. T-cell exhaustion: characteristics, causes and conversion. Immunology. 2010;129(4):474-81.

36. Wu AA, Drake V, Huang HS, Chiu S, Zheng L. Reprogramming the tumor microenvironment: tumor-induced immunosuppressive factors paralyze T cells. Oncoimmunology. 2015;4(7):e1016700.

37. Schreiber RD, Old LJ, Smyth MJ. Cancer immunoediting: integrating immunity's roles in cancer suppression and promotion. Science (New York, NY). 2011;331(6024):1565-70.

38. Garrido F, Aptsiauri N, Doorduijn EM, Garcia Lora AM, van Hall T. The urgent need to recover MHC class I in cancers for effective immunotherapy. Current Opinion in Immunology. 2016;39:44-51.

39. Palazon A, Aragones J, Morales-Kastresana A, de Landazuri MO, Melero I. Molecular pathways: hypoxia response in immune cells fighting or promoting cancer. Clinical Cancer Research. 2012;18(5):1207-13.

40. Jarnicki AG, Lysaght J, Todryk S, Mills KH. Suppression of antitumor immunity by IL-10 and TGF-beta-producing T cells infiltrating the growing tumor: influence of tumor environment on the induction of CD4+ and CD8+ regulatory T cells. Journal of Immunology. 2006;177(2):896-904.

41. Mittal SK, Cho KJ, Ishido S, Roche PA. Interleukin 10 (IL-10)-mediated Immunosuppression: MARCH-I INDUCTION REGULATES ANTIGEN PRESENTATION BY MACROPHAGES BUT NOT DENDRITIC CELLS. The Journal of biological chemistry. 2015;290(45):27158-67.

42. Wrzesinski SH, Wan YY, Flavell RA. Transforming growth factor-beta and the immune response: implications for anticancer therapy. Clinical Cancer Research. 2007;13(18 Pt 1):5262-70.

43. Bagnyukova TV, Serebriiskii IG, Zhou Y, Hopper-Borge EA, Golemis EA, Astsaturov I. Chemotherapy and signaling: How can targeted therapies supercharge cytotoxic agents? Cancer Biology & Therapy. 2010;10(9):839-53.

44. Baxevanis CN, Perez SA, Papamichail M. Cancer immunotherapy. Critical reviews in clinical laboratory sciences. 2009;46(4):167-89.

45. Yousefi H, Yuan J, Keshavarz M, Murphy J, Rezaei N. Immunotherapy of cancers comes of age2017.

46. Braun M, Perret R, Scholz G, Romero P. Peptide and Protein-Based Cancer Vaccines. In: Curiel T, editor. Cancer Immunotherapy: Springer; 2012. p. 111-46.

47. Hollingsworth RE, Jansen K. Turning the corner on therapeutic cancer vaccines2019. 7 p.

48. Arlen PM, Skarupa L, Pazdur M, Seetharam M, Tsang K, Grosenbach D, et al. Clinical Safety of a Viral Vector Based Prostate Cancer Vaccine Strategy: National Institutes of Health; 2007. 1515-20 p.

49. Ong HK, Tan WS, Ho KL. Virus like particles as a platform for cancer vaccine development. PeerJ. 2017;5:e4053.

50. Abrantes J, van der Loo W, Le Pendu J, Esteves PJ. Rabbit haemorrhagic disease (RHD) and rabbit haemorrhagic disease virus (RHDV): a review. Journal of Veterinary Research. 2012;43:12.

51. Wang X, Xu F, Liu J, Gao B, Liu Y, Zhai Y, et al. Atomic model of rabbit hemorrhagic disease virus by cryo-electron microscopy and crystallography. PLOS Pathogens. 2013;9(1):e1003132.

52. Kramer K, Al-Barwani F, Baird MA, Young VL, Larsen DS, Ward VK, et al. Functionalisation of Virus-Like Particles Enhances Antitumour Immune Responses %J Journal of Immunology Research. Journal of Immunology Research. 2019;2019:10.

53. Al-Barwani F, Young SL, Baird MA, Larsen DS, Ward VK. Mannosylation of Virus-Like Particles Enhances Internalization by Antigen Presenting Cells. PLOS One. 2014;9(8):e104523.

54. Mita AC, Mita MM, Nawrocki ST, Giles FJ. Survivin: key regulator of mitosis and apoptosis and novel target for cancer therapeutics. Clinical Cancer Research. 2008;14(16):5000-5.

55. Garg H, Suri P, Gupta JC, Talwar GP, Dubey S. Survivin: a unique target for tumor therapy. Cancer Cell International. 2016;16(1):49.

56. Gendler SJ. MUC1, The Renaissance Molecule. Journal of Mammary Gland Biology and Neoplasia. 2001;6(3):339-53.

57. Bode C, Zhao G, Steinhagen F, Kinjo T, Klinman DM. CpG DNA as a vaccine adjuvant. Expert Review of Vaccines. 2011;10(4):499-511.

58. Donaldson B, Al-Barwani F, Pelham SJ, Young K, Ward VK, Young SL. Multi-target chimaeric VLP as a therapeutic vaccine in a model of colorectal cancer. Journal for ImmunoTherapy of Cancer. 2017;5(1):69.

59. Keenan BP, Jaffee EM. Whole cell vaccines--past progress and future strategies. Seminars in Oncology. 2012;39(3):276-86.

60. Mohebtash M, Madan RA, Gulley JL, Arlen PM. Therapeutic prostate cancer vaccines: a review of the latest developments. Current Opinion in Investigational Drugs. 2008;9(12):1296-301.

61. Chen G, Gupta R, Petrik S, Laiko M, Leatherman JM, Asquith JM, et al. A feasibility study of cyclophosphamide, trastuzumab, and an allogeneic GM-CSF-secreting breast tumor vaccine for HER2+ metastatic breast cancer. Cancer Immunoly Research. 2014;2(10):949-61.

62. Hamid O, Robert C, Daud A, Hodi FS, Hwu WJ, Kefford R, et al. Safety and tumor responses with lambrolizumab (anti-PD-1) in melanoma. The New England journal of medicine. 2013;369(2):134-44.

63. Pardoll DM. The blockade of immune checkpoints in cancer immunotherapy. Nature Reviews Cancer. 2012;12(4):252-64.

64. Julia EP, Amante A, Pampena MB, Mordoh J, Levy EM. Avelumab, an IgG1 anti-PD-L1 Immune Checkpoint Inhibitor, Triggers NK Cell-Mediated Cytotoxicity and Cytokine Production Against Triple Negative Breast Cancer Cells. Front Immunol. 2018;9:2140.

65. Gwalani LA, Orange JS. Single Degranulations in NK Cells Can Mediate Target Cell Killing. The Journal of Immunology. 2018:ji1701500.

66. Restifo NP, Dudley ME, Rosenberg SA. Adoptive immunotherapy for cancer: harnessing the T cell response. Nature Reviews Immunology. 2012;12(4):269-81.

67. Huang PL. A comprehensive definition for metabolic syndrome. Disease Models & Mechanisms. 2009;2(5-6):231-7.

68. Guilherme A, Virbasius JV, Puri V, Czech MP. Adipocyte dysfunctions linking obesity to insulin resistance and type 2 diabetes. Nature Reviews Molecular Cell Biology. 2008;9(5):367-77.

69. Obesity: World Health Organisation; [Available from: https://www.who.int/topics/obesity/en/.

70. Obesity Statistics New Zealand: Ministry of Health; 2018 [Available from: https://www.health.govt.nz/nz-health-statistics/health-statistics-and-data-sets/obesity-statistics.

71. Dixon JB. The effect of obesity on health outcomes. Molecular and Cellular Endocrinology. 2010;316(2):104-8.

72. Wolin KY, Carson K, Colditz GA. Obesity and cancer. The Oncologist. 2010;15(6):556-65.

73. De Pergola G, Silvestris F. Obesity as a Major Risk Factor for Cancer. Journal of Obesity. 2013;2013.

74. Reeves GK, Pirie K, Beral V, Green J, Spencer E, Bull D, et al. Cancer incidence and mortality in relation to body mass index in the Million Women Study: cohort study. The British Medical Journal. 2007;335(7630):1134.

75. Vucenik I, Stains JP. Obesity and cancer risk: evidence, mechanisms, and recommendations. Annals of the New York Academy of Sciences. 2012;1271:37-43.

76. Zhang G, Li X, Sui C, Zhao H, Zhao J, Hou Y, et al. Incidence and risk factor analysis for sarcopenia in patients with cancer. Oncology Letters. 2016;11(2):1230-4.

77. Kim SH, Shin MJ, Shin YB, Kim KU. Sarcopenia Associated with Chronic Obstructive Pulmonary Disease. Journal of Bone Metabolism. 2019;26(2):65-74.

78. El Ridi R, Tallima H. Physiological functions and pathogenic potential of uric acid: A review. J Adv Res. 2017;8(5):487-93.

79. de Oliveira EP, Burini RC. High plasma uric acid concentration: causes and consequences. Diabetology & Metabolic Syndrome. 2012;4:12.

80. Smith E, March L. Global Prevalence of Hyperuricemia: A Systematic Review of Population-Based Epidemiological Studies [abstract]. Arthritis & Rheumatology. 2015;67.

81. Choi HK, Liu S, Curhan G. Intake of purine-rich foods, protein, and dairy products and relationship to serum levels of uric acid: the Third National Health and Nutrition Examination Survey. Arthritis Rheum. 2005;52(1):283-9.

82. George C, Minter DA. Hyperuricemia. StatPearls. Treasure Island (FL)2018.

83. Fini MA, Elias A, Johnson RJ, Wright RM. Contribution of uric acid to cancer risk, recurrence, and mortality. Clinical and Translational Medicine. 2012;1(1):16.

84. Cetin AO, Omar M, Calp S, Tunca H, Yimaz N, Ozseker B, et al. Hyperuricemia at The Time Of Diagnosis is a Factor for Poor Prognosis in Patients With Stage II and III Colorectal Cancer (Uric Acid and Colorectal Cancer). Asian Pacific Journal of Cancer Prevention. 2017;18(2):485-90.

85. Quail DF, Dannenberg AJ. The obese adipose tissue microenvironment in cancer development and progression. Nature Reviews Endocrinology. 2018.

86. Gunter MJ, Hoover DR, Yu H, Wassertheil-Smoller S, Manson JE, Li J, et al. A prospective evaluation of insulin and insulin-like growth factor-I as risk factors for endometrial cancer. Cancer Epidemiology, Biomarkers & Prevention. 2008;17(4):921-9.

87. Chan BT, Lee AV. Insulin receptor substrates (IRSs) and breast tumorigenesis. Journal of Mammary Gland Biology and Neoplasia. 2008;13(4):415-22.

88. Gallagher EJ, LeRoith D. The proliferating role of insulin and insulin-like growth factors in cancer. Trends in Endocrinology & Metabolism. 2010;21(10):610-8.

89. Renehan AG, Frystyk J, Flyvbjerg A. Obesity and cancer risk: the role of the insulin-IGF axis. Trends in Endocrinology & Metabolism. 2006;17(8):328-36.

90. Kaaks R, Rinaldi S, Key TJ, Berrino F, Peeters PH, Biessy C, et al. Postmenopausal serum androgens, oestrogens and breast cancer risk: the European prospective investigation into cancer and nutrition. Endocr Relat Cancer. 2005;12(4):1071-82.

91. Calle EE, Kaaks R. Overweight, obesity and cancer: epidemiological evidence and proposed mechanisms. Nature Reviews Cancer. 2004;4(8):579-91.

92. Matsuzawa Y. Therapy Insight: adipocytokines in metabolic syndrome and related cardiovascular disease. Nature Clinical Practice Cardiovascular Medicine. 2006;3(1):35-42.

93. Klok MD, Jakobsdottir S, Drent ML. The role of leptin and ghrelin in the regulation of food intake and body weight in humans: a review. Obesity Reviews. 2007;8(1):21-34.

94. Vona-Davis L, Rose DP. Adipokines as endocrine, paracrine, and autocrine factors in breast cancer risk and progression. Endocrine-Related Cancer. 2007;14(2):189-206.

95. Birmingham JM, Busik JV, Hansen-Smith FM, Fenton JI. Novel mechanism for obesity-induced colon cancer progression. Carcinogenesis. 2009;30(4):690-7.

96. Catalano S, Marsico S, Giordano C, Mauro L, Rizza P, Panno ML, et al. Leptin enhances, via AP-1, expression of aromatase in the MCF-7 cell line. Journal of Biological Chemistry. 2003;278(31):28668-76.

97. Cnop M, Havel PJ, Utzschneider KM, Carr DB, Sinha MK, Boyko EJ, et al. Relationship of adiponectin to body fat distribution, insulin sensitivity and plasma lipoproteins: evidence for independent roles of age and sex. Diabetologia. 2003;46(4):459-69.

98. Kelesidis I, Kelesidis T, Mantzoros CS. Adiponectin and cancer: a systematic review. British Journal of Cancer. 2006;94(9):1221-5.

99. Brakenhielm E, Veitonmaki N, Cao R, Kihara S, Matsuzawa Y, Zhivotovsky B, et al. Adiponectin-induced antiangiogenesis and antitumor activity involve caspase-mediated endothelial cell apoptosis. Proceedings of the National Academy of Sciences of the United States of America. 2004;101(8):2476-81.

100. Byrne GJ, Ghellal A, Iddon J, Blann AD, Venizelos V, Kumar S, et al. Serum soluble vascular cell adhesion molecule-1: role as a surrogate marker of angiogenesis. Journal of the National Cancer Institute. 2000;92(16):1329-36.

101. Wang Z, Aguilar EG, Luna JI, Dunai C, Khuat LT, Le CT, et al. Paradoxical effects of obesity on T cell function during tumor progression and PD-1 checkpoint blockade. Nature medicine. 2019;25(1):141-51.

102. Horowitz NS, Wright AA. Impact of obesity on chemotherapy management and outcomes in women with gynecologic malignancies. Gynecologic Oncology. 2015;138(1):201-6.

103. Griggs JJ, Mangu PB, Anderson H, Balaban EP, Dignam JJ, Hryniuk WM, et al. Appropriate chemotherapy dosing for obese adult patients with cancer: American Society of Clinical Oncology clinical practice guideline. Journal of Clinical Oncology. 2012;30(13):1553-61.

104. Moszynska-Zielinska M, Chalubinska-Fendler J, Gottwald L, Zytko L, Bigos E, Fijuth J. Does obesity hinder radiotherapy in endometrial cancer patients? The implementation of new techniques in adjuvant radiotherapy - focus on obese patients. Przegląd Menopauzalny. 2014;13(2):96-100.

105. Kroenke CH, Neugebauer R, Meyerhardt J, Prado CM, Weltzien E, Kwan ML, et al. Analysis of Body Mass Index and Mortality in Patients With Colorectal Cancer Using Causal Diagrams. The Journal of the American Medical Association Oncology. 2016;2(9):1137-45.

106. Shahjehan F, Merchea A, Cochuyt JJ, Li Z, Colibaseanu DT, Kasi PM. Body Mass Index and Long-Term Outcomes in Patients With Colorectal Cancer. Frontiers in Oncology. 2018;8(620).

107. Lennon H, Sperrin M, Badrick E, Renehan AG. The Obesity Paradox in Cancer: a Review. Current Oncology Reports. 2016;18(9):56.

108. Caan BJ, Cespedes Feliciano EM, Prado CM, Alexeeff S, Kroenke CH, Bradshaw P, et al. Association of Muscle and Adiposity Measured by Computed Tomography With Survival in Patients With Nonmetastatic Breast Cancer. The Journal of the American Medical Association Oncology. 2018;4(6):798-804.

109. Naaz A, Holsberger DR, Iwamoto GA, Nelson A, Kiyokawa H, Cooke PS. Loss of cyclin-dependent kinase inhibitors produces adipocyte hyperplasia and obesity. The FASEB Journal. 2004;18(15):1925-7.

110. Andersen CJ, Murphy KE, Fernandez ML. Impact of Obesity and Metabolic Syndrome on Immunity. Advances in Nutrition. 2016;7(1):66-75.

111. Sartipy P, Loskutoff DJ. Monocyte chemoattractant protein 1 in obesity and insulin resistance. Proceedings of the National Academy of Sciences of the United States of America. 2003;100(12):7265-70.

112. Lumeng CN, Bodzin JL, Saltiel AR. Obesity induces a phenotypic switch in adipose tissue macrophage polarization. Journal of Clinical Investigation. 2007;117(1):175-84.

113. Lagathu C, Yvan-Charvet L, Bastard JP, Maachi M, Quignard-Boulange A, Capeau J, et al. Long-term treatment with interleukin-1beta induces insulin resistance in murine and human adipocytes. Diabetologia. 2006;49(9):2162-73.

114. Sasi SP, Yan X, Enderling H, Park D, Gilbert HY, Curry C, et al. Breaking the 'harmony' of TNF-α signaling for cancer treatment. Oncogene. 2012;31(37):4117-27.

115. Ghanim H, Aljada A, Hofmeyer D, Syed T, Mohanty P, Dandona P. Circulating mononuclear cells in the obese are in a proinflammatory state. Circulation. 2004;110(12):1564-71.

116. Kanneganti TD, Dixit VD. Immunological complications of obesity. Nature Immunology. 2012;13(8):707-12.

117. Iwasaki H, Akashi K. Myeloid lineage commitment from the hematopoietic stem cell. Immunity. 2007;26(6):726-40.

118. Dixit VD. Impact of immune-metabolic interactions on age-related thymic demise and T cell senescence. Seminars in immunology. 2012;24(5):321-30.

119. Naveiras O, Nardi V, Wenzel PL, Hauschka PV, Fahey F, Daley GQ. Bone-marrow adipocytes as negative regulators of the haematopoietic microenvironment. Nature. 2009;460(7252):259-63.

120. Yang H, Youm YH, Vandanmagsar B, Rood J, Kumar KG, Butler AA, et al. Obesity accelerates thymic aging. Blood. 2009;114(18):3803-12.

121. Kono H, Chen CJ, Ontiveros F, Rock KL. Uric acid promotes an acute inflammatory response to sterile cell death in mice. Journal of Clinical Investigation. 2010;120(6):1939-49.

122. Wang Y, Ma X, Su C, Peng B, Du J, Jia H, et al. Uric acid enhances the antitumor immunity of dendritic cell-based vaccine. Scientific Reports. 2015;5:16427.

123. Hu DE, Moore AM, Thomsen LL, Brindle KM. Uric Acid Promotes Tumor Immune Rejection. Cancer research. 2004;64(15):5059-62.

124. Ghaemi-Oskouie F, Shi Y. The role of uric acid as an endogenous danger signal in immunity and inflammation. Current Rheumatology Reports. 2011;13(2):160-6.

125. Nambu A, Nakae S, Iwakura Y. IL-1β, but not IL-1α, is required for antigen-specific T cell activation and the induction of local inflammation in the delayed-type hypersensitivity responses. International Immunology. 2006;18(5):701-12.

126. Mirsoian A, Bouchlaka MN, Sckisel GD, Chen M, Pai CC, Maverakis E, et al. Adiposity induces lethal cytokine storm after systemic administration of stimulatory immunotherapy regimens in aged mice. Journal of Experimental Medicine. 2014;211(12):2373-83.

127. Sheridan PA, Paich HA, Handy J, Karlsson EA, Hudgens MG, Sammon AB, et al. Obesity is associated with impaired immune response to influenza vaccination in humans. International Journal of Obesity (London). 2012;36(8):1072-7.

128. James BR, Tomanek-Chalkley A, Askeland EJ, Kucaba T, Griffith TS, Norian LA. Diet-induced obesity alters dendritic cell function in the presence and absence of tumor growth. Journal of Immunology. 2012;189(3):1311-21.

129. Sánchez-Jiménez F, Pérez-Pérez A, de la Cruz-Merino L, Sánchez-Margalet V. Obesity and Breast Cancer: Role of Leptin. Frontiers in Oncology. 2019;9(596).

130. Murphy WJ, Longo DL. The Surprisingly Positive Association Between Obesity and Cancer Immunotherapy Efficacy. The Journal of the American Medical Association. 2019;321(13):1247-8.

131. Baey C, Yang J, Ronchese F, Harper JL. Hyperuricaemic UrahPlt2/Plt2 mice show altered T cell proliferation and defective tumor immunity after local immunotherapy with Poly I:C. PLOS One. 2018;13(11):e0206827.

132. Shuster A, Patlas M, Pinthus JH, Mourtzakis M. The clinical importance of visceral adiposity: a critical review of methods for visceral adipose tissue analysis. The British Journal of Radiology. 2012;85(1009):1-10.

133. Bergman RN, Kim SP, Catalano KJ, Hsu IR, Chiu JD, Kabir M, et al. Why Visceral Fat is Bad: Mechanisms of the Metabolic Syndrome. Obesity. 2006;14(S2):16S-9S.

134. The POUND mouse: Charles River Laboratories; [Available from: https://www.criver.com/products-services/find-model/pound-mouse?region=3616.

135. Mukherjee P, Ginardi AR, Tinder TL, Sterner CJ, Gendler SJ. MUC1-specific cytotoxic T lymphocytes eradicate tumors when adoptively transferred in vivo. Clinical Cancer Research. 2001;7(3 Suppl):848s-55s.

136. Evans M. Investigating the Effects of Chronic Low-Grade Inflammation on Cancer Immunotherapy [Honours]. Dunedin: University of Otago; 2018.

137. Efremova M, Rieder D, Klepsch V, Charoentong P, Finotello F, Hackl H, et al. Targeting immune checkpoints potentiates immunoediting and changes the dynamics of tumor evolution. Nature Communications. 2018;9(1):32.

138. McKee SJ, Young VL, Clow F, Hayman CM, Baird MA, Hermans IF, et al. Virus-like particles and α-galactosylceramide form a self-adjuvanting composite particle that elicits anti-tumor responses. Journal of Controlled Release. 2012;159(3):338-45.

139. Wells JC, Fewtrell MS. Measuring body composition. Archives of Disease in Childhood. 2006;91(7):612-7.

140. Doyle SL, Bennett AM, Donohoe CL, Mongan AM, Howard JM, Lithander FE, et al. Establishing computed tomography–defined visceral fat area thresholds for use in obesity-related cancer research. Nutrition Research. 2013;33(3):171-9.

141. Gomez-Perez SL, Haus JM, Sheean P, Patel B, Mar W, Chaudhry V, et al. Measuring Abdominal Circumference and Skeletal Muscle From a Single Cross-Sectional Computed Tomography Image: A Step-by-Step Guide for Clinicians Using National Institutes of Health ImageJ. Journal of Parenteral and Enteral Nutrition. 2016;40(3):308-18.

142. Ciudin A, Salvador R, Budoy A, Ciudin A, Spinu C, Diaconu MG, et al. Measurement of waist circumference for retrospective studies - prospective validation of use of CT images to assess abdominal circumference. Endocrinol Nutr. 2014;61(3):147-52.

143. Martin L, Birdsell L, MacDonald N, Reiman T, Clandinin MT, Murphy R, et al. Cancer cachexia in the age of obesity: skeletal muscle depletion is a powerful prognostic factor, independent of body mass index. Journal of Clinical Oncology. 2013;31(12):1539-47.

144. Fuchs G, Thevathasan T, Chretien YR, Mario J, Piriyapatsom A, Schmidt U, et al. Lumbar skeletal muscle index derived from routine computed tomography exams predict adverse post-extubation outcomes in critically ill patients. Journal of Critical Care. 2018;44:117-23.

145. Nattenmueller J, Hoegenauer H, Boehm J, Scherer D, Paskow M, Gigic B, et al. CT-based compartmental quantification of adipose tissue versus body metrics in colorectal cancer patients. European Radiology. 2016;26(11):4131-40.

146. Simoni Y, Becht E, Fehlings M, Loh CY, Koo SL, Teng KWW, et al. Bystander CD8+ T cells are abundant and phenotypically distinct in human tumour infiltrates. Nature. 2018;557(7706):575-9.

147. Gilmore J. Body mass index and health. Public Health Reports. 1999;11(1):31-43(Eng); 33-47(Fre).

148. Zhu SK, Wang ZM, Heshka S, Heo M, Faith MS, Heymsfield SB. Waist circumference and obesity-associated risk factors among whites in the third National Health and Nutrition Examination Survey: clinical action thresholds. The American Journal of Clinical Nutrition. 2002;76(4):743-.

149. Shinichiro M. Prevalence of Sarcopenia in Cancer Patients: Review and Future Directions. International Journal of Physical Medicine & Rehabilitation. 2016;- 4(- 2329-9096):- 1-8.

150. Guthrie GJ, Charles KA, Roxburgh CS, Horgan PG, McMillan DC, Clarke SJ. The systemic inflammation-based neutrophil-lymphocyte ratio: experience in patients with cancer. Crit Rev Oncol Hematol. 2013;88(1):218-30.

151. Alexander JC, Jr., Silverman NA, Chretien PB. Effect of Age and Cigarette Smoking on Carcinoembryonic Antigen Levels. The Journal of the American Medical Association. 1976;235(18):1975-9.

152. Al-Barwani F, Donaldson B, Pelham SJ, Young SL, Ward VK. Antigen delivery by virus-like particles for immunotherapeutic vaccination. Therapeutic Delivery. 2014;5(11):1223-40.

153. Ventola CL. Cancer Immunotherapy, Part 3: Challenges and Future Trends. Pharmacy and Therapeutics. 2017;42(8):514-21.

154. UBC ACC Guideline on Rodents with Ulcerated Subcutaneous Tumours: Protocol Requirements,

Monitoring, Managing and Humane Endpoints. University of British Columbia; 2018.

155. Xie QK, He WZ, Hu WM, Yang L, Jiang C, Kong PF, et al. Tumor-infiltrating lymphocyte as a prognostic biomarker in stage IV colorectal cancer should take into account the metastatic status and operation modality. Cancer Management and Research. 2018;10:1365-75.

156. Konig L, Mairinger FD, Hoffmann O, Bittner AK, Schmid KW, Kimmig R, et al. Dissimilar patterns of tumor-infiltrating immune cells at the invasive tumor front and tumor center are associated with response to neoadjuvant chemotherapy in primary breast cancer. BioMed Central Cancer. 2019;19(1):120.

157. Galon J, Costes A, Sanchez-Cabo F, Kirilovsky A, Mlecnik B, Lagorce-Pagès C, et al. Type, Density, and Location of Immune Cells Within Human Colorectal Tumors Predict Clinical Outcome. Science (New York, NY). 2006;313(5795):1960-4.

158. Zeigler-Johnson C, Morales KH, Lal P, Feldman M. The Relationship between Obesity, Prostate Tumor Infiltrating Lymphocytes and Macrophages, and Biochemical Failure. PLOS One. 2016;11(8):e0159109.

159. Ahmadzadeh M, Johnson LA, Heemskerk B, Wunderlich JR, Dudley ME, White DE, et al. Tumor antigen-specific CD8 T cells infiltrating the tumor express high levels of PD-1 and are functionally impaired. Blood. 2009;114(8):1537-44.

160. Long L, Zhang X, Chen F, Pan Q, Phiphatwatchara P, Zeng Y, et al. The promising immune checkpoint LAG-3: from tumor microenvironment to cancer immunotherapy. Genes & Cancer. 2018;9(5-6):176-89.

161. Dean L. Blood and the cells it contains. Blood Groups and Red Cell Antigens. Bethesda, MD: National Center for Biotechnology Information (US); 2005.

162. Furuncuoglu Y, Tulgar S, Dogan AN, Cakar S, Tulgar YK, Cakiroglu B. How obesity affects the neutrophil/lymphocyte and platelet/lymphocyte ratio, systemic immune-inflammatory index and platelet indices: a retrospective study. European Review for Medical and Pharmacological Sciences. 2016;20(7):1300-6.

163. Ip BC, Hogan AE, Nikolajczyk BS. Lymphocyte roles in metabolic dysfunction: of men and mice. Trends in Endocrinology & Metabolism. 2015;26(2):91-100.

164. Womack J, Tien PC, Feldman J, Shin JH, Fennie K, Anastos K, et al. Obesity and immune cell counts in women. Metabolism. 2007;56(7):998-1004.

165. Pilla L, Maccalli C. Immune Profiling of Cancer Patients Treated with Immunotherapy: Advances and Challenges. Biomedicines. 2018;6(3).

166. Hartmann FJ, Babdor J, Gherardini PF, Amir ED, Jones K, Sahaf B, et al. Comprehensive Immune Monitoring of Clinical Trials to Advance Human Immunotherapy. Cell Reports. 2019;28(3):819-31.e4.

167. Graul AI, Stringer M, Sorbera L. Cachexia. Drugs of Today (Barc). 2016;52(9):519-29.

168. Karastergiou K, Smith SR, Greenberg AS, Fried SK. Sex differences in human adipose tissues - the biology of pear shape. Biology of Sex Differences. 2012;3(1):13.

169. Caan BJ, Cespedes Feliciano EM, Kroenke CH. The Importance of Body Composition in Explaining the Overweight Paradox in Cancer-Counterpoint. Cancer research. 2018;78(8):1906-12.

170. Seo IK, Kim BJ, Kim B, Choi CH, Kim JW, Kim JG, et al. Abdominal fat distribution measured using computed tomography is associated with an increased risk of colorectal adenoma in men. Medicine (Baltimore). 2017;96(37):e8051.

171. Chargi N, Bril SI, Emmelot-Vonk MH, de Bree R. Sarcopenia is a prognostic factor for overall survival in elderly patients with head-and-neck cancer. European Archives of Oto-Rhino-Laryngology. 2019;276(5):1475-86.

172. Deng CY, Lin YC, Wu JS, Cheung YC, Fan CW, Yeh KY, et al. Progressive Sarcopenia in Patients With Colorectal Cancer Predicts Survival. American Journal of Roentgenology. 2018;210(3):526-32.

173. Shiroyama T, Nagatomo I, Koyama S, Hirata H, Nishida S, Miyake K, et al. Impact of sarcopenia in patients with advanced non–small cell lung cancer treated with PD-1 inhibitors: A preliminary retrospective study. Scientific Reports. 2019;9(1):2447.

174. 2018 Census totals by topic – national highlights. Wellington: Statistics New Zealand; 2018.

175. Heymsfield SB, Peterson CM, Thomas DM, Heo M, Schuna JM, Jr. Why are there race/ethnic differences in adult body mass index-adiposity relationships? A quantitative critical review. Obesity Reviews. 2016;17(3):262-75.

176. Rubbieri G, Mossello E, Di Bari M. Techniques for the diagnosis of sarcopenia. Clinical Cases in mineral and bone metabolism. 2014;11(3):181-4.

177. Bahadir A, Baltaci D, Turker Y, Turker Y, Iliev D, Ozturk S, et al. Is the neutrophil-to-lymphocyte ratio indicative of inflammatory state in patients with obesity and metabolic syndrome? The Anatolian Journal of Cardiology. 2015;15(10):816-22.

178. Mosli RH, Mosli HH. Obesity and morbid obesity associated with higher odds of hypoalbuminemia in adults without liver disease or renal failure. Diabetes, Metabolic Syndrome and Obesity: Targets and Therapy. 2017;10:467-72.

179. Jain S, Gautam V, Naseem S. Acute-phase proteins: As diagnostic tool. Journal of Pharmacy and Bioallied Sciences. 2011;3(1):118-27.

180. Knekt P, Hakulinen T, Leino A, Heliovaara M, Reunanen A, Stevens R. Serum albumin and colorectal cancer risk. European Journal of Clinical Nutrition. 2000;54(6):460-2.

181. Can B, Kara O, Kizilarslanoglu MC, Arik G, Aycicek GS, Sumer F, et al. Serum markers of inflammation and oxidative stress in sarcopenia. Aging Clinical and Experimental Research. 2017;29(4):745-52.

182. Kim EY, Kim YS, Seo JY, Park I, Ahn HK, Jeong YM, et al. The Relationship between Sarcopenia and Systemic Inflammatory Response for Cancer Cachexia in Small Cell Lung Cancer. PLOS ONE. 2016;11(8):e0161125.

183. Lin J, Zhang W, Huang Y, Chen W, Wu R, Chen X, et al. Sarcopenia is associated with the neutrophil/lymphocyte and platelet/lymphocyte ratios in operable gastric cancer patients: a prospective study. Cancer Management and Research. 2018;10:4935-44.

Appendix

Supplementary figures

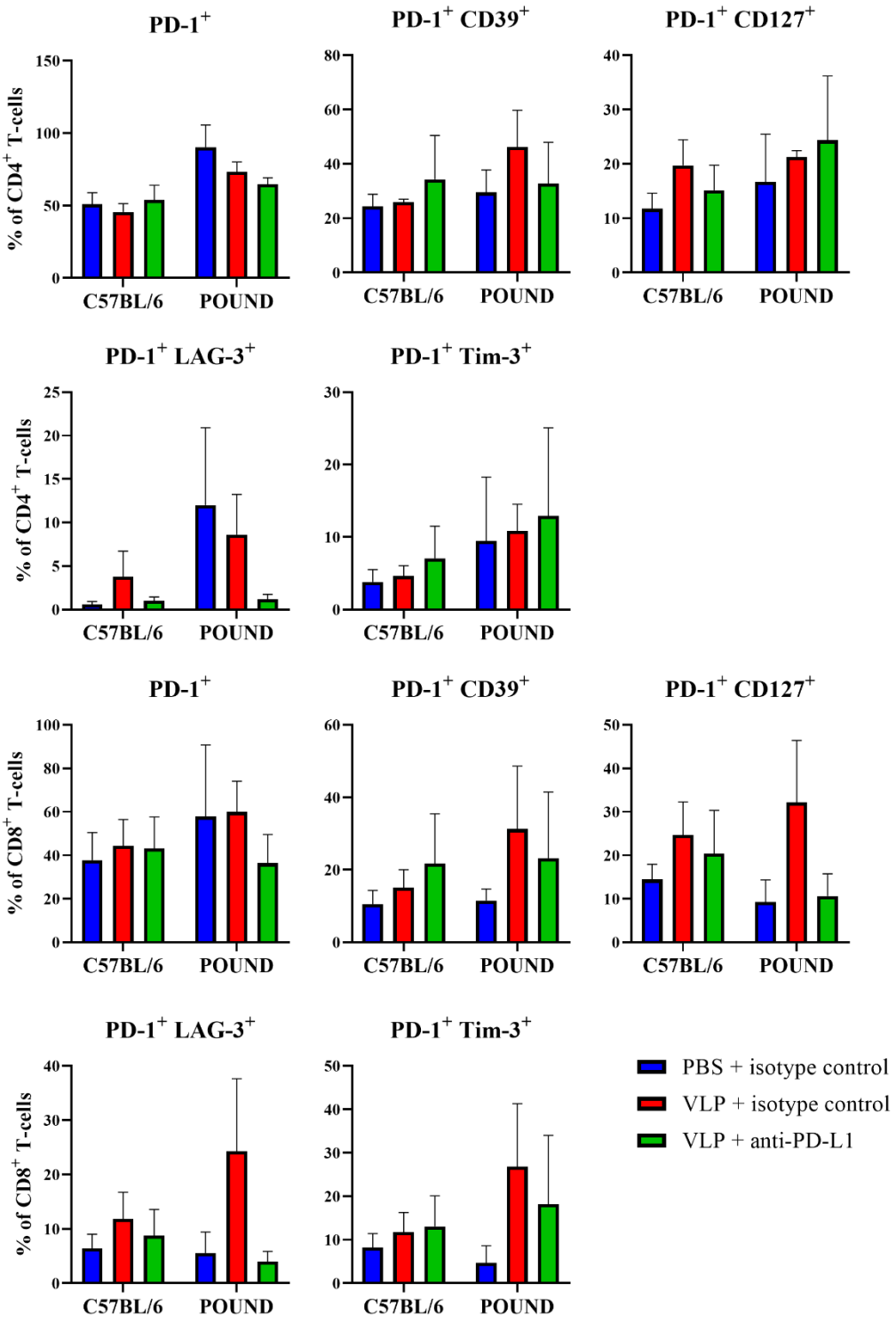

Supplementary Figure 1: Markers of T-cell exhaustion in spleens of C57mg.MUC1 mice

The results represent the mean (± SEM) of five mice per treatment group. Statistical differences were determined by using a one-way ANOVA.

Recipes

Alsever's Solution

20 g dextrose

8 g sodium citrate

0.55 g citric acid

4.2 g NaCl

1 L Milli-Q deionised water

Complete Phosphate-Buffered Solution (cPBS)

5.2 g NaH_2PO_4

23.66 g Na_2HPO_4

17.54 g NaCl

2 L distilled water

C57mg.MUC1 Cell Media

45 mL Dulbecco's Modified Eagle Medium (Gibco)

5 mL (10%) Foetal Calf Serum (FCS) (Moregate Biotech)

150 µg/mL geneticin (G418) (Gibco)

Dulbecco's Phosphate-Buffered Solution (DPBS)

10 g Dulbecco's PBS powder (Gibco)

1 L Milli-Q deionised water

Sterile filtered

Ethylenediaminetetraacetic acid (EDTA) solution

1 mM EDTA in DPBS

Fluorescence-Activated Cell Sorting (FACS) buffer

1 g (1%) bovine serum albumin

0.1 g (0.1%) NaN_3

2 mM EDTA

1 L 10x PBS

Sterile filtered, dilute 1:9 in Milli-Q deionised water

MC-38 Cell Media

45 mL Dulbecco's Modified Eagle Medium

5 mL (10%) Foetal Calf Serum (FCS)

8% Paraformaldehyde (PFA) Fixation Buffer

8 g paraformaldehyde

100 mL FACS buffer

Red Blood Cell Lysis Buffer

4.15 g NH_4Cl

0.5 g $KHCO_3$

0.0186 g EDTA

500 mL Milli-Q deionised water

Sterile filtered

Trypan blue solution

0.25 g Trypan blue powder (Sigma-Aldrich)

100 mL 1 x PBS solution

Sterile filtered